Synthesis and Characterization of Ruthenium(II) Complexes with 2-(4'-*N*,*N*-diethylaminophenylazo)pyridine Ligands

Nararak Leesakul

Master of Science Thesis in Inorganic Chemistry

Prince of Songkla University

2000

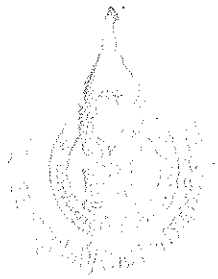

Thesis Title	Synthesis and Characterization of Ruthenium(II) with 2-(4'-*N,N*-diethylaminophenylazo)pyridine Ligands
Author	Miss Nararak Leesakul
Major Program	Inorganic Chemistry

Advisory Committee

Kanidtha Hansongnern .....Chairman

(Dr. Kanidtha Hansongnern)

.....Committee

(Dr. Walailak Puetpaiboon)

Orawan Sirichote .....Committee

(Asst. Prof. Dr. Orawan Sirichote)

Examining Committee

Kanidtha Hansongnern .....Chairman

(Dr. Kanidtha Hansongnern)

.....Committee

(Dr. Walailak Puetpaiboon)

Orawan Sirichote .....Committee

(Asst. Prof. Dr. Orawan Sirichote)

Adisorn Ratanaphan .....Committee

(Asst. Prof. Dr. Adisorn Ratanaphan)

The Graduate School, Prince of Songkla University, has approved this thesis as partial fulfillment of the requirement for the Master of Science degree in Inorganic Chemistry.

P. Trisdikoon .....

(Assoc. Prof. Dr. Piti Trisdikoon)

Dean, Graduate School

ชื่อวิทยานิพนธ์	การสังเคราะห์และศึกษาคุณสมบัติของสารประกอบเชิงซ้อนของโลหะรูทีเนียมกับลิแกนด์ 2-(4'-N,N-diethylaminophenylazo)pyridine
ผู้เขียน	นางสาวนรารักษ์ หลีสกุล
สาขาวิชา	เคมีอนินทรีย์
ปีการศึกษา	2543

บทคัดย่อ

สารประกอบเชิงซ้อน $Ru(L)_2Cl_2$ (L = dmazpy และ deazpy) สามารถเตรียมจากปฏิกิริยาระหว่าง $Ru(dmso)_4Cl_2$ กับ ลิแกนด์ 2-(4'-*N,N*-dimethylaminophenylazo)pyridine (dmazpy, 1) และ 2-(4'-*N,N*-diethylaminophenylazo)pyridine (deazpy, 2) ซึ่งเป็นอนุพันธ์ของ 2-(phenylazo)pyridine (azpy, 3) และสามารถแยก ไอโซเมอร์ ที่เกิดขึ้นได้ 2 ชนิด คือ ไอโซเมอร์แบบซิส (*cis*) และ ไอโซเมอร์แบบทรานส์ (*trans*) ผลจากการศึกษาโครงสร้าง คุณสมบัติทางเคมี และคุณสมบัติทางไฟฟ้าเคมี พบว่า ลิแกนด์ dmazpy และ deazpy มีความสามารถในการเป็นตัวรับไพอิเล็กตรอน (π-acceptor) น้อยกว่า ลิแกนด์ azpy แต่มีความสามารถในการเป็นตัวให้ซิกมาอิเล็กตรอน (σ-donor) ที่ดีกว่าลิแกนด์ azpy ในโครงสร้างของสารประกอบเชิงซ้อน คุณสมบัติดังกล่าวสามารถทำให้รูทีเนียมอิออน (Ru(II)) ในสารประกอบเชิงซ้อนที่มีลิแกนด์ดังกล่าว มีความเสถียรมากกว่า สารประกอบเชิงซ้อนของรูทีเนียมกับลิแกนด์ azpy

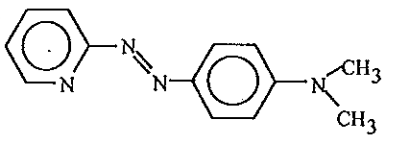

1

dmapy

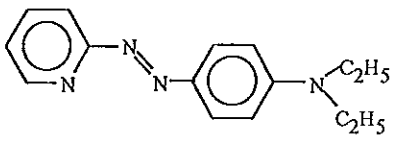

2

deazpy

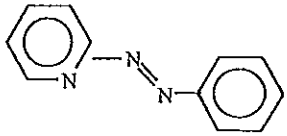

3

azpy

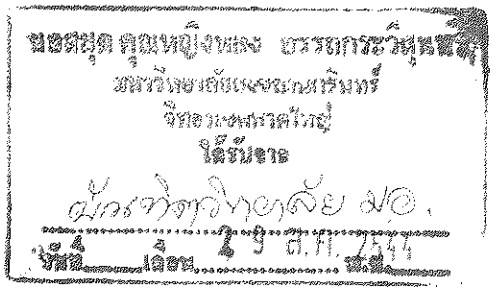

Thesis Title	Synthesis and Characterization of Ruthenium(II) with 2-(4'-*N,N*-diethylaminophenylazo)pyridine Ligands.
Author	Miss Nararak Leesakul
Major Program	Inorganic Chemistry
Academic Year	2000

ABSTRACT

The complexes of $Ru(L)_2Cl_2$ (L = dmazpy และ deazpy) were prepared from the reactions between $Ru(dmso)_4Cl_2$ complexes and 2-(4'-*N,N*-dimethyl aminophenylazo) pyridine (dmazpy, 1) and 2-(4'-*N,N*-diethylaminophenylazo)pyridine (deazpy, 2) ligands. Both of ligands are the derivatives of 2-(phenylazo)pyridine (azpy, 3). The isolated isomeric complexes from these reactions were determined to be *cis* and *trans* configurations. Results from structural determination, chemical properties and electrochemistry indicated that dmazpy and deazpy ligands are weaker π-acceptors than that of azpy. Nevertheless, dmazpy and deazpy ligands have greater σ-donor ability than azpy, and stabilize Ru(II) center better than the azpy ligand.

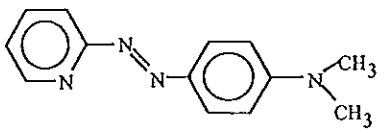

1

dmapy

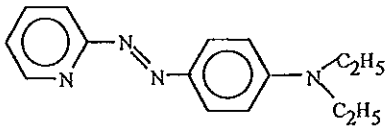

2

deazpy

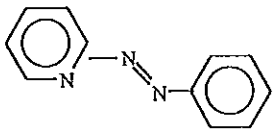

3

azpy

Acknowledgment

I would like to thank my supervisor, Dr. Kanidtha Hansongnern who provided support, helpful criticism, valuable advice, guidance and kindness throughout this thesis. The thesis cannot be completed without her support.

I am indebted to Assistant Professor Dr. Orawan Sirichote, Dr. Walailak Puetpaiboon, my co-advisors who gave their time in reviewing the text and suggested the improvement of the report. I am also grateful to Assistant Professor Dr. Adisorn Ratanaphan, the examining committee for his kind comments and correction the report.

I am certainly indebted to Assistant Professor Dr. Chaveng Pakawatchai for his advice on the Xtal program to study crystal structures.

I would like to express my gratitude to Professor Dr. Alan M. Bond, Department of Chemistry, Faculty of Science, Monash University, Australia for the great support in solving single crystal complexes and for grants of using cyclic voltammetry instruments. I also would like to extend my sincere thanks to Dr. Paul A. Keller, Department of Chemistry, University of Wollongong for his helpful in Electrospray mass spectrometry and 300 MHz ^{1}H NMR spectroscopy experiments. I am also indebted to Associate Professor Dr. Sumpan Wongnawa for the valuable comments on my thesis.

I would like to thank the Department of Chemistry, Faculty of Science, Prince of Songkla University for all necessary laboratory apparatus and chemical supplies used throughout this research.

I would like to thank Postgraduate Education and Research Program in Chemistry (PERCH) and Graduate School, Prince of Songkla University for partial support of this research.

I am especially grateful to my parents for their love and supports.

My deepest thanks is extended to Miss Sirintip Tanchatchawal, Miss Uraiwan Seateaw, Miss Sriwipa Onganusorn, my beloved friends and all Ch.432's members for their kind helps and encouragement.

Nararak Leesakul

Contents

Contents (continued)

List of Tables

List of Tables (continued)

List of Tables (continued)

List of Figures

List of Figures (continued)

List of Figures (continued)

List of Figures (continued)

Lists of Abbreviations

azpy	=	2-(phenylazo)pyridine
dmazpy	=	2-(4'-*N*,*N*-dimethylaminophenylazo)pyridine
deazpy	=	2-(4'-*N*,*N*-diethylaminophenylazo)pyridine
L	=	ligand
r, R	=	correlation coefficient
Hz	=	hertz
v / v	=	volume by volume
mins	=	minutes
Å	=	angstrom unit
°	=	degree
ppm	=	part per million
δ	=	chemical shift
nm	=	nanometer
mV/s	=	millivolt per second
V	=	Volt
A	=	Ampere
mmol	=	millimole
g	=	gram
A.R. grade	=	Analytical reagent grade
rel. abun.	=	relative abundance
λ	=	wavelength
ε	=	molar extinction coefficient
h	=	hour
mL	=	milliliter

Chapter 1

INTRODUCTION

1.1 Introduction

Ruthenium is a chemical element which has symbol Ru, atomic number 44. The element is a britten gray-white metal of low natural abundance. It is a second transition series element in the Periodic Table. The electronic configuration is [Kr] $(4d)^7(5s)^1$. The most common isotope is 102 and most common oxidation state are II, III and IV. The ruthenium metal is not oxidized by air at room temperature, but it is oxidized at high temperatures (more than 900 °C). From this property, ruthenium compounds have been used a lot of applications. The applications of ruthenium compounds such as the ruthenium tetraoxide complex (RuO_4) which is the precursor for synthesis hydrated ruthenium trichloride complex ($RuCl_3.3H_2O$) and used as an oxidant for organic compounds. The $RuCl_3.3H_2O$ complex is the most common starting material for preparation other useful ruthenium complexes (Carol, 1993). The ruthenium(II) complexes with chelating polypyridyl ligand groups, particularly, 2,2'-bipyridine (bpy) and derivatives of bpy such as $[Ru(bpy)_3]^{2+}$ and $Ru(dcb)_2X_2$ (dcb = 4,4'-$(COOH)_2$-2,2'-bipyridine and X = Cl^-, Br^-, I^-, SCN^-, H_2O) complexes, are extensively used as the most efficient and stable redox sensitizers on nanocrystalline TiO_2 solar cell for conversion light to electrical energy. (Meyer, 1997). Other application of ruthenium(II) complexes with polypyridyl ligands is the complex of $[Ru(phen)_2dppz]^{2+}$ (phen = 1,10-phenanthroline, dppz = dipyridophenazene), acting as luminescent probes in DNA. It is useful in optically probing the kind of DNA bases. However, these various applications are related to chemical properties of complexes containing different ligands.

The polypyridyl ligands such as bpy and phen are symmetric ligands which have σ−donor and π−acceptor properties. In addition, ruthenium(II) is well recognized

as a metal ion capable of entering dπ–pπ back bonding with polypyridyl ligands. This gives rise to stabilize ruthenium(II) and their complexes show interesting properties. For example, charge transfer luminescence is another property in the complex of $[Ru(bpy)_3]^{2+}$ that useful for acting as a catalyst of water photolysis (Krause and Krause, 1980).

Besides, bpy and phen ligands containing the azoimine (-N=N-C=N-) moiety are better π–acceptor toward ruthenium(II). One of this type is 2-(phenylazo)pyridine (azpy). The azpy ligand is an asymmetric ligand, and is stronger π–acidity ligand than bpy. The chemistry and application of ruthenium(II) complexes with azpy ligand have been extensively studied. The *cis*- and *trans*- isomeric complexes of $Ru(azpy)_2Cl_2$ show the in Vitro cytotoxicity activity in tumor cell lines (Aldrik *et al.*, 2000). Besides, the complexes of α–$Ru(azpy)_2(NO_3)_2$ (*cis*-$Ru(azpy)_2(NO_3)_2$) show the strong binding of DNA-model bases (Holtze *et al.*, 2000). Furthermore, $Ru(azpy)_2Cl_2$ complexes are catalysts in epoxidation reaction (Barf and Sheldon, 1995). The progress in azoimine chemistry of azpy leads to further investigation on other heterocyclic complexes,ligands such as 2-(phenylazo)imidazole (aai) in $Ru(aai)_2Cl_2$(Misra *et al.*, 1998) and 2-(phenylazo)pyrimidine (papm) in $Ru(papm)_2Cl_2$ (Santra *et al.*, 1999).

In the present work, ruthenium(II) complexes, $Ru(L)_2Cl_2$ (where L were 2-(4'-*N,N*-dimethylaminophenylazo)pyridine (dmazpy), 2-(4'-*N,N*-diethylaminophenylazo) pyridine (deazpy)) were synthesized and characterized. The dmazpy and deazpy ligands are derivatives of azpy containing electron-donating substituents, $-NR_2$ (where R = CH_3, C_2H_5 in dmazpy and deazpy, respectively). The π-accepting properties of these ligands were also investigated and compared with those in $Ru(azpy)_2Cl_2$ complexes. The chemical properties of the complexes were studied by X-ray diffraction, spectroscopic and cyclic voltammetric techniques.

It is interesting to know how the -NR_2 groups effect the chemistry of $Ru(L)_2Cl_2$. The structures of azpy, dmazpy and deazpy are shown in Figure 1.

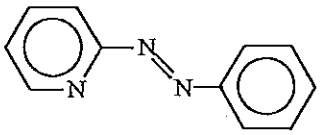

2-(phenylazopyridine) (azpy)

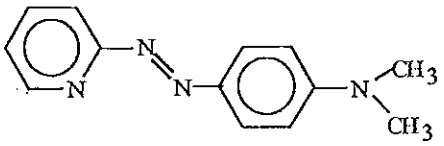

2-(4'-*N*,*N*-dimethylaminophenylazo)pyridine (dmazpy)

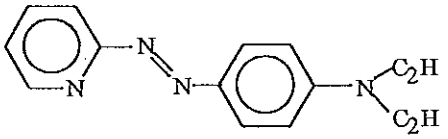

2-(4'-*N*,*N*-diethylaminophenylazo)pyridine (deazpy)

Figure 1. The structures of azpy, dmazpy and deazpy ligands.

From the structures, dmazpy and deazpy are asymmetric ligands. In priciple, the six coordination of RuL_2Cl_2 (L = dmazpy and deazpy) complexes give five possible geometrical isomers (Figure 2) similar to $Ru(azpy)_2Cl_2$ complexes.

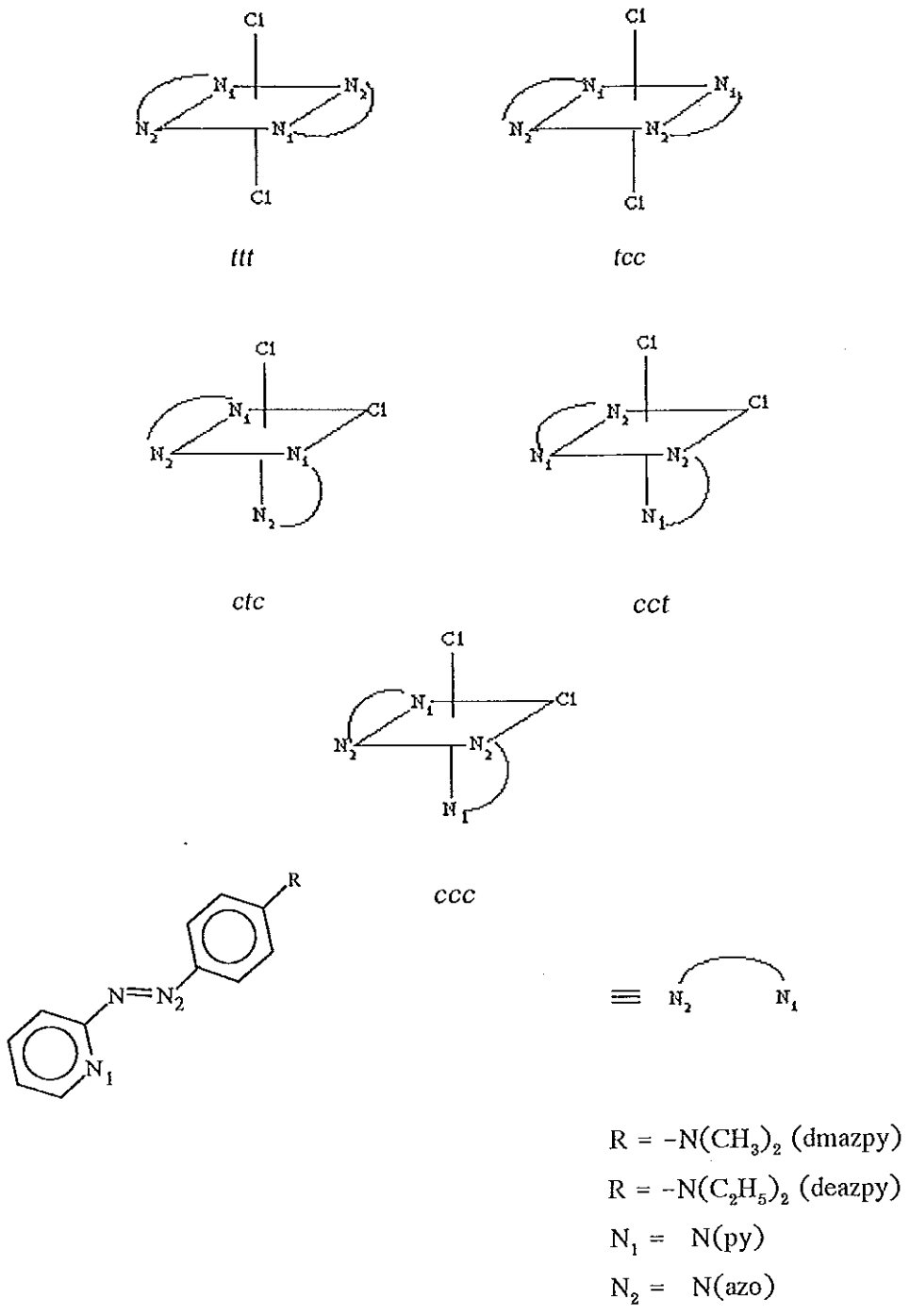

Figure 2. Five possible isomers of RuL_2Cl_2 (L = dmazpy and deazpy) complexes.

The structures of possible isomers are described in order of coordination pairs as Cl, N(pyridine : N_1) and N(azo : N_2). The two isomers of each complex are obtained from the experiments and established to *trans-cis-cis (tcc)* and *cis-trans-cis (ctc)* configurations. The structures of *tcc*-Ru(dmazpy)$_2$Cl$_2$, *tcc*-Ru(deazpy)$_2$Cl$_2$ and *ctc*-Ru-(dmazpy)$_2$Cl$_2$ complexes have been confirmed by X-ray crystallography. Eventhough the single crystal of the *ctc*-Ru(deazpy)$_2$Cl$_2$ isomer is not available, but it can be confirmed by spectroscopic techniques. Whereas, three isomers of Ru(azpy)$_2$Cl$_2$ complexes, which are *trans-cis-cis (tcc)*, *cis-trans-cis (ctc)* and *cis-cis-cis (ccc)* complexes, were isolated (Krause and Krause, 1980). The isomeric complex of *ccc*-Ru (L)$_2$Cl$_2$ (L = dmazpy and deazpy) are not obtained. However, the isolated complexes have interesting chemical properties and show different spectroscopic results between *cis* and *trans* configurations.

1.2 Literature reviews

Evans *et al.*, (1973) studied of dichlorotetrakis (dimethylsulfoxide)ruthenium (II), Ru(dmso)$_4$Cl$_2$ which are common precursors to synthesize other ruthenium(II) complexes. Ru(dmso)$_4$Cl$_2$ was characterized by infrared and NMR techniques. Results indicated that there were mixed sulphur and oxygen coordination sites.

Krause and Krause, (1980) studied of azpy ligands and three isomeric complexes of Ru(azpy)$_2$Cl$_2$. The complexes of Ru(azpy)$_2$Cl$_2$ were synthesized from both Ru(dmso)$_4$Cl$_2$ and RuCl$_3$.3H$_2$O complexes and the different isomers were obtained. These complexes were characterized by infrared spectroscopy, ^{13}C NMR spectroscopy, UV-Vis absorption spectroscopy and cyclic voltammetry.

Krause and Krause, (1984) synthesized and characterized the complexes of Ru $(Naz)_2Cl_2$ (Naz = 2-((4'-nitrophenyl)azo)pyridine by infrared spectroscopic, UV-Vis absorption spectroscopic and Differential pulse voltammetric techniques. In comparison with $Ru(azpy)_2Cl_2$ complexes, the Naz ligand can stabilize ruthenium(II) greater than the azpy ligand. This was due to the inductive effect of the nitro group in Naz ligands as it is stronger π-acceptor properties than that in azpy complexes. The supporting data were obtained by UV-Vis absorption, infrared spectroscopic and electrochemical techniques. The UV-Vis absorption spectroscopic data of Naz complexes showed the bathochromic shifted MLCT transition from the azpy complexes. For electrochemical data, the Ru(II/III) couple in Naz complexes occurred at higher potentials than the azpy complexes.

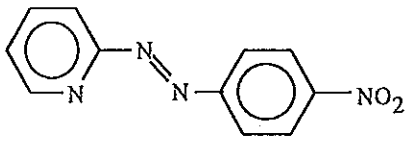

2-((4'-nitrophenyl)azo)pyridine

Misra, *et al.*, (1998) studied new azoimidazole ligands (L) which belong to the class of 1-methyl-2-(arylazo)imidazoles and 1-benzyl-2-(arylazo)imidazoles (R= H, CH_3, OCH_3, Cl, NO_2) as shown below. The reactions between $RuCl_3.3H_2O$ with these ligands in ethanol afforded RuL_2Cl_2 complexes. They reported the synthesis, spectra, redox properties and single crystal X-ray structures of two isomers of ruthenium(II) complexes with these ligands. These azoimidazole ligands are better π-acceptor ligands than bpy and phen but weaker than azpy. Furthermore, the properties of ruthenium-imidazole complexes are of interest for their antitumor activities.

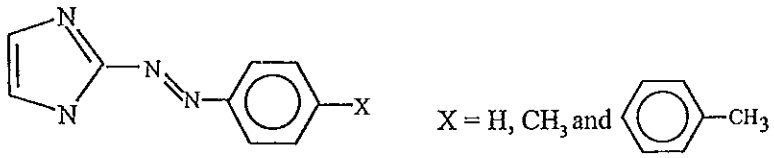

1-methyl-2-(arylazo)imidazoles

Santra *et al.*, (1999) synthesized and isolated three isomers of Ru-$(aapm)_2Cl_2$ (aapm = 2-(arylazo)pyrimidine) complexes. They were determined as *trans-cis-cis (tcc), cis-trans-cis (ctc)* and *cis-cis-cis (ccc)* configurations with refered to the order of coordination pairs as Cl, N(pyrimidine), N(azo). The isomers of *tcc* and *ccc* were confirmed by X-ray crystallography. Both of these structures, the Ru-N(azo) distances were shorter than Ru-N(pyrimidine) distances indicating stronger bonding of the former and the $Ru(aapm)_2Cl_2$ π-interaction was localized in the Ru-N(azo) fragment. The structure of all isomers were studied by infrared and ^{1}H-NMR spectroscopy. In addition, the cyclic voltammetric data showed the Ru(III)/Ru(II) couple at higher potential than those in $Ru(bpy)_2Cl_2$, $Ru(azpy)_2Cl_2$ and $Ru(aai)_2Cl_2$ (aai = 2- aryl azoimidazole) complexes. Then the order of the π-acidity of ligands can be arranged as; bpy < azoimidazole < azopyrimidine.

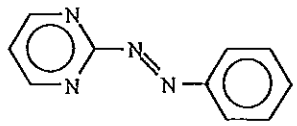

2-(arylazo)pyrimidine

Velders *et al.*, (2000) investigated the three isomeric of $Ru(azpy)_2Cl_2$ complexes (*ctc*-Cl, *ccc*-Cl, *tcc*-Cl) which showed different in Vitro cytroxicity activity. The *ctc*-$Ru(azpy)_2Cl_2$ isomer showed high cytotoxicty against a series of tumor cell lines while the *ccc*-Cl and the *tcc*-Cl showed low to moderate cytotoxicity. In addition, the structure of *tcc*-Cl isomer was confirmed by a single crystal X-ray diffraction. The *tcc*-Cl isomer has two Cl atoms in trans configuration, but the pyridines and azo groups are in *cis* geometry. Furthermore, the binding of DNA bases with the *ctc*-$Ru(azpy)_2Cl_2$ was studied and compared with the related complexes such as *cis*-$Ru(bpy)_2Cl_2$. The binding of the *ctc*-Cl isomer with guanine and purine bases are sterically less hindered

than that in *cis*-$Ru(bpy)_2Cl_2$ complexes therefore, the *ctc* isomer was found to show high cytotoxicity against a series of tumor-cell lines.

Crutchley and Lever, (1982) reported the synthesis of $Ru(bpy)_3Cl_3.3.5H_2O$, $Ru(bpz)_3.1.5(CH_3)_2CO$, $[Ru(bpz)_2(CH_3CN)(Cl)][PF_6].1/2H_2O$, $Ru(bpz)_2Cl_2.H_2O$, $Ru(bpy)_2Cl_2$, $Mo(CO)_4bpz$ and $W(CO)_4bpz$ (bpz = 2,2'-bipyrazine, bpy = 2,2'-bipyridine) complexes. These complexes were characterized by spectroscopic and electrochemical methods. The electrochemistry and the photoanation of bipyrazyl and bipyridyl metal complexes were carried out. Their purpose was to develop the photosensitizer in solar energy conversion. The results showed that bipyrazyl was not a greater π−acceptor than bipyridyl. The bipyridyl ligand was the strong σ−donor, which cause an enhancement of π−back donation with π−donor metals.

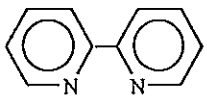

2,2'-bipyridine (bpy)

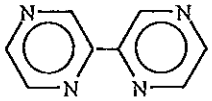

2,2'-bipyrazine (bpz)

Goswami *et al.*, (1981) studied two types of ruthenium(II) complexes, RuX_2L_2 and $[Ru(bpy)_2L](ClO_4)_2$ (X = Cl, Br, I ; L = 2-(phenylazo)pyridine (azpy) or 2-(m-tolylazo)pyridine (tap) ; 2,2'-bipyridine(bpy)). These complexes were characterized by infrared and UV-Vis absorption spectroscopy. In addition, the ^1H NMR spectrum of the $Ru(tap)_2X_2$ showed methyl signal in $CDCl_3$ solvent. The redox activities were done by cyclic voltammetric technique in acetonitrile and dichloromethane solvents. The RuX_2L_2 complexes showed Ru(II/III) couple at higher potential than that of *cis*-$Ru(bpy)_2Cl_2$ and several other dichlororuthenium (II) species. The azopyridine ligand can stabilize (with respect to oxidation potential) ruthenium(II) better than bpy.

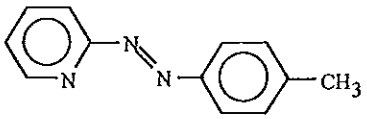

2-(m-tolylazo)pyridine (tap)

Seal and Ray, (1984) investigated the structures of two isomers of Ru-$(azpy)_2Cl_2$ complex were *cis-trans-cis* (*ctc*) and *cis-cis-cis* (*ccc*) configuration (refered to Cl, N (pyridine) and N(azo) atoms respectively). Refinement parameters of the *ctc*-Ru$(azpy)_2$ Cl_2 complex (C_2 symmetry) were R=0.051 and R_w = 0.070. Whereas, the refinement parameters of the *ccc*-Ru$(azpy)_2Cl_2$ complex (C_1 symmetry) were 0.054 and R_w = 0.074. Both complexes are distorted octahedral. The angles of Cl-Ru-Cl are nearly 90°. However, N(py)-Ru-N(azo) angles were found ca. 76°. Furthermore, Ru-N(azo) distances were shorter than Ru-N(py) distance due to powerful π-backbonding of the azo function.

Panneerselvam *et al.*, (2000) reported the crystal structure of the [protonated 2-(phenylazo)pyridine and protonated2-(4-hydroxyphenylazo)pyridine (3:1)] tetrafluoroborate compound. The results from X-ray data indicated that the protonation occurs at N(azo) atom and it was more strongly basic than N(pyridine). The azpy compound was normally liquid at ambient temperature but this crystal structure was stabilized by intramolecular H bonding, N-H-N and van der Waals force.

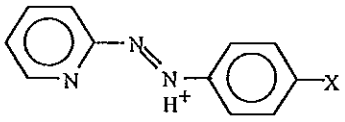

Protonated azpy X = H (3 times) and OH^- (1 time)

Bao *et al.*, (1988) established the method for conversion the *tcc*-Ru$(azpy)_2Cl_2$ (or γ form) to the *ctc*-Ru$(azpy)_2Cl_2$ (*ctc*, α form) and the *trans-γ*-Ru- $(azpy)_2Cl_2$ to the *ctc*-Ru$(azpy)_2Cl_2$ (*ccc*, β form) isomers. The conversion can be done by using hydroxide ion as catalyst in the mixture of water-ethanol and water-dichloromethane which gave α and β isomer respectively.

Holtze *et al.*, (2000) reported the synthesis and characterization of the α-[Ru (azpy)$_2$(NO$_3$)$_2$] complex. The structure of α-[Ru(azpy)$_2$(NO$_3$)$_2$] were determined by X-ray crystallography. The binding of the DNA-model bases 9-ethylguanine and guanosine also has been studied and compared with bis-(bipyridyl) ruthenium(II) complex. The binding DNA complexes have been identified by ^{1}H and 2D NMR spectroscopy.

Irving *et al.*, (1953) showed the stability constants of some metal chelates of 2-(4'-*N,N*-dimethylaminophenylazo)pyridine (dmazpy). The dmazpy can act as an indicator in measuring other metal-complex stability constants. Stability constants for 1:1 chelated of dmazpy with metals at 25°C, pH 6 and ionic strength 0.15 fall in order Cu > Hg > Ni > Co > Zn > Mn > Ca, Mg. They also described the protonated forms in different pH.

Sadler and Bard, (1968) reviewed the electrochemical reduction of aromatic azo compounds in dimethylformamide solutions. It was studied by cyclic voltammetric and other electrochemical techniques. It was also studied the UV-Vis absorption spectroscopy. The electrochemical reductions of these compounds were generally similar to that of aromatic hydrocarbons in aprotic media. The reduction couple occured two steps which one electron transfer.

1.3 Objectives

1. To prepare the Ru(L)$_2$Cl$_2$ (L = dmazpy and deazpy) complexes
2. To characterize and to study of chemistry and electrochemistry of their complexes.
3. To compare the π-acceptor property of azpy, dmazpy and deazpy ligands.
4. To demonstrate the effect of electron-donating groups to chemical properties of Ru(II) complexes.

Chapter 2

METHOD OF STUDY

2.1 Chemicals

2.1.1 Materials from Fluka AG, Switzerland

Ruthenium(III)chloride, $RuCl_3$, A.R grade

2-aminopyridine, C_5H_5N, A.R grade

2.2.2 Materials from Lab-Scan

Dimethyl sulphoxide, DMSO, A.R grade

acetonitrile, CH_3CN, A.R grade

2.2.3 Materials from Carlo Erba

Chloroform, $CHCl_3$, A.R grade

N,N-dimethylformamide, A.R grade

Sodium hydroxide, NaOH, A.R grade

2.2.4 Materials from Merck

Acetone, CH_3COCH_3, A.R grade

Dichloromethane, CH_2Cl_2, A.R grade

Ethanol, C_2H_5OH, A.R grade

Methanol, CH_3OH, A.R grade

2.2.5 Materials from Aldrich Chemical Company, Inc.

N,N-dimethyl-1,4-nitrosoaniline, A.R grade

N,N-diethyl-1,4-nitrosoaniline, A.R grade

Nitrosobenzene, A.R grade

2.2.6 The solvents, dichloromethane, hexane and ethyl acetate for column chromatography were purified by distillation and collected from their boiling points.

2.2 Instruments

2.2.1 X-ray diffraction data were collected on a CCD X-ray Diffractometer with TeXsan program.

2.2.2 UV-Vis absorption spectra were monitored in the 200-820 nm range by Hewlett Packard 8452A diode array spectrophotometer.

2.2.3 Electrospray mass spectra were recorded on VG Quattro triple quadrupole Mass Spectrometer.

2.2.4 Infrared spectra were recorded with either Perkin Elmer Spectrum GX FTIR-spectrophotometer (4,000-400 cm^{-1}) or Perkin Elmer 783 Infrared Spectrophotometer (400-200 cm^{-1}) from KBr pellets.

2.2.5 Proton nuclear magnetic resonance spectra (^1H NMR) were recorded on a Varian UNITY SNOVA 500 MHz FTNMR spectrometer and 300 MHz Varian UNITY NMR 165 FT-NMR Spectrometer at ambient temperature. Tetramethylsilane (TMS) at 0.00 ppm. The residual protons of $CDCl_3$ at 7.25 ppm were used as internal reference.

2.2.6 Electrochemical measurements were carried out using cyclic voltammetric technique. The measurements were obtained from Cypress system version 5.5 computer controlled electroanalysis system. A platinum disk was used as the working electrode. A platinum gauze was the counter electrode and $AgNO_3/Ag$ was used as the reference electrode. Ferrocene was added as an internal reference to the electrochemical cell. The supporting electrolyte was tetrabutylammonium hexafluorophosphate (TBAH) in acetonitrile solvent.

2.2.7 The measurement of melting points of all compounds were used the Thomas Hoover Capillary melting point apparatus which can measure in the range 30-300 °C.

2.3 Synthesis of ligands.

2.3.1 Synthesis of 2-(phenylazo)pyridine ligand (azpy).

The synthesis of 2-(phenylazo)pyridine ligands was prepared by modified literature method (Krause and Krause, 1980). 2-aminopyridine (3.88 g, 41.2 mmol) reacted with nitrosobenzene (4.03 g, 37.6 mmol) in 13.5 mL NaOH (25 M) and 2 mL benzene with stirring. The solution was heated on the steam bath for 45 mins. The mixture was extracted with 5 x 50 mL of benzene. The mixture solution was evaporated to have a small volume. Purification was carried out by column chromatography technique on silica and the mixed solution of hexane: ethyl acetate (9:2) was used to be the mobile solvent. The isolated product was orange liquid (28.0 % yield, mp 32-34 °C).

2.3.2 Synthesis of 2-(4'-*N,N*-dimethylaminophenylazo)pyridine ligand (dmazpy).

The 2-(4'-*N,N*-dimethylaminophenylazo)pyridine ligand was obtained from the reaction of 2-aminopyrimidine and *N,N*-dimethyl-1,4-nitrosoaniline. The *N,N*-dimethyl-1,4-nitrosoaniline (1.502 g, 0.01 mol) was slightly added to the warm solution of 2-aminopyridine (0.940 g, 0.01 mol) at 70°C in the presence of 11.6 mL 25 M NaOH in toluene stirring was continued and 4 mL of acetonitrile was also added. After this period the mixture was carried out under refluxing conditions for 9 hours. The expected dark red ligands might be soluble in the toluene portion. Reaction mixture was filtered and extracted with 50 mL toluene for 5 times. The mixture solution was evaporated to

be less small volume. Purification was carried out by column chromatography on silica column. The red ligands were eluted with 9:1 hexane : ethyl acetate (yield 28.0%, mp 80 °C)

2.3.3 Synthesis of 2-(4'-*N,N*-diethylaminophenylazo)pyridine ligand (deazpy).

The 2-(4'-*N,N*-diethylaminophenylazo)pyridine ligands was synthesized by using the same procedure as *N,N*-dimethyl-2-(phenylazo)pyridine ligand. But *N,N*-diethylnitrosoaniline (1.602 g, 0.01 mol) was replaced the *N,N*-dimethylnitroso aniline and the reaction gave 12.7 % yeild with mp 80 °C.

2.4 Synthesis of complexes.

2.4.1 Synthesis of $Ru(dmso)_4Cl_2$ complexes

The $Ru(dmso)_4Cl_2$ complex was prepared according to the literature method. (Evan *et al.*, 1973). Ruthenium trichloride trihydrate, $RuCl_3.3H_2O$ (0.2 g, 0.8 mmol) was refluxed in dimethylsulfoxide (1 mL, 3.2 mmol) for 5 mins. The solution was cooled to room temperature and 4 mL of acetone was added. The reaction mixture was stored in a desiccator for 7-10 days. The yellow to orange crystals was filtered and washed with diethyl ether. The yields were 72.0 %. The decomposed temperature is 120 °C.

2.4.2 Synthesis of *trans*-$Ru(azpy)_2Cl_2$ complexes

$Ru(dmso)_4Cl_2$ complex (0.024 g, 0.06 mmol) and azpy ligands (0.019 g, 0.13 mmol) were refluxed in chloroform (15 mL) for 72 hours. The mixture was filtered and evaporated to dryness. The solution was dissolved in small amount of distilled dichloromethane. Purification the complexes by using column chromatography on silica

and the mixed solvents as dichloromethane and ethyl acetate (9:1) were eluting solvent. The green band of the *trans*-$Ru(azpy)_2Cl_2$ complexes were isolated. The green complexes were evaporated and precipitated with dichloromethane (28.6 %).

2.4.3 Synthesis of *trans*-$Ru(dmazpy)_2Cl_2$ complex

$Ru(dmso)_4Cl_2$ complex (0.024 g, 0.05 mmol) and deazpy ligands (0.026 g, 0.13 mmol) were refluxed in chloroform (15 mL) for 72 h. The solution became orange to dark purple consequently. The complex solution was filtered and evaporated to dryness. The obtained solid was purified by using column chromatography on silica gel. The green band of *trans*-$Ru(dmazpy)_2Cl_2$ complex were isolated from toluene and acetonitrile (2:1) mixture. The yield of *trans*-$Ru(dmazpy)_2Cl_2$ complexes was 0.016 g (52.4 %). Crystals of *trans*-$Ru(dmazpy)_2Cl_2$ complexes were obtained from a dichloromethane-ethanol and 0.1 M HCl mixture (2:1:0.5 v/v).

2.4.4 Synthesis of *cis*-$Ru(dmazpy)_2Cl_2$ complex

This complex was prepared similarly to *trans*-$Ru(dmazpy)_2Cl_2$ complex. The purple band was isolated chromatography. The *cis*-$Ru(dmazpy)_2Cl_2$ complexes were recrystallized from toluene and dichloromethane mixture (4:1 v/v) at room temperature for 4 days. The yield was 0.011 g (38.3 %).

2.4.5 Synthesis of *trans*-$Ru(deazpy)_2Cl_2$ complex

The synthesis was prepared similarly to *trans*-$Ru(dmazpy)_2Cl_2$ complex. The dmazpy ligands were replaced by an equivalent amount of deazpy (0.030 g, 0.13 mmol). The yield was 54.0 %.

2.4.6 Synthesis of *cis*-$Ru(deazpy)_2Cl_2$ complex

The synthesis was prepared similarly to *trans*-$Ru(dmazpy)_2Cl_2$ complex. The dmazpy ligands was replaced by an equivalent amount of deazpy and the purple band was isolated chromatography. The yield was 30.8 %.

2.5 Methods for determination structures

2.5.1 Single crystal X-ray crystallography

X-ray crystallography is the most precise and comfortable technique for determination the actual structures. The principal of this technique is the radiation of X-ray through single crystal with the most intense of K line. Some of X-ray which interacts with the crystal are transmitted and some of them are diffracted with the angle of 2θ. That diffracted X-ray enter to the detector. In this work, the CCD is used as detector. The TeXan programs is used for solving crystal data and the Xtal program was used to study the crystal structures.

2.5.2 Electrospray mass spectrometry (ES-MS)

ES-MS is a new technique which allows pre-existing ions to be very gently transferred from solution to gas phase with minimal fragmentation, followed by conventional mass analysis. The ES technique has been developed to study inorganic and organometallic structures (Colton, 1995). ES-MS technique is used to confirm molecular structure by consideration of m/z values. All peaks in the mass spectra will be identified by the most intense peak in the isotope mass distribution.

2.5.3 Proton Nuclear Magnetic Resonance Spectrometry (^{1}H-NMR)

^{1}H-NMR is another technique to identify structures of compounds or complexes. It is related to molecular arrangement. The chemical shifts and spin-spin coupling

constants from nuclear magnetic resonance spectra are sensitive to electron density at the nucleus which depend on the specific to more electronegative atoms. However, NMR parameters are also affected by other features.

2.5.4 Infrared spectrometry (IR)

IR is an useful technique to determine the functional groups which composed in compounds. The compounds have to absorb the Infrared frequencies range. For this research complexes absorb in the IR medium region (4,000-200 cm^{-1}) for molecular vibration. The absorbed IR molecules are IR active which give the stretching or bending modes of bonding in molecules at different frequencies.

2.5.5 UV-Visible absorption spectrometry (UV-Vis)

The chromophores in complex molecule can absorb energy in the UV-Visible range and consequently change electronic transitions. The correlated electrons are all valence electrons, bonding orbital and non-bonding electrons which stay in different energy levels. The electrons are excited and shifted to higher energy level followed by selection rules. However, the UV-Vis absorption is a roughly technique for characterization complexes but it is very useful for the describing colored. Besides, it is the comfortable technique in qualitative and quantitative analysis.

2.5.6 Cyclic voltammetry (CV)

The cyclic voltammetry is an electrochemical method which leads to the knowledge of redox phenomena. It can be used to investigate the rates and mechanisms of metal-charge transfer reactions, kinetic studies, and so on. It shows current-potential curve which is called cyclic voltammogram. In general, a typical voltammetric experiment utilizes three types of electrodes (Eklund and Bond, 1998).

- the working electrode

this is the electrode at which the reaction of interest takes place, e.g. the simple one-electron oxidation-reduction processes are given below

$$A \rightleftharpoons A^{+} + e^{-} \quad \text{(oxidation)}$$

$$B + e^{-} \rightleftharpoons B^{-} \quad \text{(reduction)}$$

These electrodes are typically made an inert and electrically conducting material. The common electrodes are made of Platinum and some forms of carbon (i.e. glassy carbon or graphite).

- the reference electrode

This electrode provides a fixed reference couple against the potential of working electrode measured, e.g. the Ag/Ag^{+} electrode which the potentials are accurately known relative to the standard hydrogen electrode (SHE).

- the counter/auxillary electrode

An auxillary electrode consists of a large surface area piece of platinum (wire or gauze) or carbon (disk or rod) placed directly into the test solution. Since the current flows through the counter electrode, it must have a sufficiently large surface area relative to working electrode to prevent limitation of current flowing in the total circuit. The current measured in a voltammetric experiment flows between the working and counter electrode.

Chapter 3

RESULTS

The results in this investigation were divided into 3 sections as followed :

3.1 The studies on synthesis and characterization of dmazpy and deazpy Ligands.

3.2 The studies on synthesis and characterization of $Ru(dmso)_4Cl_2$ and $Ru(L)_2Cl_2$ (L = dmazpy and deazpy) complexes.

3.3 Electrochemistry of ligands and complexes.

3.1 Synthesis and characterization of dmazpy and deazpy ligands.

3.1.1 Synthesis of dmazpy and deazpy Ligands.

2-(4'-*N,N*-dimethylaminophenylazo)pyridine (dmazpy) and 2-(4'-*N,N*-diethyl aminophenylazo)pyridine (deazpy) ligands are synthesized by coupling of 4-*N,N*-dimethyl-1,4-nitrosoaniline or *N,N*-diethyl-1,4-nitrosoaniline with 2-aminopyridine respectively in separated mixture of 25 M NaOH and toluene. Purification was done by column chromatography which described previously. The reaction are followed by equation (1) and (2).

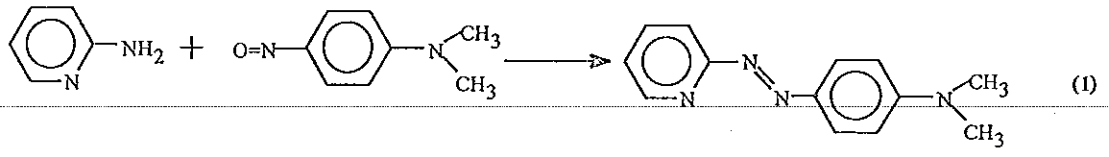

(1)

2-aminopyridine *N,N*-dimethyl-1,4-nitrosoaniline 2-(4'-*N,N*-dimethylaminophenylazo)pyridine (dmazpy)

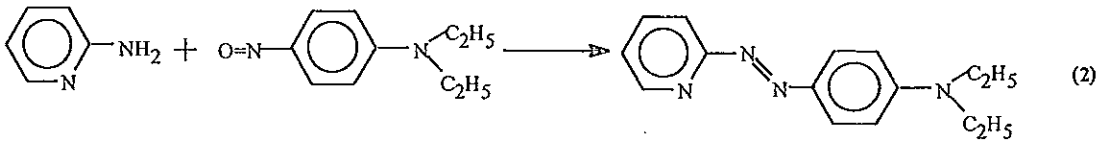

(2)

2-aminopyridine *N,N*-diethyl-1,4-nitrosoaniline 2-(4'-*N,N*-diethylaminophenylazo)pyridine (deazpy)

Ligands were prepared in small yields because of many side reactions. The yield of dmazpy and deazpy ligand were 28 % and 12.7 %, respectively. The solubilities of dmazpy and deazpy were summarized in Table 1.

Table 1. Solubility of dmazpy and deazpy ligands.

solvents	solubility
hexane	+++
toluene	+++
dichloromethane	+++
chloroform	+++
ethyl acetate	+++
acetone	+++
acetonitrile	+++
dimethylformamide	+++
dimethylsulfoxide	+++
ethanol	+++
methanol	+++
*water	+++
*0.1 M HCl	+++
*0.1 M NaOH	+++

The symbol of solubility, +++ represents the completely soluble of ligand 0.0030 g in 10 mL of solvents. The * represents the changing of ligand's color in a solvent.

Those ligands are soluble in almost solvents because their structures also have organic parts soluble in organic solvents and N atoms which can make H-bonding with water molecules. However, the orange ligands have immediately changed color into deep pink when they dissolved in acid due to the protonation at N atoms (Klotz and Wing, 1953).

3.1.2 Characterization of dmazpy and deazpy ligands.

The structures of dmazpy and deazpy were determined by using these techniques

- Electrospray mass spectrometry
- Proton Nuclear Magnetic Resonance spectrometry
- Infrared spectrometry
- UV-Visible absorption spectrophotometry

3.1.2.1 Electrospray mass spectrometric data of dmazpy and deazpy ligands

The electrospray mass spectra and the electrospray mass spectroscopic data of dmazpy ligands are displayed in Figure 3 and detail in Table 2 whereas, the deazpy are shown in Figure 4 and details in Table 3. From the data, the maximum peaks in an isotropic mass distribution are exactly closed to molecular weight of ligands. Therefore, it can confirm the ligand structures.

Table 2. Electrospray mass spectroscopic data of dmazpy ligand.

m/z	stoichiometry	equivalent species	rel. abun.
227.1	$[dmazpy+H]^+$	$[M+H]^+$	100

MW of the dmazpy ligand = 226.2 = M

Table 3. Electrospray mass spectrometric data of deazpy ligand.

m/z	stoichiometry	equivalent species	rel. abun.
255.3	$[deazpy+H]^+$	$[M+H]^+$	100
256.2	$[deazpy+2H]^+$	$[M+2H]^+$	37

MW of the deazpy ligand = 254.2 = M

Both of dmazpy and deazpy ligands show the parent peaks which are one protonation at *m/z* 227.1 and 255.3 for dmazpy and deazpy, respectively.

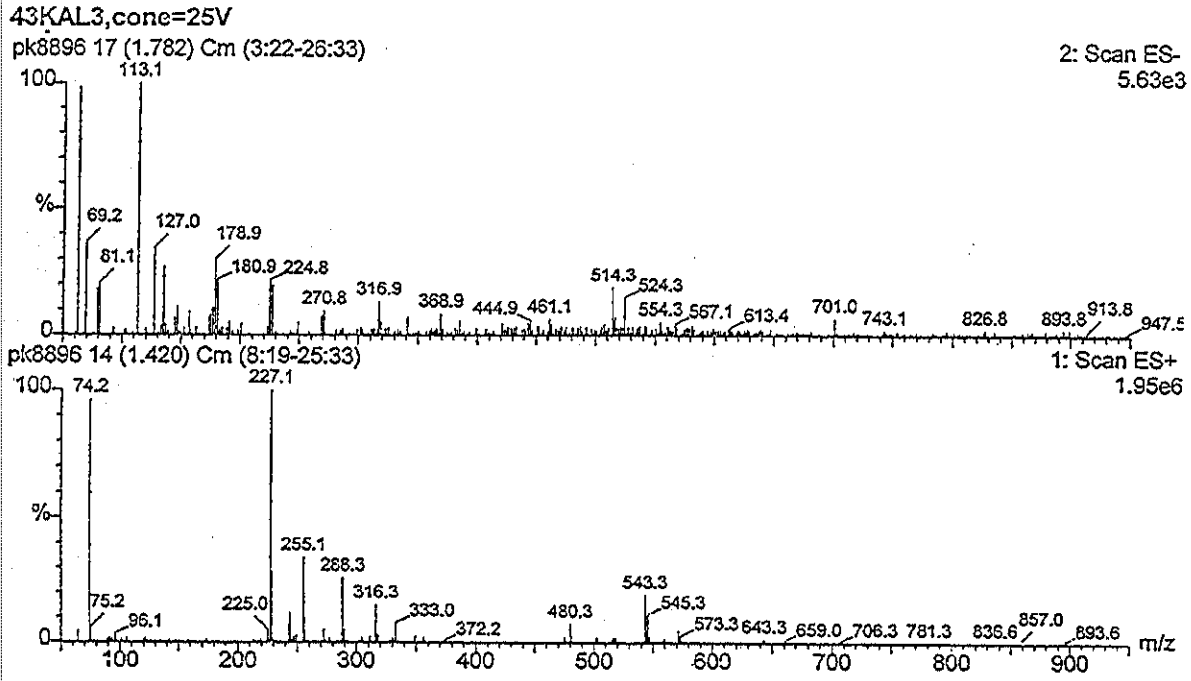

Figure 3. Electrospray mass spectrum of 2-(4'-*N*,*N*-dimethylaminophenylazo)pyridine

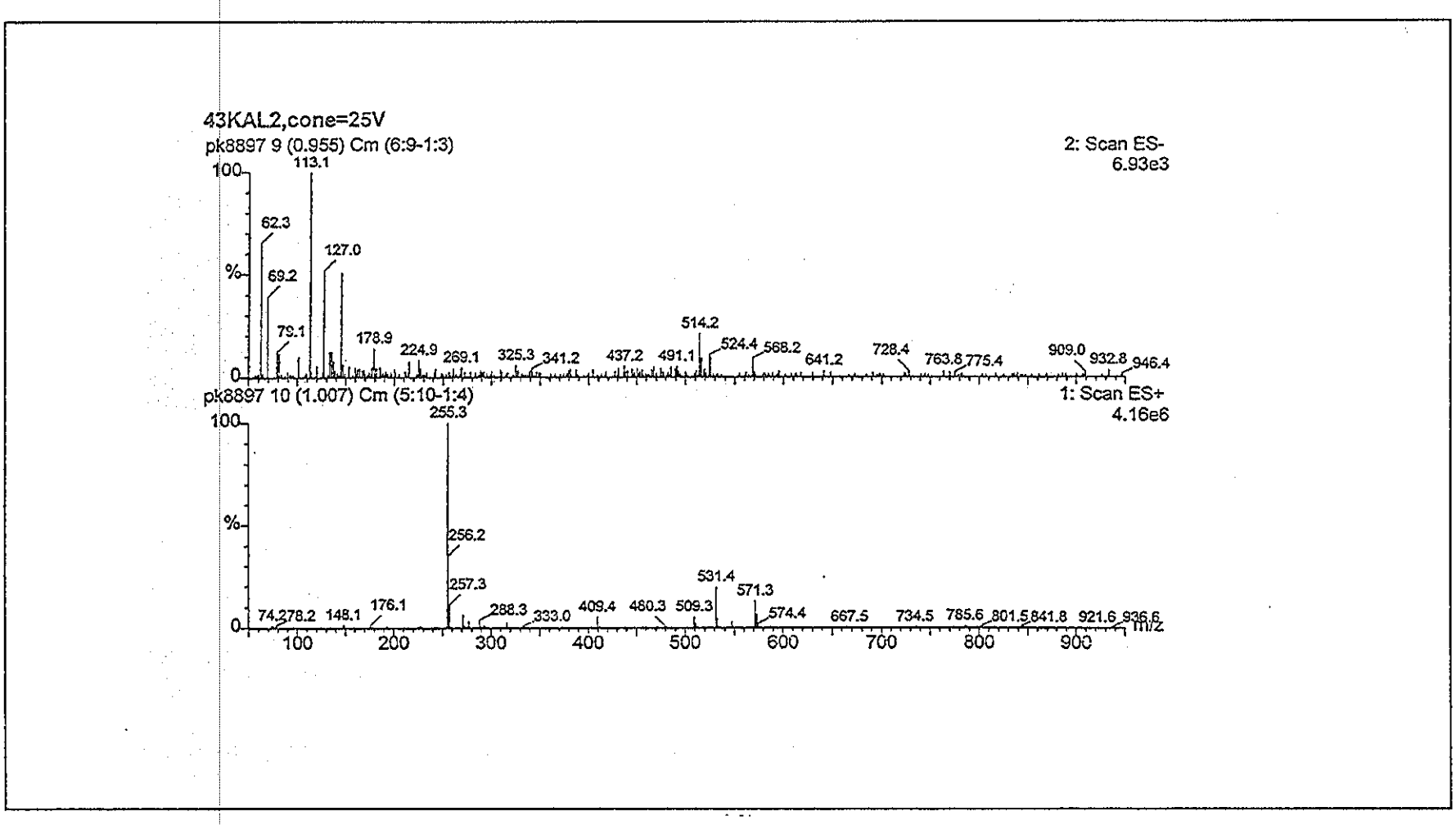

Figure 4. Electrospray mass spectrum of 2-(4'-*N,N*-diethylaminophenylazo)pyridine

3.1.2.2 ^{1}H NMR spectroscopic results of dmazpy and deazpy ligands

The chemical shifts (δ, ppm) and J-coupling (Hz) of free dmazpy and deazpy (Table 4 and 5) are reported in part per million (ppm) downfield from tetramethylsilane (TMS, $(CH_3)_4Si$) solution. The ^{1}H NMR spectra are displayed in Figure 6 and 7. TMS was set at 0 ppm and was used as reference for $CDCl_3$ solutions. The types of protons in dmazpy are divided into 7 groups but 8 groups for deazpy as shown in Figure 5.

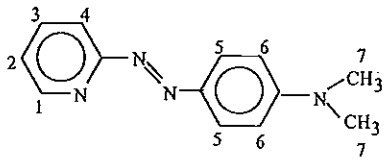

dmazpy

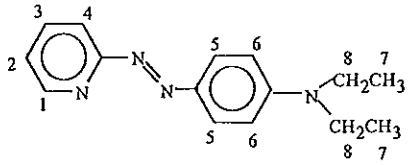

deazpy

Figure 5. Structure of dmazpy and deazpy ligands with proton numbering systems.

Table 4. ^{1}H NMR data for dmazpy

H-position	J-coupling (Hz)	δ (ppm)	amounts of H	peak
1	7.5	8.678	1	dd
4	9	8.012	1	dd
2	7.8,7.5	7.828	1	dt
5	8.5	7.762	2	d
3	7,7	7.286	1	dt
6	9	6.754	2	d
7	-	3.100	6	s

d = doublet dd = doublet of doublet dt = doublet of triplet s = singlet

Table 5. ^{1}H NMR data for deazpy

H-position	J-coupling (Hz)	δ (ppm)	amounts of H	peak
1	7.5	8.668	1	dd
4	9	7.987	1	dd
2	8,7.5	7.818	1	dt
5	8	7.751	2	d
3	7,7	7.271	1	dt
6	9	6.724	2	d
8	7.5,7,7	3.464	4	q
7	7,7.5	1.239	6	t

d = doublet dd = doublet of doublet dt = doublet of triplet

t = triplet q = quatet

The ^{1}H NMR results are used to support the structures of both ligands. The results of ^{1}H NMR of dmazpy and deazpy are very similar to each other. The chemical shift of corresponding protons in both ligands resonate at sligthly different values. The detail of each signal can be described below.

The proton-1 is on pyridine located next to pyridine nitrogen atom which gives signal at most downfield. The proton signal is splited by the proton-2 (J = 7.5 Hz) and by the proton-3 (J = 1.5 Hz). Therefore, the signal is doublet of doublet (dd) peak.

The proton-2 located next to proton-1. The signal of this proton is doublet of triplet. The spliting of triplet peaks (J = 7.5-8 Hz) is observed for coupling with proton-1 and proton-3. Then each of triplet peak is splited to doublet peaks (J= 1.5 Hz) from long range coupling with proton-4.

The proton-3 is the proton which is opposite to pyridine nitrogen. The proton is less effected from nitrogen atom than that of the proton-2 thus the chemical shift value is less than that of proton-2. The signal of this proton is also doublet of triplet peaks. It is splited by the proton-2 and 4 (J = 7 Hz) and by the proton-1 (J = 1.5 Hz).

The proton-4 located next to the proton-3 and it is effected from nitrogen of azo function. The signals might be at downfield more than proton-2,3. It occurs at upfield than that in proton-1. The signal is doublet of doublet peaks. It is splited by proton-3 (9 Hz) and by the proton-2 (J = 1.5 Hz).

The proton-5 are two equivalent protons on phenyl ring located closed to azo nitrogen. The rotation of phenyl ring leads the proton-5 signal showed at upfield than proton-4. The proton-5 interacts with proton 6 and give the doublet peaks with J-coupling 8-8.5 Hz.

The proton-6 are two equivalent protons located next to the proton-5. The signal is also doublet of doublet peaks. The signal is splited by the proton-5 (J = 9 Hz).

The proton-7 are the methyl protons ($-CH_3$). In case of dmazpy, the signal is singlet peak of 6 protons whereas, deazpy shows triplet peaks with 6 protons. The signal in deazpy is due to the methylene ($-CH_2-$) protons with J-coupling 7,7.5 Hz .

The proton-8 are the methylene protons of deazpy ligand. The signal of this proton is quatet peaks from the interaction with methyl proton (J-coupling 7, 7.5, 7 Hz).

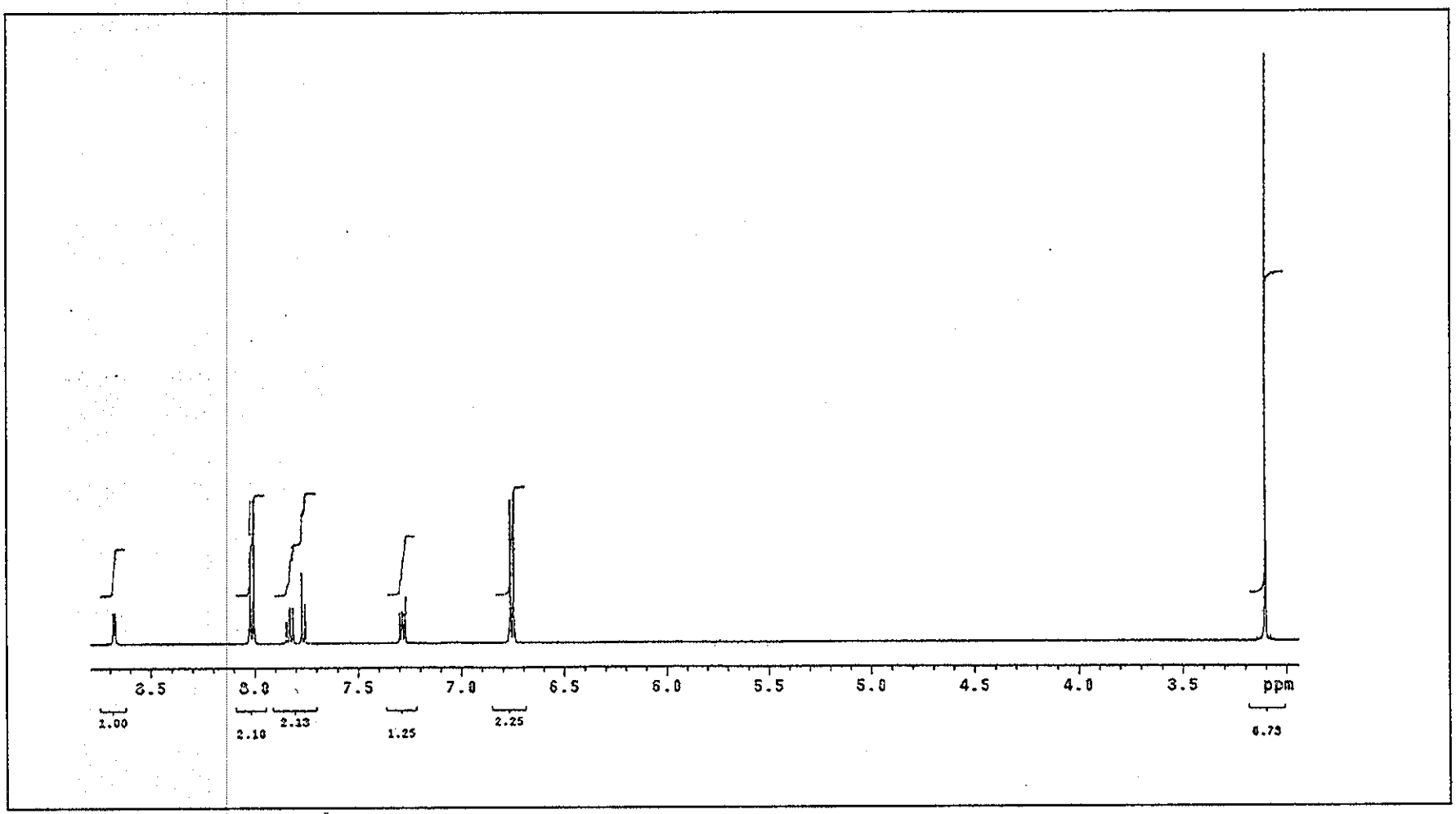

Figure 6. ^{1}H NMR spectrum of 2-(4'-*N*,*N*-dimethylaminophenylazo)pyridine

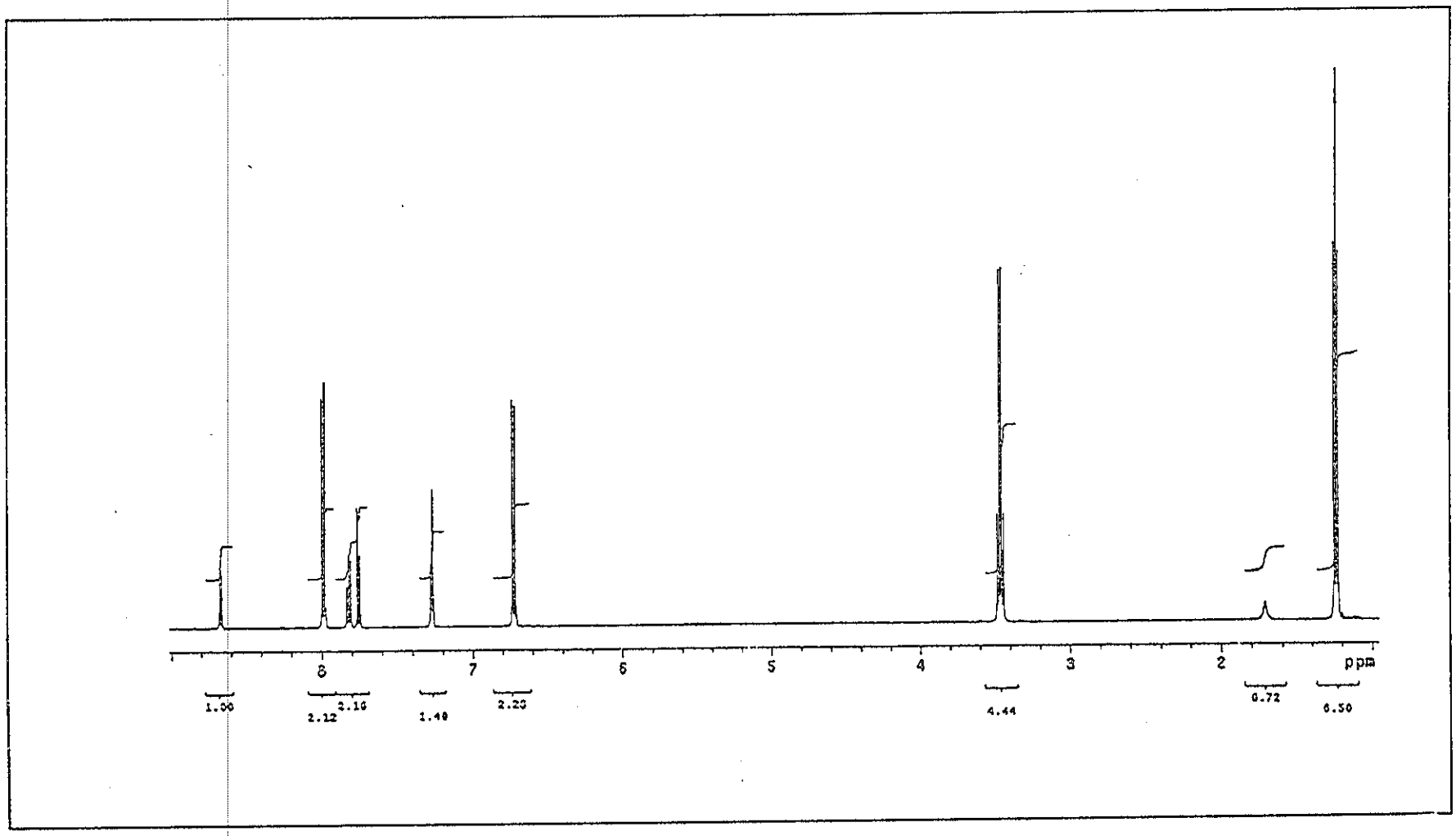

Figure 7. ^{1}H NMR spectrum of 2-(4'-*N*,*N*-diethylaminophenylazo)pyridine

3.1.2.3 Infrared (IR) spectrometric results of dmazpy and deazpy ligands

Infrared spectra of dmazpy and deazpy were recorded in the range 4000-400 cm^{-1} shown in Figure 8 and 9 respectively. Both ligands show bands near 1600 to 500 cm^{-1}. Some characteristic frequencies are summarized in Table 6 and 7 respectively.

Table 6. IR data of 2-(4'-*N,N*-dimethylaminophenylazo)pyridine (dmazpy)

vibrational modes	frequencies (cm^{-1})
sp^2 C-H stretching	3080(s)
N=N stretching	1399(s)
C=N stretching	1603(s)
C=C stretching	1603(s) 1524(s) 1460(w) 1449(m)
C-H bending of para disubstituted benzene	825(s)

s = strong, m = medium and w = weak

Table 7. IR data of 2-(4'-*N,N*-diethylaminophenylazo)pyridine (deazpy)

vibrational modes	frequencies (cm^{-1})
sp^2 C-H stretching	3080(s)
N=N stretching	1396(s)
C=N stretching	1600(s)

vibrational modes	frequencies (cm^{-1})
C=C stretching	1600(s) 1515(s) 1480(m) 1470(m)
C-H bending of para disubstituted benzene	825(m)
C-H bending of ethyl chain	790(m)

s = strong, m = medium

Some characteristic peaks for determining structure of dmazpy and deazpy ligands are in the 1600-1400 cm^{-1} region. They are C=C and C=N stretching modes of pyridine and phenyl ring. These modes show strong to medium absorption at the frequencies similar to azpy results. The C=C and C=N stretching modes of azpy appear at 1584, 1578, 1498 and 1495 cm^{-1} (Krause and Krause, 1980).

The most important peak is N=N stretching mode which used for considering the π-acid property in azo complexes . The N=N stretching of both ligands show the intense peak at very closely frequencies to each other. It occurs at 1399 cm^{-1} in dmazpy and at 1396 cm^{-1} in deazpy. Meanwhile, the N=N stretching frequency shows of azpy ligand shows peak at higher frequency, 1420 cm^{-1} (Krause and Krause, 1980). This result indicates that the N=N bond of the free azpy ligand is stronger than those of dmazpy and deazpy ligands. The decrease of N=N bond order in dmazpy and deazpy could be due to the substituents ($-NR_2$) which are electron donating groups and will be discussed in details later.

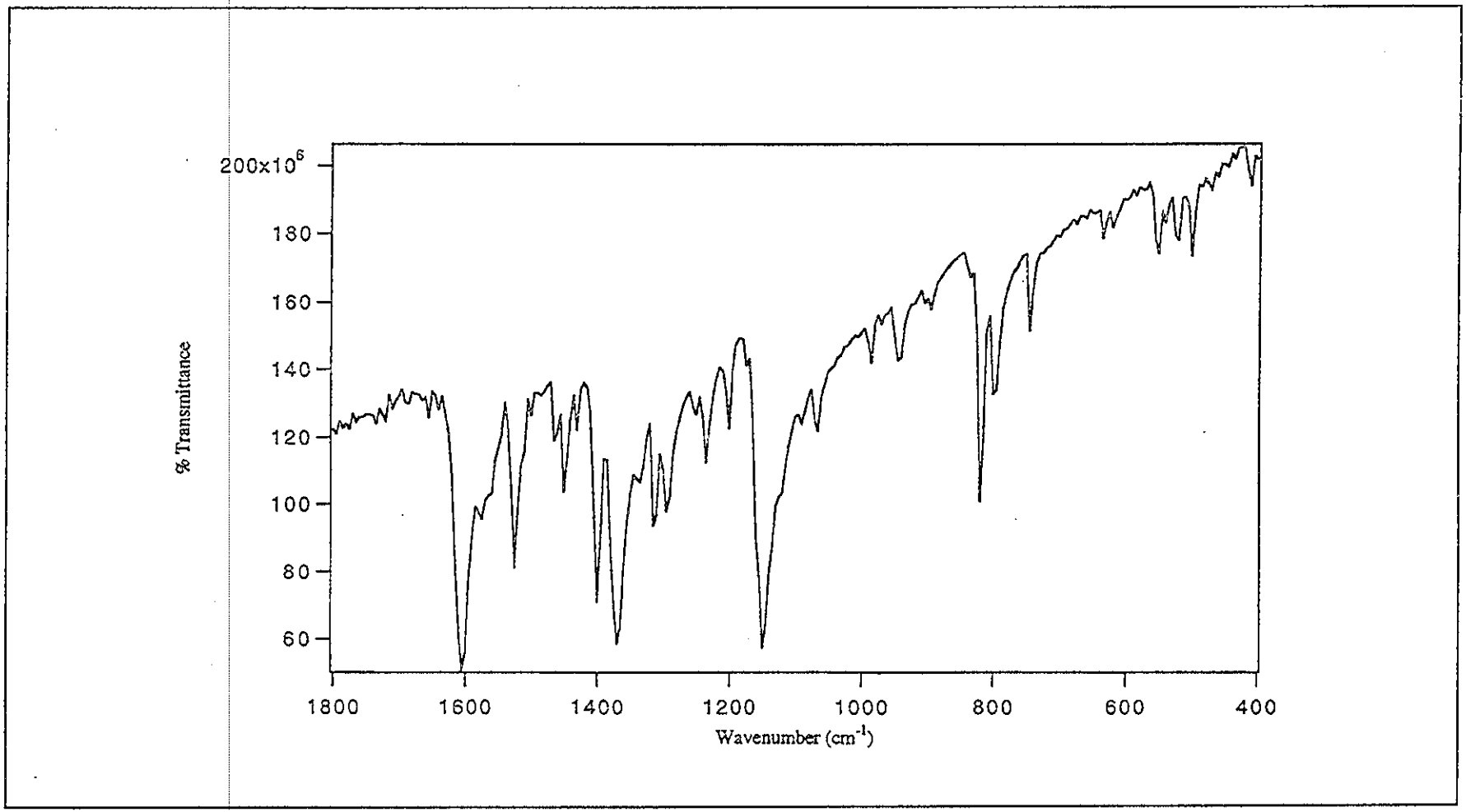

Figure 8. IR spectrum of 2-(4'-*N*,*N*-dimethylaminophenylazo)pyridine

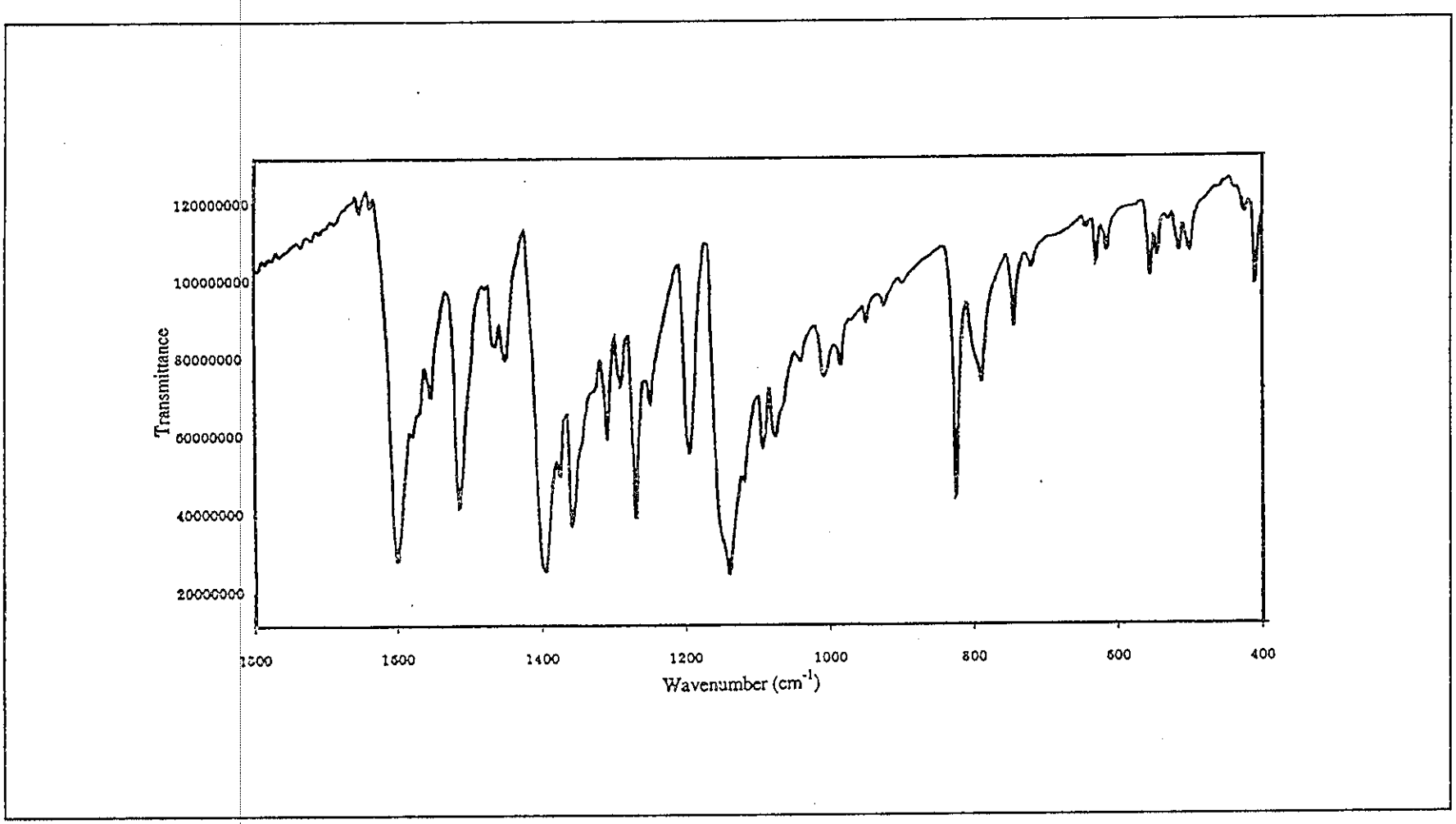

Figure 9. IR spectrum of 2-(4'-*N*,*N*-diethylaminophenylazo)pyridine

3.1.2.4 UV-Visible absorption spectra of dmazpy and deazpy

The absorption spectra of azpy, dmazpy and deazpy in $CHCl_3$ were shown in Figure 10, 11 and 12, respectively. In addition, their absorption spectra were also studied in CH_2Cl_2, $CHCl_3$, DMSO and CH_3CN and the summarized data was listed in Table 8.

Table 8. The UV-Vis spectral data of azpy, dmazpy and deazpy ligands.

Compounds	Maximum Wavelength, nm (ε^a x 10^{-4}, $M^{-1}cm^{-1}$) in solvents			
	$CHCl_3$	CH_2Cl_2	DMSO	CH_3CN
Azpy	320 (1.18)	320 (1.56)	320 (1.96)	316 (1.90)
Dmazpy	430 (2.86)	432 (2.92)	436 (3.60)	422 (3.30)
Deazpy	438 (3.20)	436 (3.00)	444 (3.26)	432 (4.20)

[a]Molar Extinction coefficient.

The azoimine ligand groups always show two absorption bands which are assigned as n →π* and π→π* transitions as observed in 200-500 nm. The absorption spectrum of azpy exhibited the maximum intense band of π→π* transition at the higher energy (320 nm, ε ~ 20,000 $M^{-1}cm^{-1}$) and gave the weak band of n →π* transition at the lowest energy (~450, ε ~ 950 $M^{-1}cm^{-1}$). In contrast to the derivative ligands, both dmazpy and deazpy showed the absorption intense bands of π→π* transition at lower energy (~430-440 nm, ε ~ 20,000 $M^{-1}cm^{-1}$). whereas, the n →π* the transition was shifted to higher energy(~274 nm, ε ~ 1,000 $M^{-1}cm^{-1}$) which close to the solvent cut-off.

Furthermore, dmazpy and deazpy showed slightly solvent effect. The polar solvents lead to bathochromic shift (red shift) of π→π* transition.

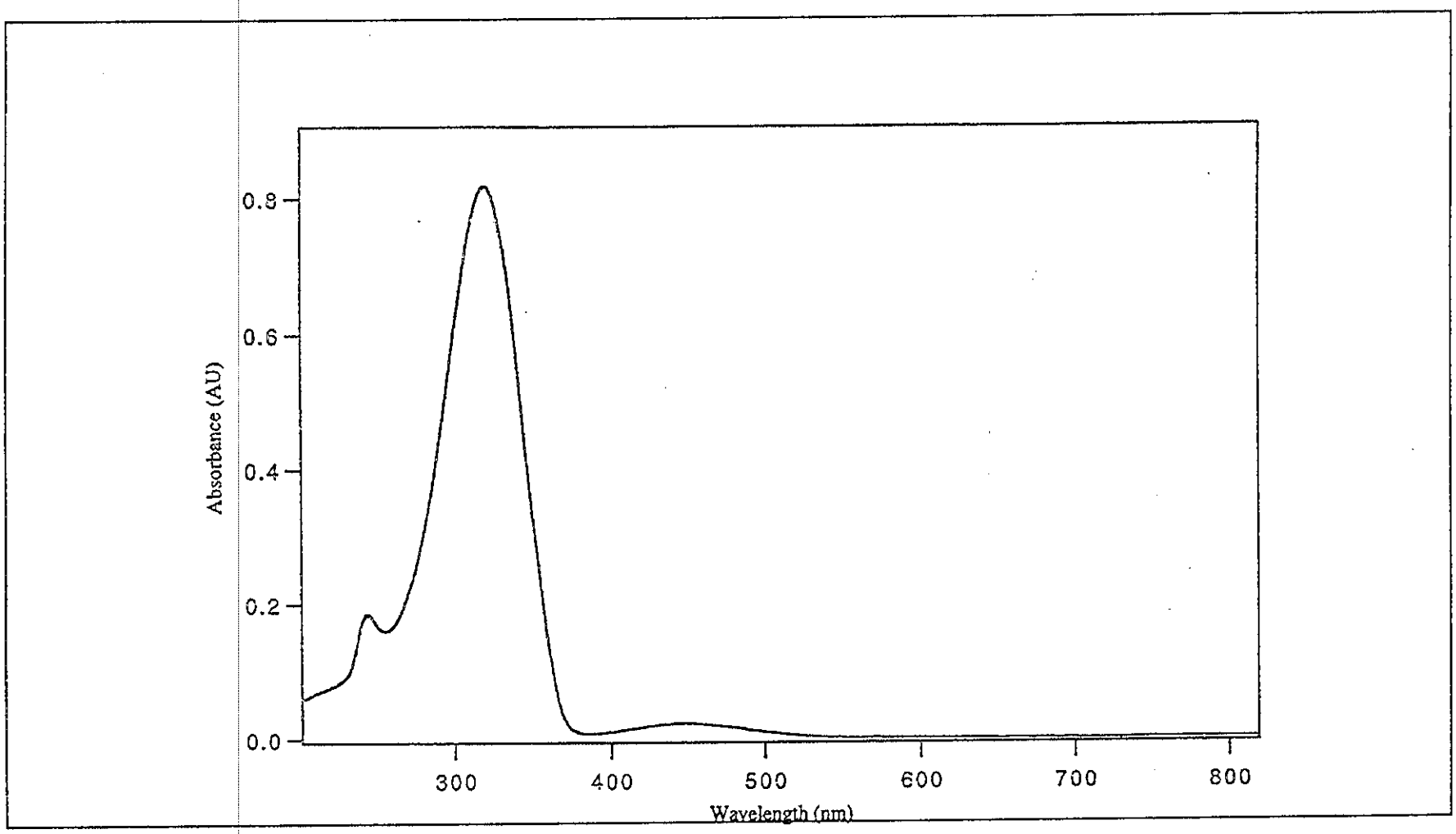

Figure 10. UV-Vis absorption spectrum of 2-(phenylazo)pyridine in $CHCl_3$

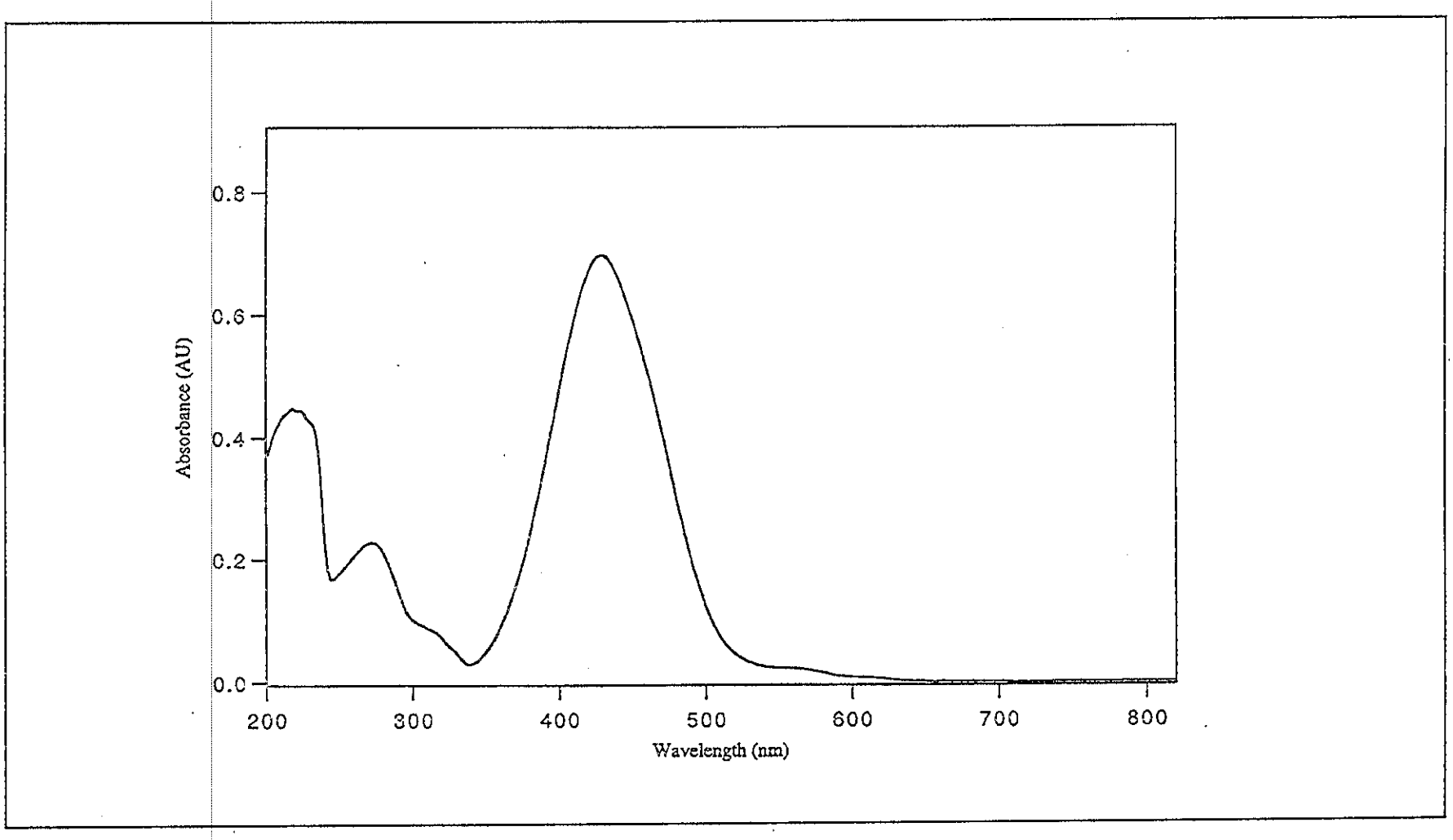

Figure 11. UV-Vis absorption spectrum of 2-(4'-*N*,*N*-dimethylaminophenylazo)pyridine in $CHCl_3$.

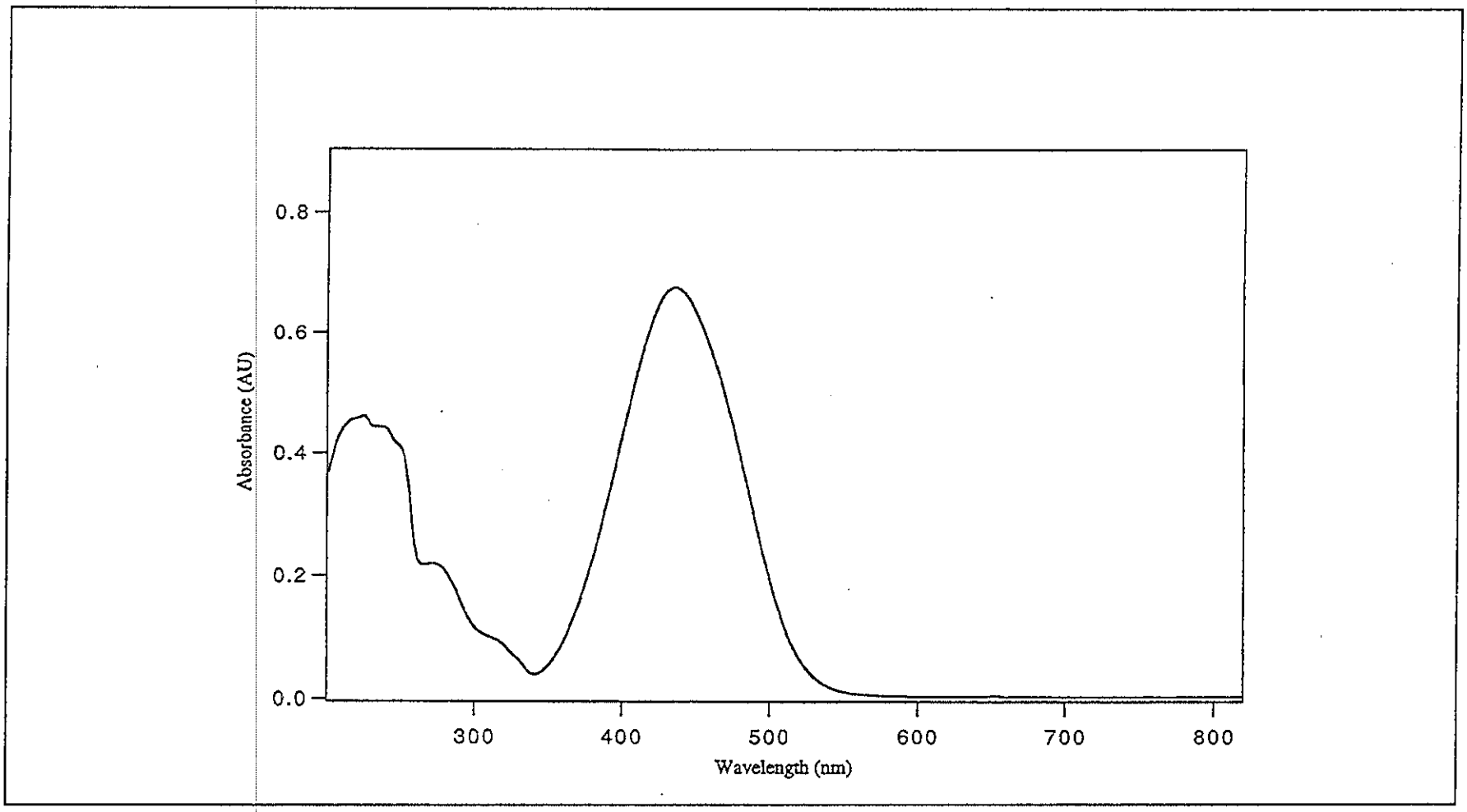

Figure 12. UV-Vis absorption spectrum of 2-(4'-*N*,*N*-diethylaminophenylazo)pyridine in $CHCl_3$

3.2 Synthesis and characterization of $Ru(L)_2Cl_2$ complexes (L = dmazpy and deazpy).

3.2.1 Synthesis and Characterization of $Ru(dmso)_4Cl_2$ complexes

$Ru(dmso)_4Cl_2$ complexes were used as starting materials for synthesis RuL_2Cl_2 (L = dmazpy and deazpy) complexes and prepared according to the literature procedure (Evan *et al.*, 1973). The structure of $Ru(dmso)_4Cl_2$ complex was studied by IR spectroscopy. Table 9 listed the results obtained on examining the IR spectra of this complex (as shown in Figure 13).

Table 9. IR data of 2-(4'-*N,N*-diethylaminophenylazo)pyridine (deazpy)

vibrational modes	frequencies (cm^{-1})
sp^2 C-H stretching	3000, 2908(m)
C-H déformation	1403(m)
S-O stretching S bonded	1120, 1100(s)
C-S stretching	720 (s)
Ru-S stretching	480(m)
CSO symmetric deformation	430(s)
CSO asymmetric deformation	390(m)
Ru-Cl	350(m)

A complete assignment of all bands are in the range 4000-200 cm^{-1}. There are some important bands to specify the isomer of this complex.

The first characteristic band is the SO stretching. It has been known that the dimehylsulfoxide $(CH_3)_2SO$ was bonded to metal ions via S or O atoms. The data from literature review (Evan *et al.*, 1973) suggested that if the S atom was bonded, there was a strong broad band with splitting of SO stretching observed at 1090-1120 cm^{-1}. Whereas, if the O-bonded there was a strong SO stretching at 915 cm^{-1}. In this work, the synthesized $Ru(dmso)_4Cl_2$ complex showed only the strong band with splitting at 1100-1120 cm^{-1}. This indicated that the S atom was bonded to the ruthenium center. The second characteristic band is a Ru-Cl stretching bands in far IR region. It appeared as the single bands at 350 cm^{-1}. Finally, Ru-S or Ru-O stretching frequencies was observed in the range 500-400 cm^{-1}. The band at 480 cm^{-1} can be assigned to either Ru-S and Ru-O stretching. From these IR data supported with *cis*- and *trans*-$Ru(dmso)_4Cl_2$ structures which S bonded.

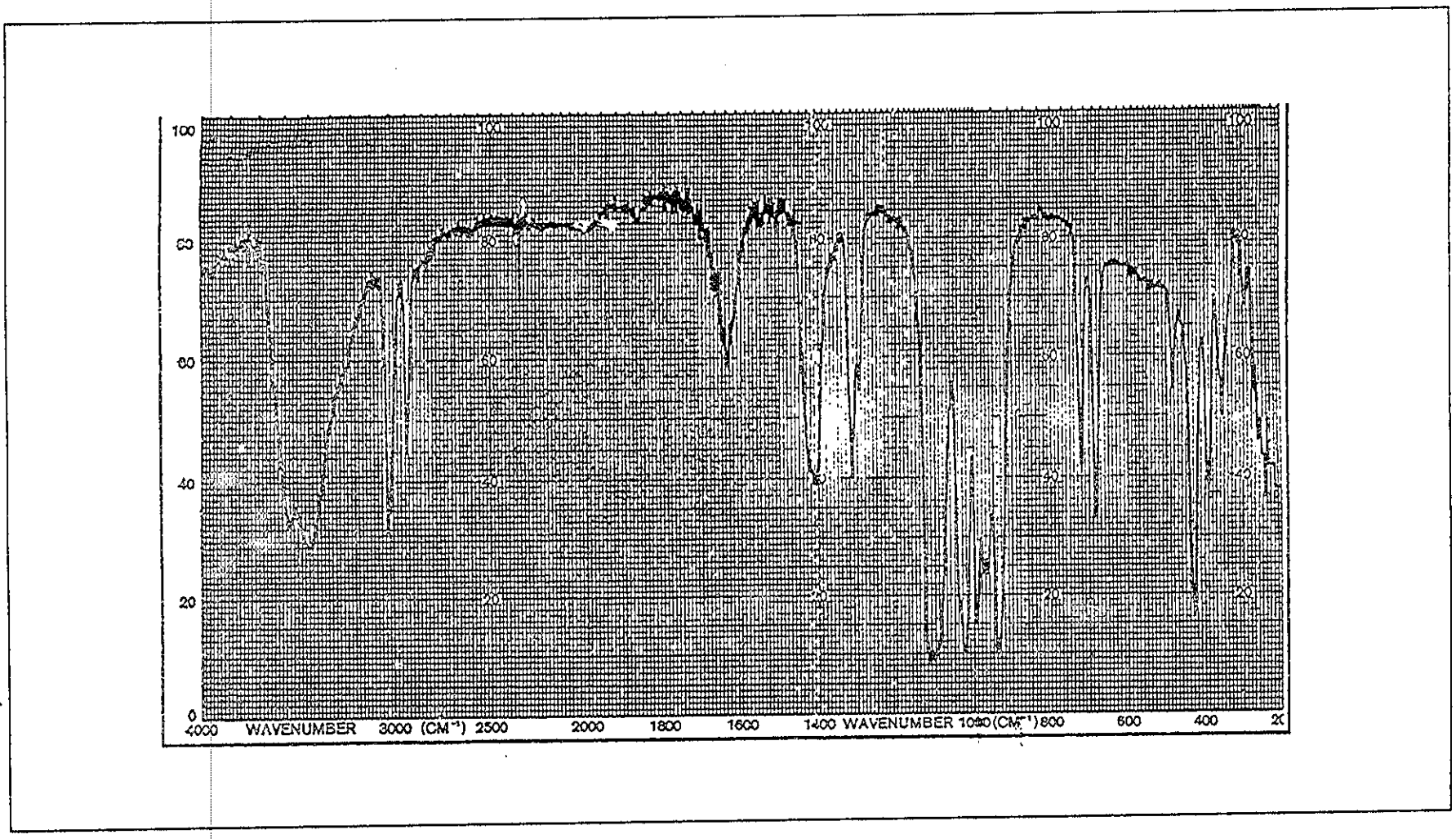

Figure 13. IR spectrum $Ru(dmso)_4Cl_2$

3.2.2 Synthesis of $Ru(L)_2Cl_2$ complexes (L = dmazpy and deazpy)

The $Ru(dmazpy)_2Cl_2$ and $Ru(deazpy)_2Cl_2$ were synthesized from the reaction between $Ru(dmso)_4Cl_2$ complexes with dmazpy and deazpy ligands in chloroform respectively. The orange reaction mixture became purple after refluxed for 40 mins. The solution was refluxed for 72 h.

The $Ru(dmazpy)_2Cl_2$ or $Ru(deazpy)_2Cl_2$ complexes show three colorful isomers on TLC plate when ethyl acetate is used as a mobile solvent. They are green, purple and violet with diferrent R_f values. The R_f values of green complexes are 0.82 for Ru $(dmazpy)_2Cl_2$ and 0.90 for $Ru(deazpy)_2Cl_2$. The purple compounds give R_f values of $Ru(dmazpy)_2Cl_2$ at 0.76 and 0.80 for $Ru(deazpy)_2Cl_2$. The violet band was collected in a very small amount and the R_f values of $Ru(dmazpy)_2Cl_2$ and $Ru(deazpy)_2Cl_2$ are 0.75. In general, there are five possible isomeric compounds. However, only two forms of each complex are isolated from column chromatography. They are green and purple.

The green complex is less polar than the purple therefore the green band was first obtained from column chromatography. The purple band came out later after eluted with mixed solvents of 2:1 (v/v) toluene : acetonitrile.

The characterization of $Ru(L)_2Cl_2$ complexes are on the basis of many techniques. One of them is single crystal X-ray diffraction. The green-$Ru(dmazpy)_2Cl_2$ was recrystallized from CH_2Cl_2 + EtOH + 0.1 M HCl (2:1:0.5 v/v). Whereas, the purple- $Ru(dmazpy)_2Cl_2$ was recrystallized from CH_2Cl_2 + toluene + CH_3CN (2:1:1 v/v). The crystals of green- $Ru(deazpy)_2Cl_2$ were obtained from CH_2Cl_2 + toluene + CH_3CN (2:2:1 v/v). The solubilities of all complexes are similar as summarized in Table 10.

Table 10. The solubilities of *cis*- and *trans*-$Ru(L)_2Cl_2$

solvents	solubility
hexane	-
toluene	-
dichloromethane	++
chloroform	++
ethyl acetate	+
acetone	+
acetonitrile	+
dimethylformamide	++
dimethylsulfoxide	++
methanol	+
ethanol	+
water	-
*0.1 M HCl	+
*0.1 M NaOH	+

- nonsoluble + slightly soluble ++ moderately soluble

* color changed

The solubility, ++ represents that the amount of complexes less than 0.0012 g can completely dissolve in 10 mL, + represents that the amount of complexes 0.0005-0.0008 g can completely dissolve in 10 mL. The - represents the non soluble 0.0005 g of complexes in 10 mL. The * shows the changing of ligand color in a solvent.

The solubility of complexes is useful for recrystallization. The suitable solvents may be selected from solvent in which compounds have different solubilities.

3.2.3 Characterization of $Ru(L)_2Cl_2$ complexes (L = dmazpy and deazpy)

The structures of isolated complexes of $Ru(L)_2Cl_2$ (L = dmazpy and deazpy) were characterized by using these following techniques.

3.2.3.1 Electrospray mass spectrometry

3.2.3.2 Infrared spectrometry

3.2.3.3 UV-Visible absorption spectrophotometry

3.2.3.4 Protons Nuclear Magnetic Resonance

3.2.3.5 Single crystal X-ray diffraction

3.2.3.1 Electrospray Mass Spectroscopic results of $Ru(L)_2Cl_2$ complexes

In general, this technique cannot provide us about the structures of compounds directly. However, in this research, the electrospray mass spectrometry is important technique to confirm the molecular mass of complexes. In general, one cannot assign the type of isomer based on the electrospray mass spectra (ES-MS). However, in this work showed the different results from ES-MS data between *trans*- and *cis*- isomers. In addition, their structures have been confirmed by ^{1}H-NMR and X-ray diffraction techniques. Therefore, in this work results from mass spectra can be used to determine the isomer of an unknown complex. It will be discussed in details later.

ES-MS of the possitive ion of a solution of *trans*- and *cis*-$Ru(L)_2Cl_2$ (L = dmazpy and deazpy) give the abandant peaks which are listed in Table 11 for *trans*-Ru $(dmazpy)_2Cl_2$, Table 12 for *trans*-$Ru(deazpy)_2Cl_2$, Table 13 for *cis*-$Ru(dmazpy)_2Cl_2$ and Table 14 for *cis*-$Ru(deazpy)_2Cl_2$. The electrospray mass spectra are displayed in Figure 13-16 respectively.

Table 11. Electrospray mass spectroscopic data of *trans*-$Ru(dmazpy)_2Cl_2$ complex

m/z	stoichiometry	equivalent species	rel. abun.
626.2	$[Ru(dmazpy)_2 2HCl_2]^+$	$[M+2H]^+$	75
288.3	$[Ru(NC_5H_4N{=}NC_6H_5 4H]^+$	$[M\text{-}2Cl\text{-}dmazpy\text{-}N(C_2H_5)_2]^+ +4H$	60
171.0	$[RuCl_2]^+$	$[RuCl_2]^+$	95

MW of the *trans*-$Ru(dmazpy)_2Cl_2$ complex = 624.38 = M

MW of the dmazpy ligand = 226.2

Even the mass spectrum contains several peak, The intense peak at m/z 626.1 is assigned to $[Ru(dmazpy)_2 2HCl_2]^+$ ion. This peak is an evidence to support the mass of the complex (MW = 624.38). The $[Ru(dmazpy)_2 2HCl_2]^+$ is unstable at higher ion source energy. It undergoes significant decomposition to give 2 major species-complex in two pathways. First, the molecular ion lost two chlorine atoms, one ligand and the $-N(CH_3)_2$ substituent of another remained dmazpy this gives rise to a peak $[Ru(NC_5H_4N{=}NC_6H_5 4H]^+$ at m/z 288.3. The other species which is the most intense peak at m/z 171.0 is assigned to $[RuCl_2]^+$ ion.

Table 12. Electrospray mass spectrometric data of *trans*-$Ru(deazpy)_2Cl_2$ complex

m/z	stoichiometry	equivalent species	rel. abun.
681.2	$[Ru(deazpy)_2HCl_2]^+$	$[M+H]^+$	85
288.3	$[Ru(NC_5H_4N{=}NC_6H_5 4H]^+$	$[M\text{-}2Cl\text{-}deazpy\text{-}N(C_2H_5)_2]^+ +4H$	80

MW of the *trans*-Ru(deazpy)$_2$Cl$_2$ complex = 680.38 = M

MW of the deazpy ligand = 254.25

The intense peak at 681.2 is assigned to [Ru(deazpy)$_2$HCl$_2$]$^+$ ion. This is the main peak which supports the molecular mass of the complex (MW. = 680.38). The [Ru(deazpy)$_2$HCl$_2$]$^+$ loses two chlorine atoms, one ligand and the substituent of another remained deazpy like the [Ru(dmazpy)$_2$Cl$_2$] complex. It also gives intense peak at m/z 288.3.

Table 13. Electrospray mass spectrometric data of *cis*-Ru(dmazpy)$_2$Cl$_2$ complex

m/z	stoichiometry	equivalent species	rel. abun.
589.0	[Ru(dmazpy)$_2$Cl]$^+$	[M-Cl]$^+$	100
591.1	[Ru(dmazpy)$_2$2HCl]$^+$	[M+2H-Cl]$^+$	80
588.1	[Ru(dmazpy)$_2$Cl-H]$^+$	[M-H-Cl]$^+$	60

MW of the *cis*-Ru(dmazpy)$_2$Cl$_2$ complex = 624.38 = M

MW of the dmazpy ligand = 226.25

The abundant peaks are the peaks at m/z 589.0, 591.1 and 588.1 of the positive ion ES-MS. These ions are assigned [Ru(dmazpy)$_2$Cl]$^+$, [Ru(dmazpy)$_2$2HCl]$^+$ and [Ru (dmazpy)$_2$Cl-H]$^+$, respectively.

Table 14. The Electrospray mass spectrometric data of *cis*-$Ru(deazpy)_2Cl_2$ complex

m/z	stoichiometry	equivalent species	rel. abun.
644.9	$[Ru(deazpy)_2Cl]^+$	$[M\text{-}Cl]^+$	40
413.2	$[Ru(NC_5H_4N{=}NC_2H)(NC_5H_4N{=}NC_6H_3)]^+$	$[M\text{-}2Cl, -C_4H_4N(C_2H_5)_2 - N(C_2H_5)_2\text{-}2H]^+$	80
391.3	$[Ru(NC_5H_4N{=}NH)(NC_5H_4N{=}NC_6H_5)]^+$	$[M\text{-}2Cl, -C_6H_5N(C_2H_5)_2 - N(C_2H_5)_2 + H]^+$	100
288.2	$[Ru(NC_5H_4N{=}NC_6H_54H]^+$	$[M\text{-}2Cl + 4H - N(C_2H_5)_2]^+$	70

MW of the *cis*-$Ru(deazpy)_2Cl_2$ complex = 680.64 = M

MW of the deazpy ligand = 254.25 = L_1,L_2

Although the single crystals of *cis*-$Ru(deazpy)_2Cl_2$ have not been obtained but the structure of this complex can be confirmed to be the *cis*- configuration based on results of electrospray mass spectrum. This is due to the pattern of the losing Cl atoms to give peak at m/z 644.9 which is similar to those of *cis*-$Ru(dmazpy)_2Cl_2$. Besides, the fragmentation of the *cis*-$Ru(deazpy)_2Cl_2$ displayed the complicate abundant peaks at m/z 413.2 and 391.3. The peak at m/z 413.2 is the species which lost the two Cl atoms, the sustituent $-N(C_2H_5)_2$ and fragmented the phenyl to be acetylene molecule.

The most abundant peak is at m/z 319.2. It may come from the fragmentation of the species at m/z 413.2 to lose the acetylene molecule.

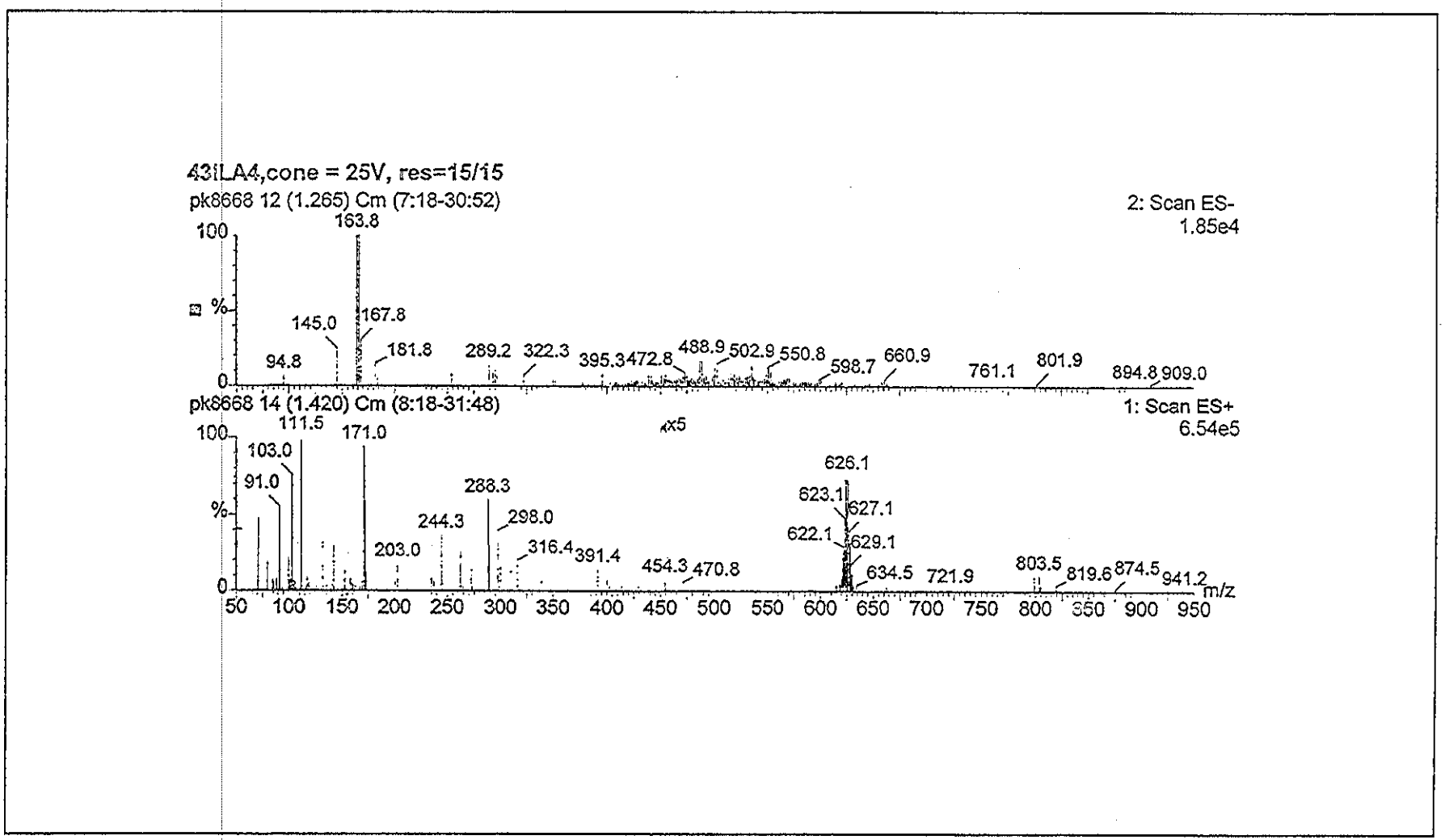

Figure 14. Electrospray mass spectrum of *trans*-Ru(dmazpy)$_2$Cl$_2$

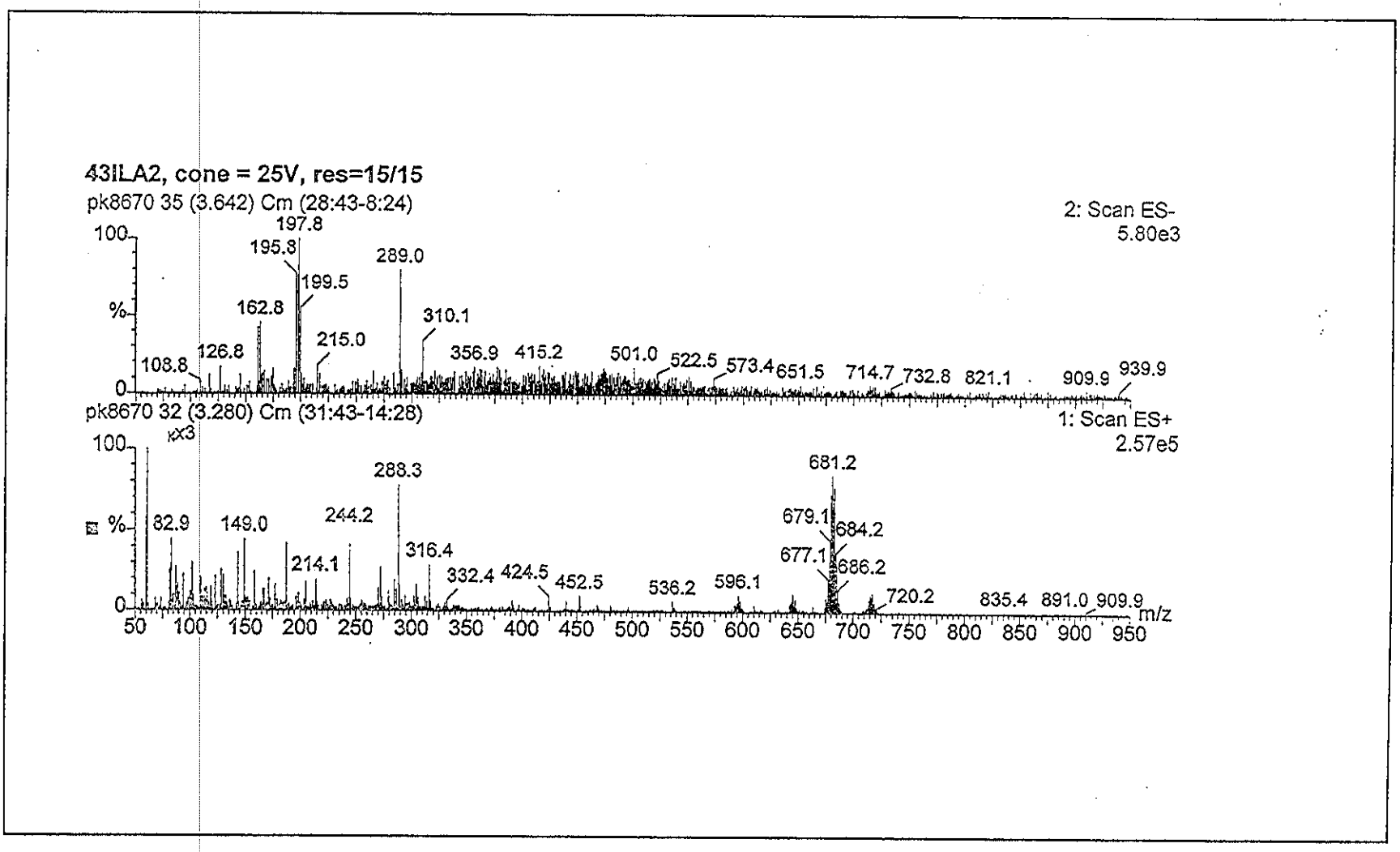

Figure 15. Electrospray mass spectrum of *trans*-Ru(deazpy)$_2$Cl$_2$

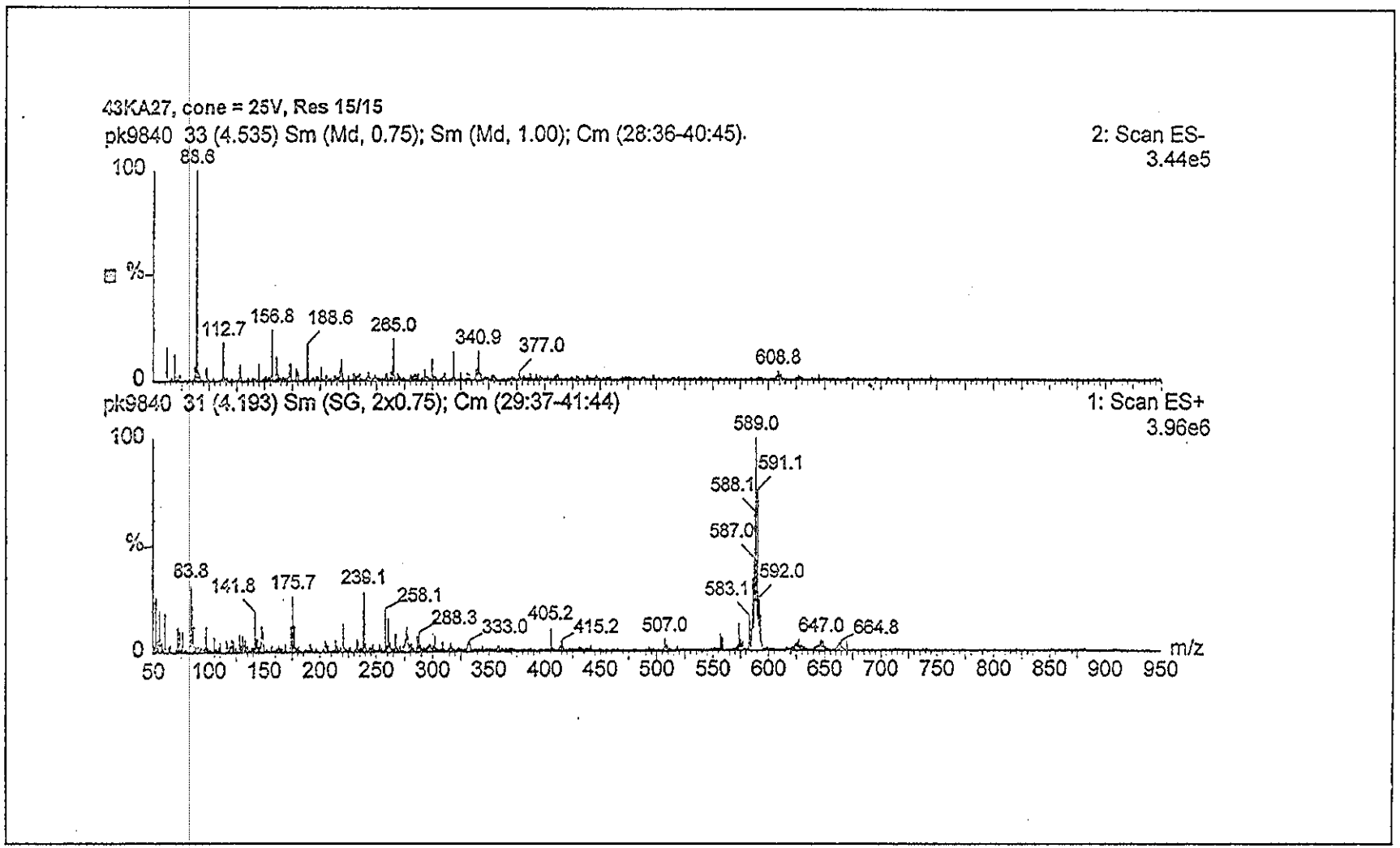

Figure 16. Electrospray mass spectrum of *cis*-Ru(dmazpy)$_2$Cl$_2$

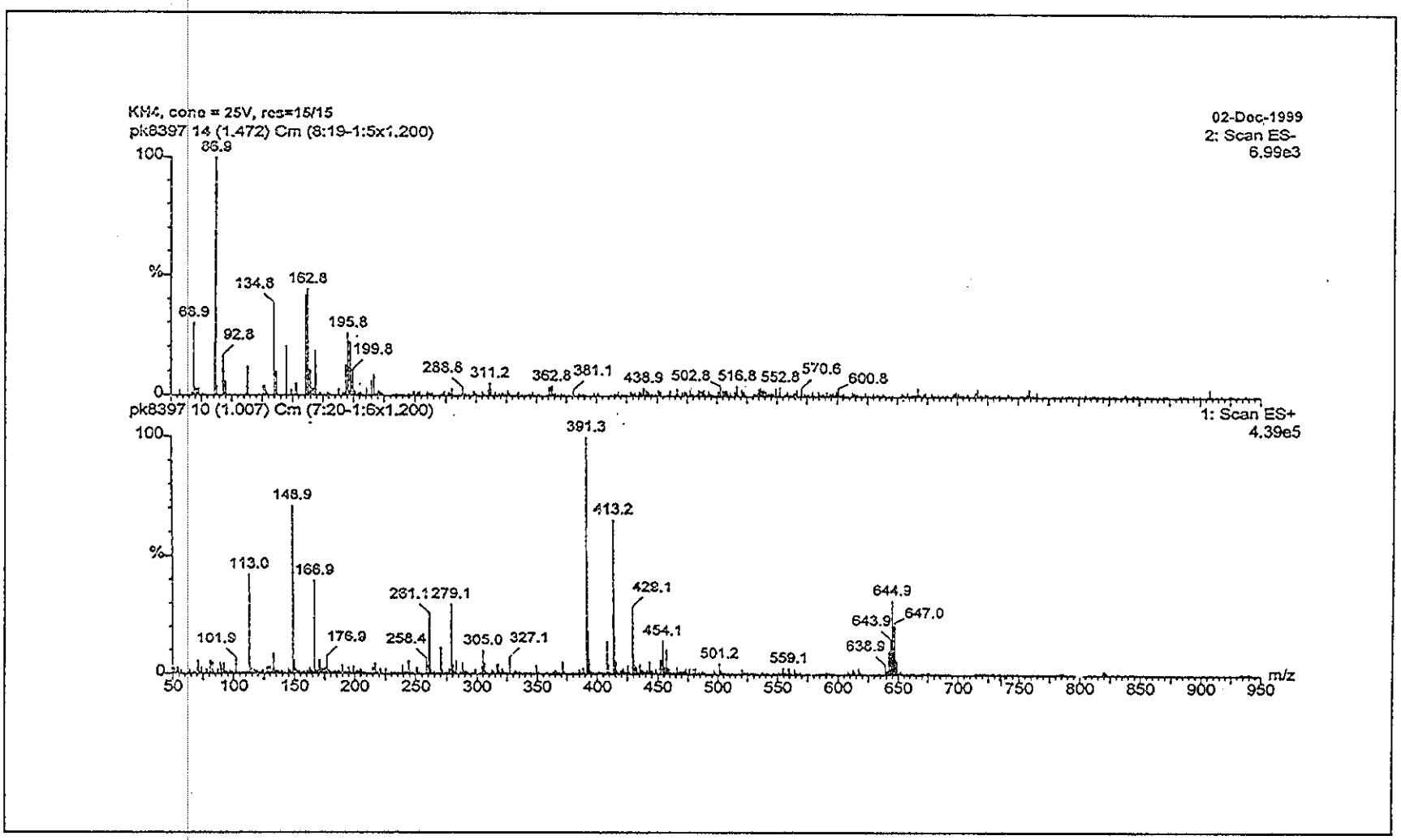

Figure 17. Electrospray mass spectrum of *cis*-Ru(deazpy)$_2$Cl$_2$

3.2.3.2 Infrared Spectroscopic data of $Ru(L)_2Cl_2$ (L = dmazpy and deazpy)

Infrared data of $Ru(L)_2Cl_2$ (L = dmazpy and deazpy) complexes are significant in the range 1600-200 cm^{-1}. Some characteristic frequencies are shown in Table 15 for *trans*-$Ru(dmazpy)_2Cl_2$, Table 16 for *trans*-$Ru(deazpy)_2Cl_2$, Table 17 for *cis*-Ru $(dmazpy)_2Cl_2$ and Table 18 for *cis*-$Ru(deazpy)_2Cl_2$. The Infrared spectra can be shown in Figure 18-21 respectively.

Table 15. Infrared Stretching Modes (cm^{-1}) of *trans*-$Ru(dmazpy)_2Cl_2$

compounds	Stretching Modes (cm^{-1})			
	N=N	Ru-N(azo)	Ru-N(py)	Ru-Cl
trans-$Ru(dmazpy)_2Cl_2$	1250	375	355	310
[a] *trans*- $Ru(azpy)_2Cl_2$	1290	370, 295	350, 280	315, 305
dmazpy	1399	-	-	-
azpy	1421	-	-	-

[a] data from literature review (Krause and Krause, 1980)

Table 16. Infrared Stretching Modes (cm^{-1}) of *trans*-$Ru(deazpy)_2Cl_2$

Compounds	Stretching Modes (cm^{-1})			
	N=N	Ru-N(azo)	Ru-N(py)	Ru-Cl
trans-$Ru(deazpy)_2Cl_2$	1243	-	-	310
[a] *trans*- $Ru(azpy)_2Cl_2$	1290	370, 295	350, 280	315, 305
deazpy	1396	-	-	-
azpy	1421	-	-	-

[a] data from literature review (Krause and Krause, 1980)

Table 17. Infrared Stretching Modes (cm^{-1}) of *cis*-$Ru(dmazpy)_2Cl_2$

compounds	stretching Modes (cm^{-1})			
	N=N	Ru-N(azo)	Ru-N(py)	Ru-Cl
cis-$Ru(dmazpy)_2Cl_2$	1249	370, 280	345, 270	305
[a] *cis*- $Ru(azpy)_2Cl_2$	1290	376, 280	358, 268	308, 336
dmazpy	1399	-	-	-
azpy	1421	-	-	-

[a] data from literature review (Krause and Krause, 1980)

Table 18. Infrared Stretching Modes (cm^{-1}) of *cis*-$Ru(deazpy)_2Cl_2$

compounds	stretching Modes (cm^{-1})			
	N=N	Ru-N(azo)	Ru-N(py)	Ru-Cl
cis-$Ru(deazpy)_2Cl_2$	1251	275	255	310
[a] *cis*- $Ru(azpy)_2Cl_2$	1290	376, 280	358, 268	308, 336
deazpy	1396	-	-	-
azpy	1421	-	-	-

[a] data from literature review (Krause and Krause, 1980)

In general, characteristic peaks of all isomeric complexes are the sharp single peak of C=N stretching modes which are observed at closed frequencies in the range 1592-1600 cm^{-1}. The results are also in the N=N stretching modes.

The N=N stretching frequencies of each isomer of $Ru(L)_2Cl_2$ (L = dmazpy and deazpy) complexes are not much different from each other. The *trans*-$Ru(deazpy)_2Cl_2$ complex seems to show this peak at lower frequencies than other forms. However, the N=N stretching modes in complexes are shifted to lower frequencies from free ligand, which is a good indication of π-acceptor property of the ligands. In comparison with these complexes, the N=N streching modes of the azpy complexes are indicated that N=N stretching modes of azpy complexes occurred at higher frequencies than those in the dmazpy and deazpy complexes. It should be from the substituents effect in dmazpy and deazpy.

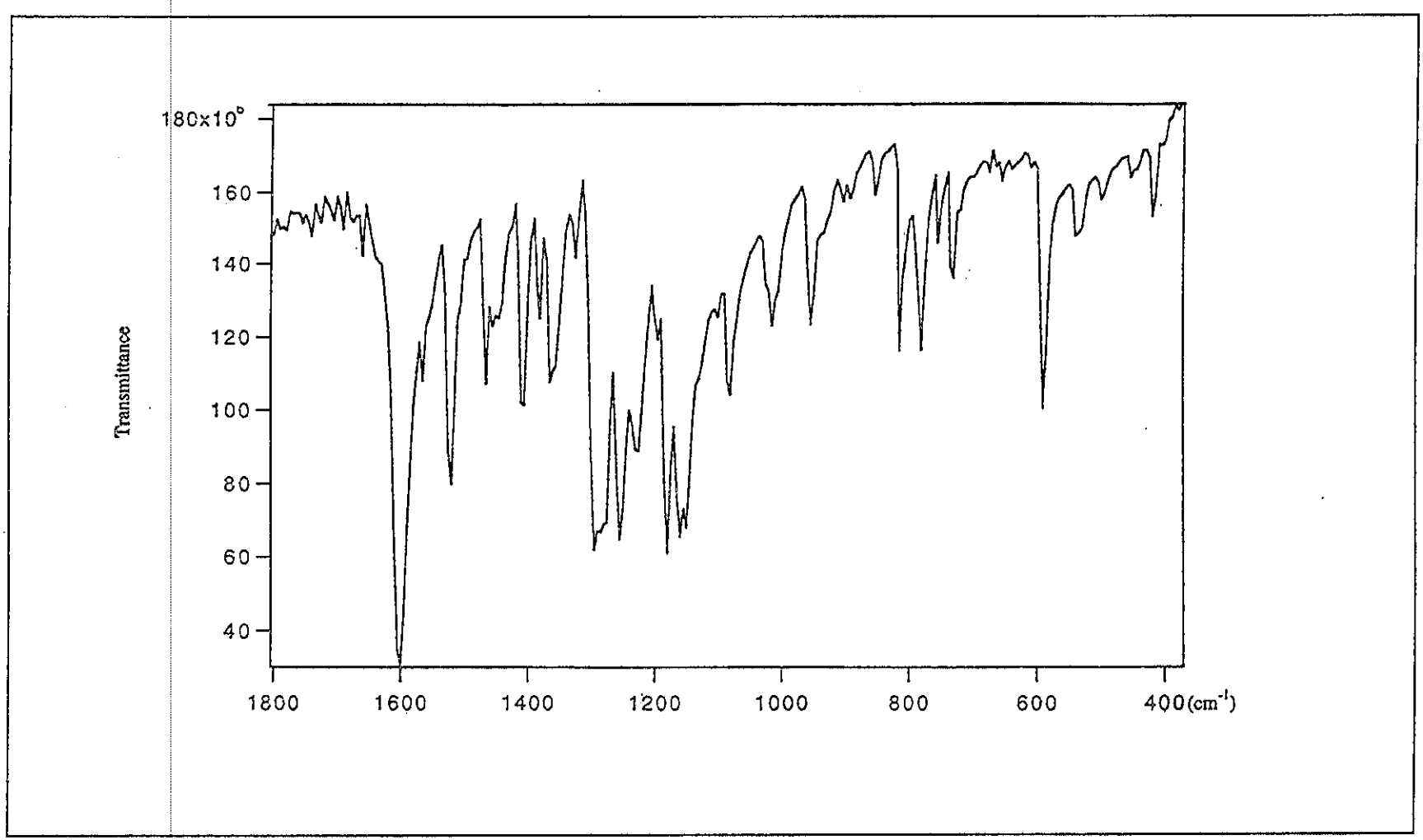

Figure 18. IR spectrum of *trans*-$Ru(dmazpy)_2Cl_2$

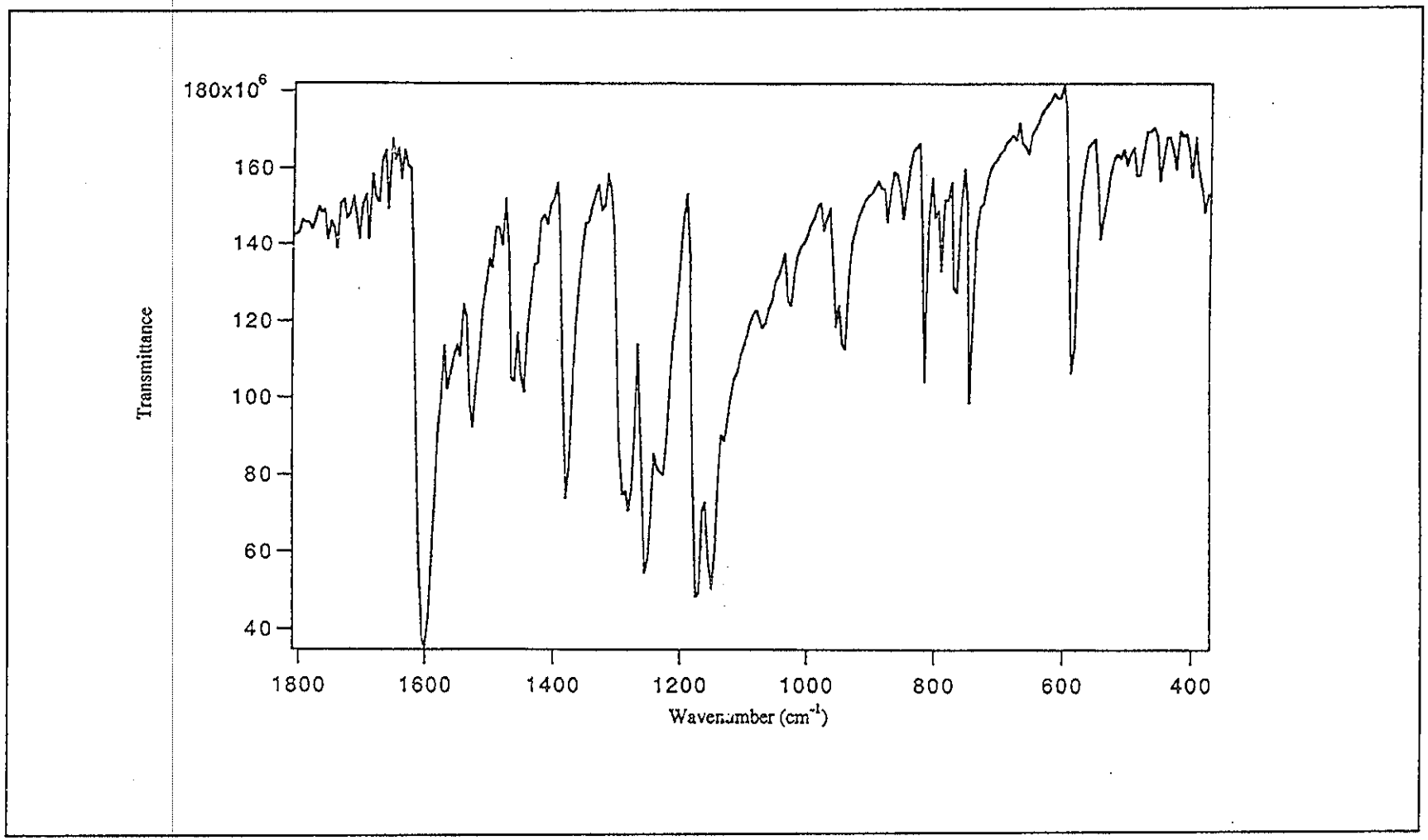

Figure 19. IR spectrum of *trans*-Ru(deazpy)$_2$Cl$_2$

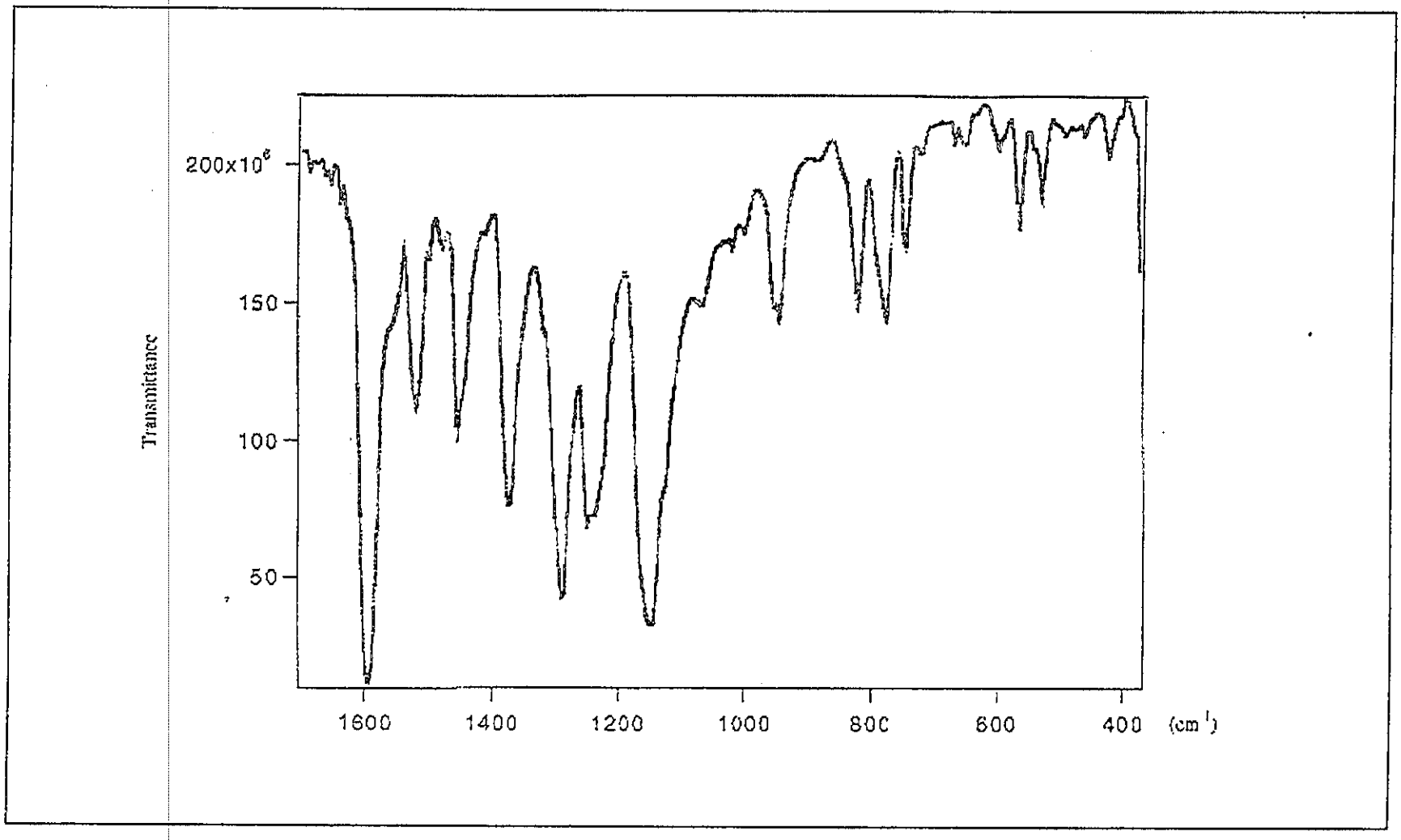

Figure 20. IR spectrum of *cis*-Ru(dmazpy)$_2$Cl$_2$

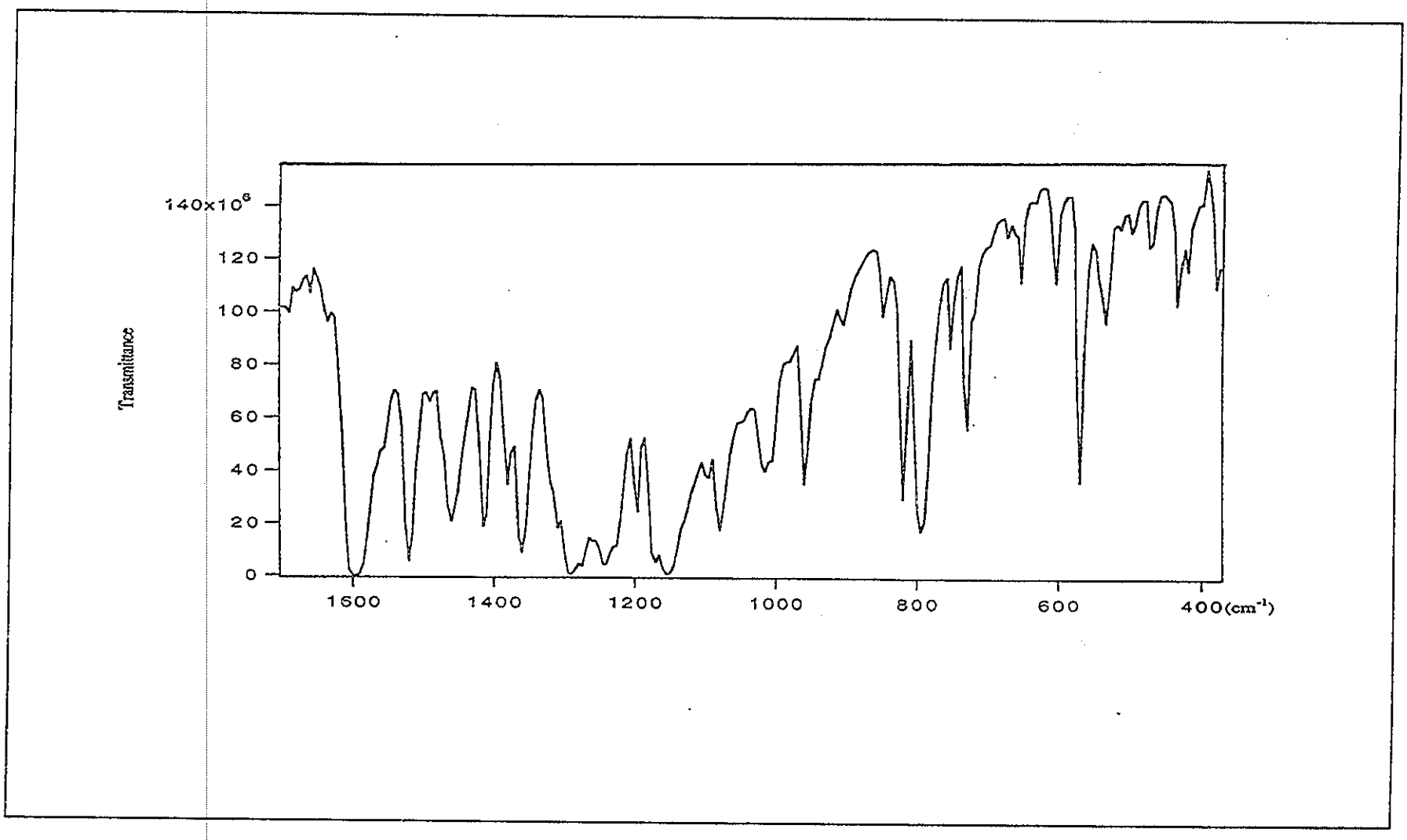

Figure 21. IR spectrum of *cis*-Ru(deazpy)$_2$Cl$_2$

3.2.3.3 UV-Vis absorption spectroscopic results of $Ru(L)_2Cl_2$ (L = dmazpy and deazpy)

The absorption spectra of the $Ru(L)_2Cl_2$ (L = dmazpy and deazpy) complexes and free ligands were studied in various solvents in the range 200-820 nm. The absorption data of all complexes are summarized in Table 19 for *trans*-$Ru(dmazpy)_2Cl_2$, Table 20 for *trans*-$Ru(deazpy)_2Cl_2$, Table 21 for *cis*- $Ru(dmazpy)_2Cl_2$ and Table 22 for *cis*-$Ru(deazpy)_2Cl_2$. The Infrared spectra of four complexes are shown in Figure 22-25, respectively.

Table 19. UV-Vis spectral data of *trans*-$Ru(dmazpy)_2Cl_2$.

compounds	Maximum Wavelength, nm (ε^a x 10^{-4}, $M^{-1}cm^{-1}$) in solvents				
	$CHCl_3$	CH_2Cl_2	DMF	DMSO	CH_3CN
trans-$Ru(azpy)_2Cl_2$	410 (0.96)	406 (1.00)	400 (0.91)	404 (0.97)	400 (0.94)
	632 (1.20)	636 (1.25)	640 (1.13)	644 (1.23)	636 (1.21)
trans-$Ru(dmazpy)_2Cl_2$	482 (1.58)	486 (1.26)	490 (1.52)	484 (1.51)	494 (1.24)
	630 (2.37)	638 (2.65)	640 (2.15)	652 (2.46)	640 (2.04)

[a]Molar Extinction coefficient.

Table 20. The absorption spectra of *trans*-$Ru(deazpy)_2Cl_2$.

compounds	maximum wavelength, nm (ε^a x 10^{-4}, $M^{-1}cm^{-1}$) in solvents				
	$CHCl_3$	CH_2Cl_2	DMF	DMSO	CH_3CN
trans-$Ru(azpy)_2Cl_2$	410 (0.96)	406 (1.00)	400 (0.91)	404 (0.97)	400 (0.94)
	632 (1.20)	636 (1.25)	640 (1.13)	644 (1.23)	636 (1.21)
trans-$Ru(deazpy)_2Cl_2$	484 (1.23)	486 (1.38)	490 (1.64)	492 (1.61)	490 (1.46)
	636 (2.52)	640 (1.44)	644 (2.65)	648 (2.64)	644 (2.35)

[a]Molar Extinction coefficient.

Table 21. UV-Vis spectral data of *cis*-$Ru(dmazpy)_2Cl_2$.

compounds	maximum Wavelength, nm (ε^a x 10^{-4}, $M^{-1}cm^{-1}$) in solvents				
	$CHCl_3$	CH_2Cl_2	DMF	DMSO	CH_3CN
cis-$Ru(azpy)_2Cl_2$	577 (1.07)	-	-	574 (1.10)	-
cis-$Ru(deazpy)_2Cl_2$	506 (3.61) 636 (1.42)	506 (3.73) 640 (1.47)	506 (3.93) 650 (1.40)	510 (3.93) 654 (1.50)	506 (3.72) 638 (1.46)

[a]Molar Extinction coefficient.

Table 22. UV-Vis spectral data of *cis*-$Ru(deazpy)_2Cl_2$

compounds	maximum Wavelength, nm (ε^a x 10^{-4}, $M^{-1}cm^{-1}$) in solvents				
	$CHCl_3$	CH_2Cl_2	DMF	DMSO	CH_3CN
cis-$Ru(azpy)_2Cl_2$	[b]577 (1.07)	-	-	[b]574 (1.10)	-
cis-$Ru(dmazpy)_2Cl_2$	496 (2.28) 628 (0.82)	498 (2.13) 630 (0.78)	502 (1.78) 640 (0.61)	506 (2.07) 654 (0.81)	498 (2.46) 632 (1.21)

[a]Molar Extinction coefficient. [b] data from literature review (Krause and Krause, 1980)

The absorption spectra of complexes were recorded in both ultraviolet (200-400 nm) and visible regions (400-820 nm). The intense bands in the UV region arise from ligands-based $n\rightarrow\pi^*$ and $\pi\rightarrow\pi^*$ transitions, whereas the bands in the visible region are assigned to $d\pi(Ru)\rightarrow\pi^*$ transition.

The transition in visible region is metal to ligand charge transfer (MLCT) with two broad intense bands. The shape of absorption spectra in *trans*-$Ru(dmazpy)_2Cl_2$ and *trans*-$Ru(deazpy)_2Cl_2$ complexes is very similar but different from those of both *cis*-forms. The *trans*-$Ru(L)_2Cl_2$ (L = dmazpy and deazpy) (green complex) show the most intense (ε~20,000) bands in the range 630-650 nm and the less intense (ε~15,000) bands in the range 482-494 nm. In contrast with *cis*-$Ru(L)_2Cl_2$ (purple complex), they show the most intense (ε~20,000-40,000) bands in the range 496-506 nm and the less intense (ε~10,000) bands at 628-654 nm in various solvents. In addition, the lowest energy absorption bands of all complexes are shifted when the polarity of solvents is increased, the absorption occurred at lower energy than that of $Ru(azpy)_2Cl_2$ complex.

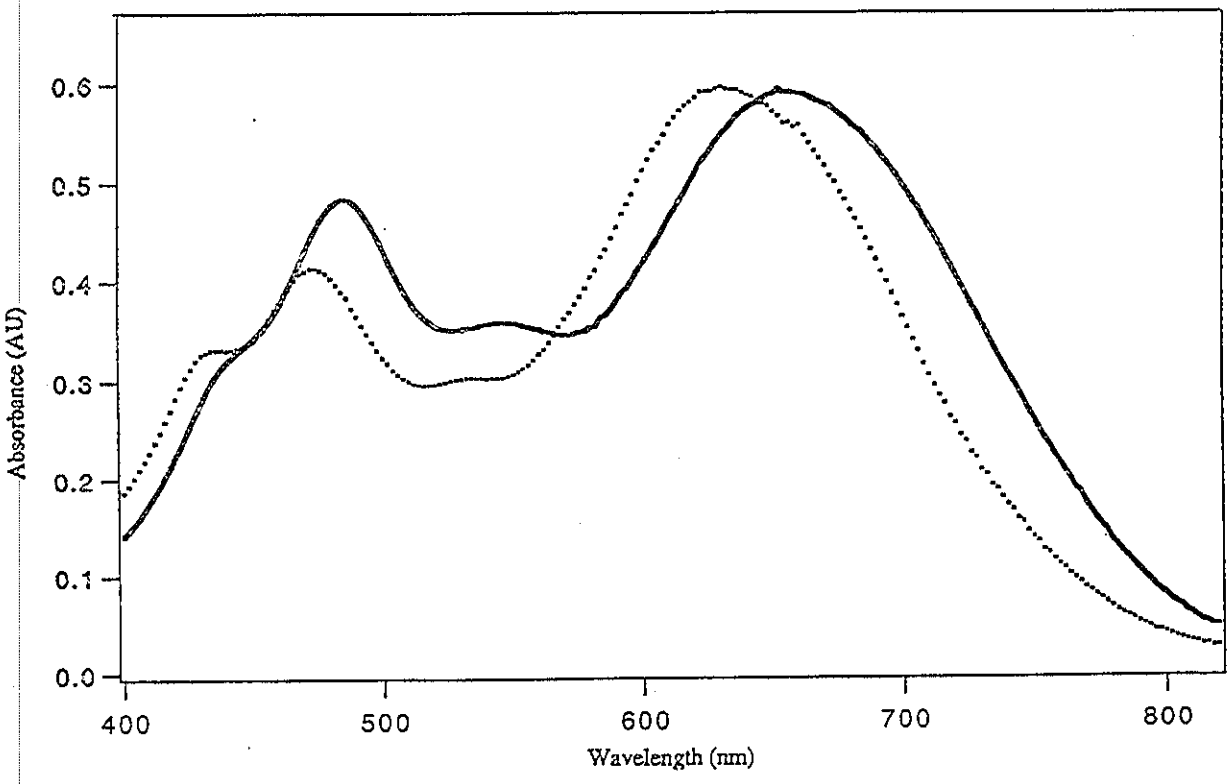

Figure 22. UV-Vis absorption spectra of *trans*-$Ru(dmazpy)_2Cl_2$ in dimethylsulfoxide (__) and $CHCl_3$ (...)

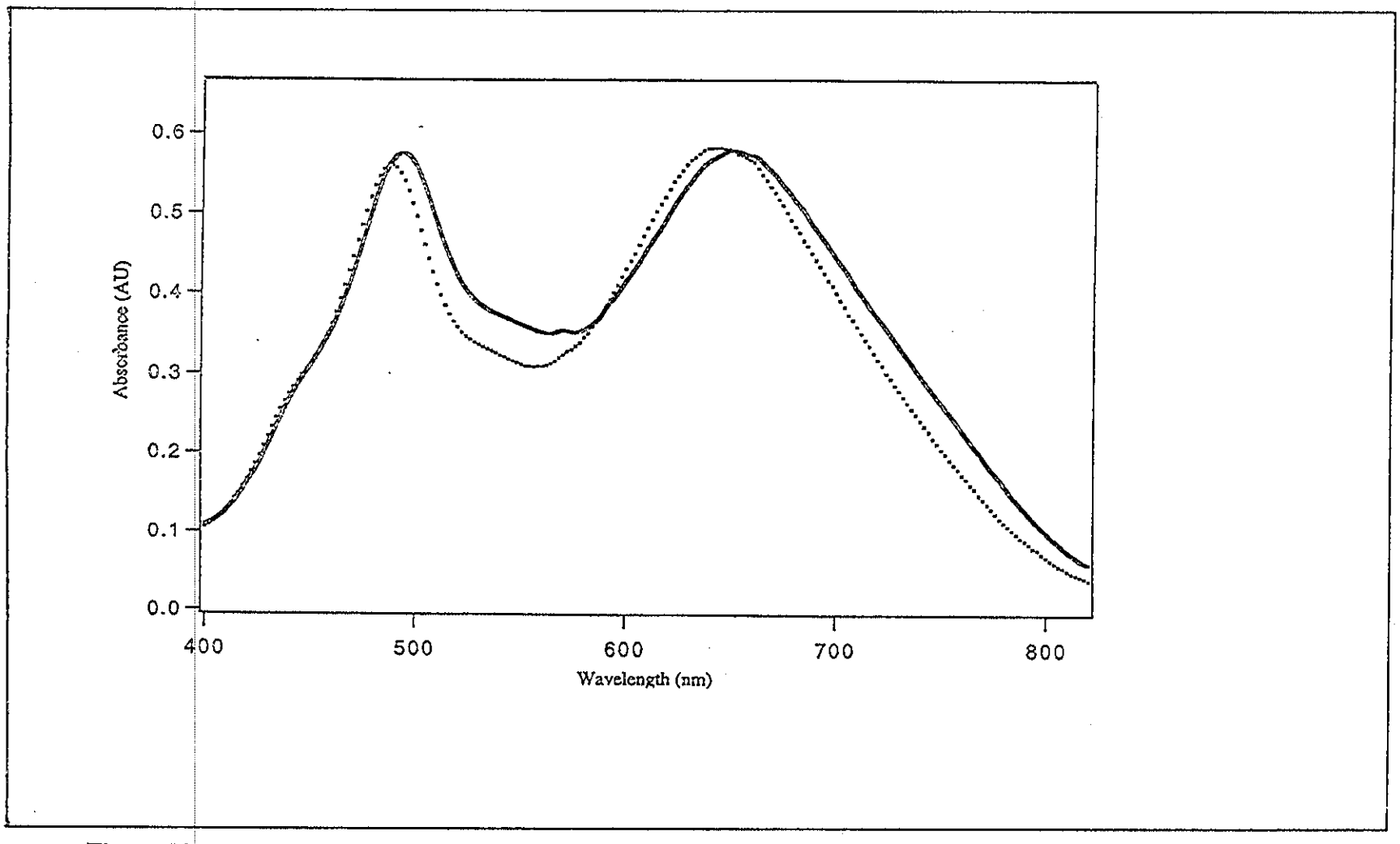

Figure 23. UV-Vis absorption spectra of *trans*-$Ru(deazpy)_2Cl_2$ in dimethylsulfoxide (__) and $CHCl_3$ (...)

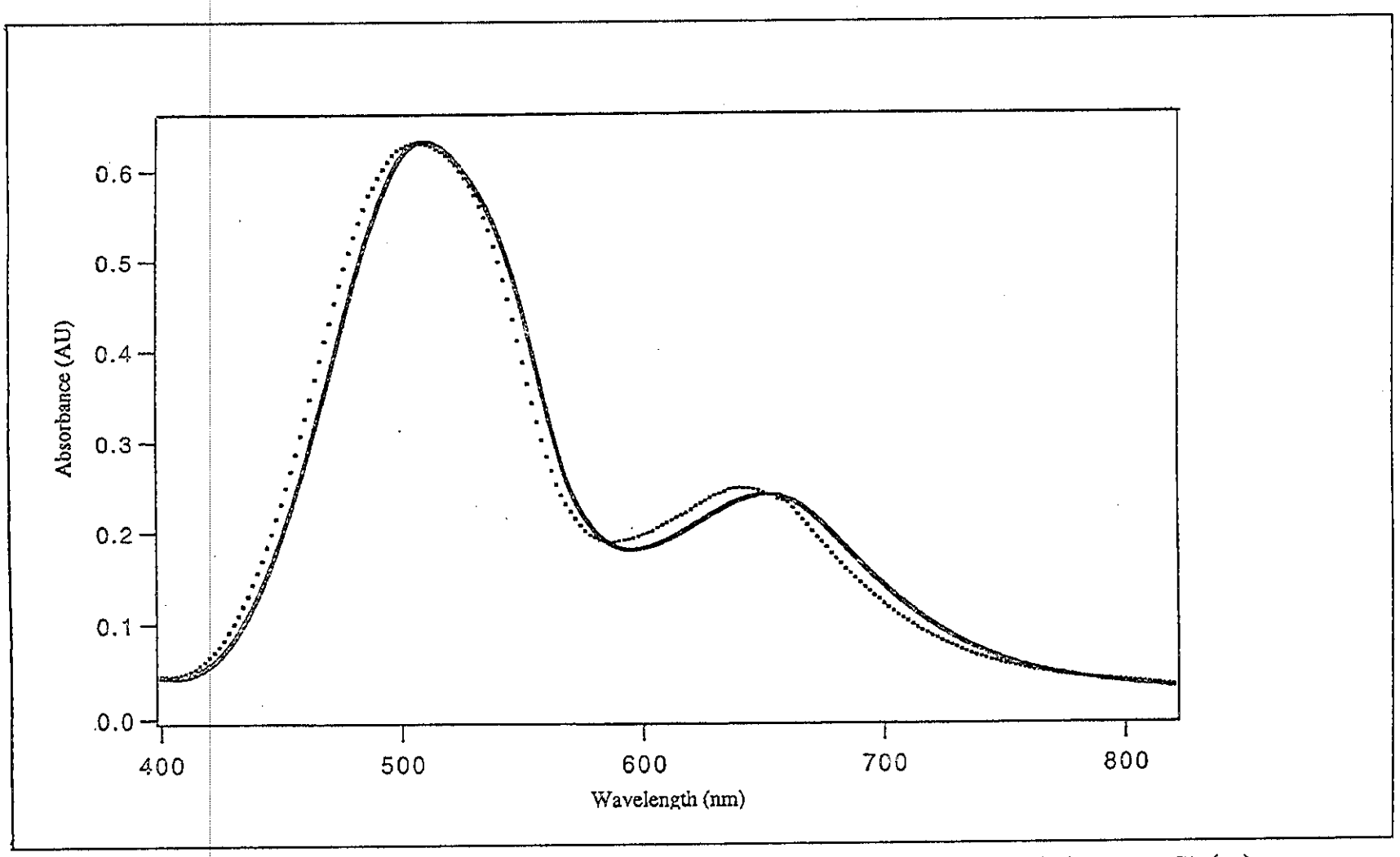

Figure 24. UV-Vis absorption spectra of *cis*-$Ru(dmazpy)_2Cl_2$ in dimethylsulfoxide (__) and $CHCl_3$ (...)

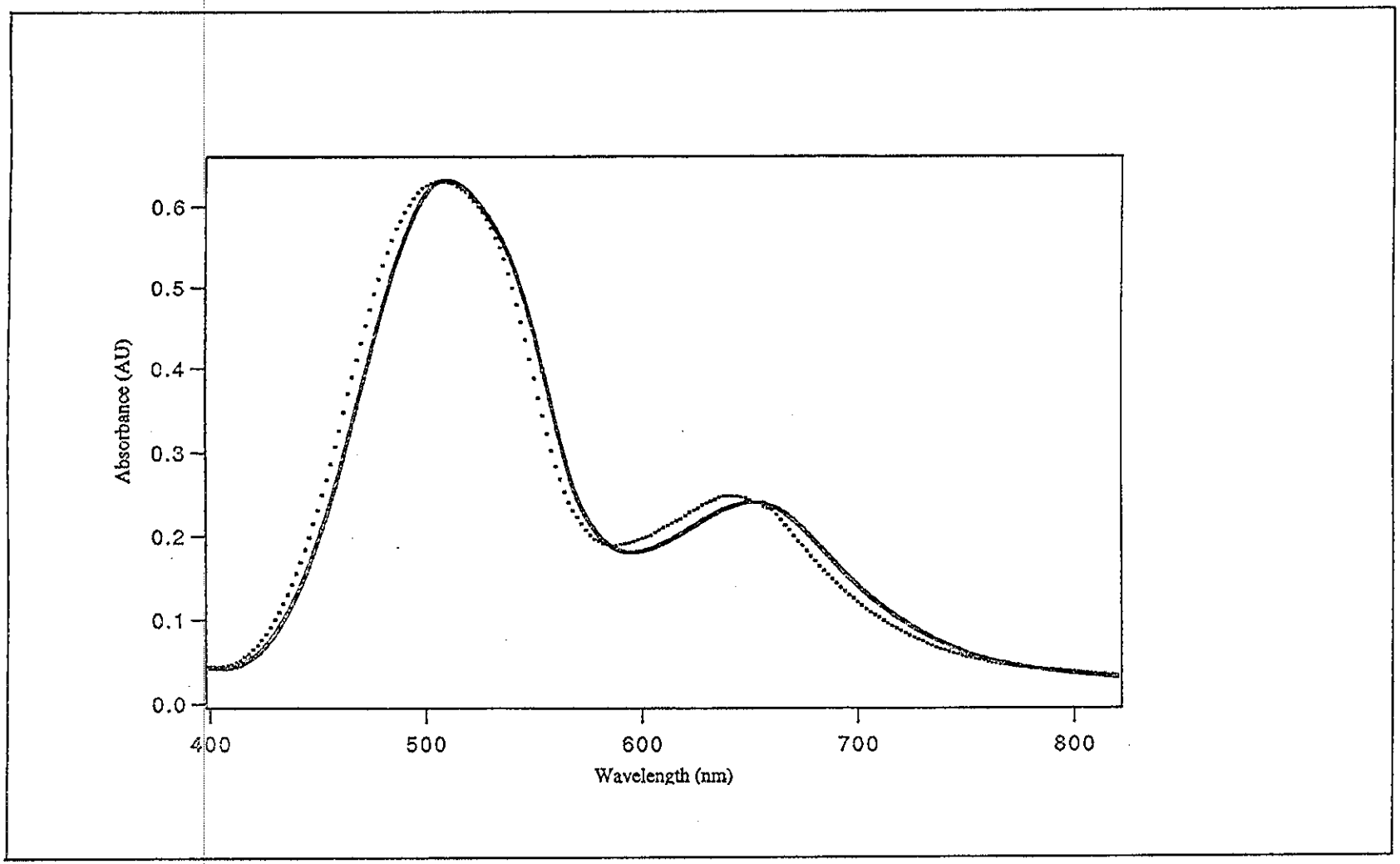

Figure 25. UV-Vis absorption spectra of *cis*-$Ru(deazpy)_2Cl_2$ in dimethylsulfoxide (__) and $CHCl_3$ (...)

3.2.3.4 ^{1}H NMR spectroscopic results of $Ru(L)_2Cl_2$ (L = dmazpy and deazpy) complexes.

Results from ^{1}H-NMR analysis are useful to characterize the isomeric structures of the complexes. The ^{1}H-NMR spectra of *trans*-and *cis*-$Ru(L)_2Cl_2$ show only one set of ligand peaks, indicating two equivalent ligands therefore the complexes must be symmetric due to the C_2 axis. The symmetries are C_{2v} for *trans*-$Ru(L)_2Cl_2$ and C_2 for *cis*-$Ru(L)_2Cl_2$ complexes. The protons can be divided into 7 groups in case of *trans*-and *cis*-$Ru(dmazpy)_2Cl_2$ and 8 groups for *trans*-and *cis*-$Ru(deazpy)_2Cl_2$. The structures with proton numbering systems are shown in Figure 26 and 27. The symbol of ' is referred to the equivalent proton. The ^{1}H-NMR spectra of *trans*-$Ru(dmazpy)_2Cl_2$, *trans*-$Ru(deazpy)_2Cl_2$, cis-$Ru(dmazpy)_2Cl_2$ and *cis*-$Ru(deazpy)_2Cl_2$ are displayed in Figure 28-31 respectively. The summarized data of ^{1}H-NMR analysis are shown in Table 23-26.

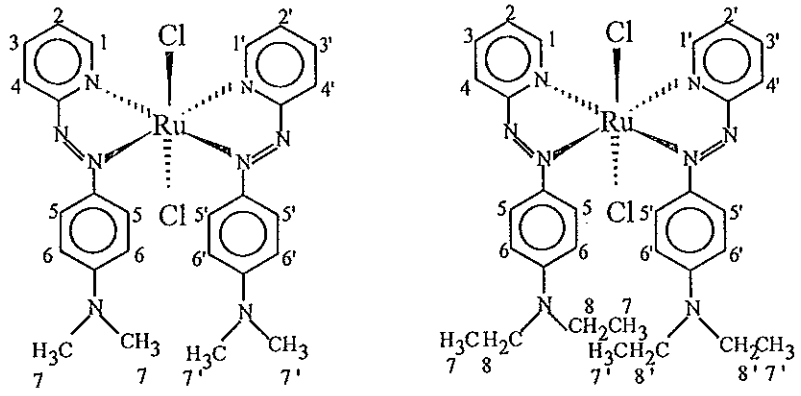

Figure 26. The structure of *trans*-$Ru(dmazpy)_2Cl_2$ and *trans*-$Ru(deazpy)_2Cl_2$ complex with proton numbering systems.

Table 23. ^{1}H NMR data for *trans*-Ru(dmazpy)$_2$Cl$_2$ complex.

H-position	J-coupling (Hz)	δ (ppm)	amounts of H	peak
1,1'	9	8.933	2	d
4,4'	8.5	8.417	2	d
2,2'	7.5,8	8.056	2	dt
5,5'	8,7.5	7.619	4	d
3,3'	-	7.602	2	dt
6,6'	9	6.206	4	d
7,7'	-	2.995	12	s

d = doublet dt = doublet of triplet s = singlet

Table 24. ^{1}H NMR data for *trans*-Ru(deazpy)$_2$Cl$_2$ complex

H-position	J-coupling (Hz)	δ (ppm)	amounts of H	peak
1,1'	9	8.923	2	d
4,4'	9	8.441	2	d
2,2'	8,7.5	8.028	2	dt
5,5'	6,6.5	7.720	4	d
3,3'	9.3	7.582	2	dt
6,6'	9.3	6.230	4	d
8,8'	9,7.2,9	3.314	8	q
7,7'	7.2,9	1.152	12	t

d = doublet dt = doublet of triplet t = triplet q = quartet

The pattern of ^{1}H NMR signals of *trans*-Ru(dmazpy)$_2$Cl$_2$ and *trans*-Ru(deazpy)$_2$ Cl$_2$ are similar to that in the free ligands, but different in chemical shifts. The signal of protons on pyridine ring and the proton on 5,5' in *trans*-Ru(L)$_2$Cl$_2$ complexes are shifted to downfield. In case of *trans*-Ru(deazpy)$_2$Cl$_2$ complexes, the protons of alkyl

groups are found quatet and triplet, respectively. This is due to ligand coordinated with Ru(II) and effects from Cl atoms in complexes. However, ^{1}H NMR spectra of complexes are more complicate than that of free ligands.

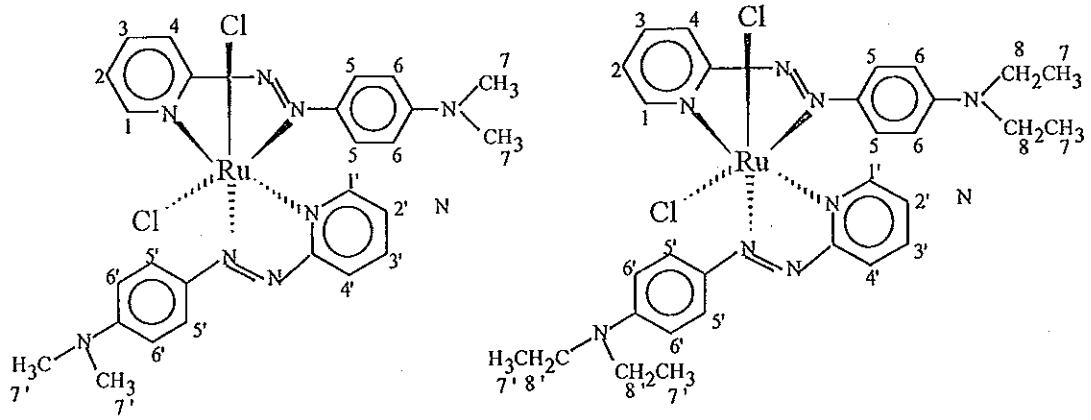

Figure 27. The structures of *cis*-Ru(dmazpy)$_2$Cl$_2$ and *cis*-Ru(deazpy)$_2$Cl$_2$ complexes with proton numbering systems.

Table 25. ^{1}H NMR data for *cis*- Ru(dmazpy)$_2$Cl$_2$ complex

H-position	J-coupling (Hz)	δ (ppm)	amounts of H	peak
1,1'	9.0	9.517	2	d
4,4'	8.0	8.342	2	d
2,2'	7.5,8.0	7.434	2	dt
3,3'	8.5,8.5	7.529	2	dt
5,5'	9.5	6.814	4	d
6,6'	9.0	6.234	4	d
7,7'	-	2.989	12	s

d = doublet dt = doublet of triplet s = singlet

Table 26. ^{1}H NMR data for *cis*-Ru(deazpy)$_2$Cl$_2$ complex

H-position	J-coupling (Hz)	δ (ppm)	amounts of H	peak
1,1'	7.5	9.506	2	d
4,4'	8.8	8.348	2	d
2,2'	7.5,8.0	7.900	2	dt
3,3'	7.0,7.0	7.413	2	dt
5,5'	9.0	6.790	4	d
6,6'	9.0	6.240	4	d
7,7'	7.0,7.0,7.1	3.305	8	q
8,8'	7.2,7.1	1.660	12	t

d = doublet dt = doublet of triplet t = triplet q = quartet

The ^{1}H NMR results of *cis*-Ru(deazpy)$_2$Cl$_2$ are similar to those of *cis*-Ru (dmazpy)$_2$Cl$_2$ but slightly different from those in *trans*- isomers and the free ligands. The signals of protons on pyridine ring are observed at downfield than phenyl protons, proton-1,1' because of the effects from Cl and pyridine nitrogen atoms in *cis*-position. Therefore, the proton-1,1' of *cis*-complexes are shifted further downfield as doublet signal at 9.51 ppm. This is shifted from that of free ligands about 0.90 ppm and from *trans*- Ru(deazpy)$_2$Cl$_2$ 0.60 ppm.

The chemical shifts of proton-3,3' and proton-5,5' can be used to identify the *cis*- and *trans*- isomers. In case of the *trans*- isomers, the signal of proton-5,5' move downfield than proton-3,3' but the *cis*- isomers give the opposite results due to different position of Cl atoms in their structures.

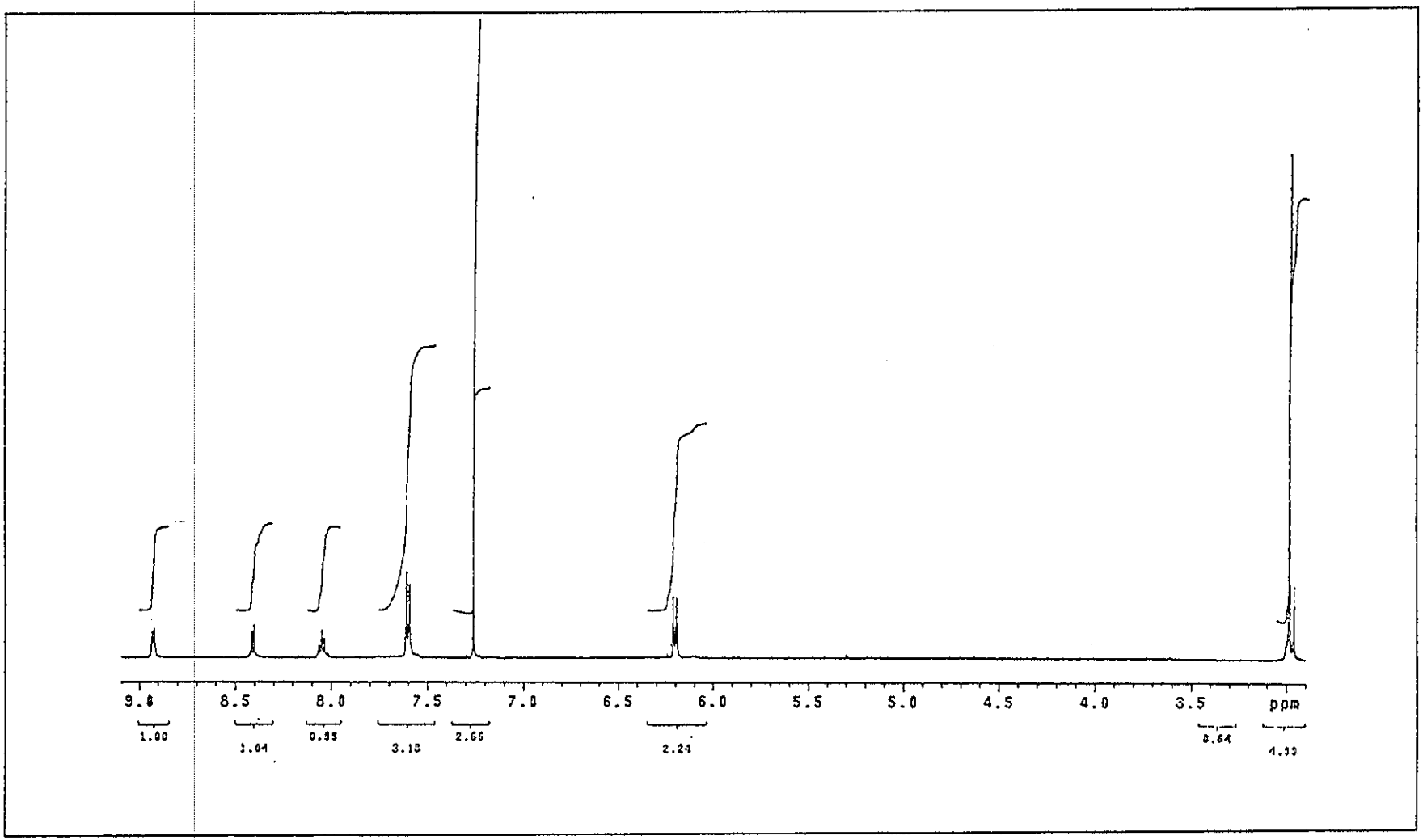

Figure 28. ^{1}H NMR spectrum of *trans*-Ru(dmazpy)$_2$Cl$_2$

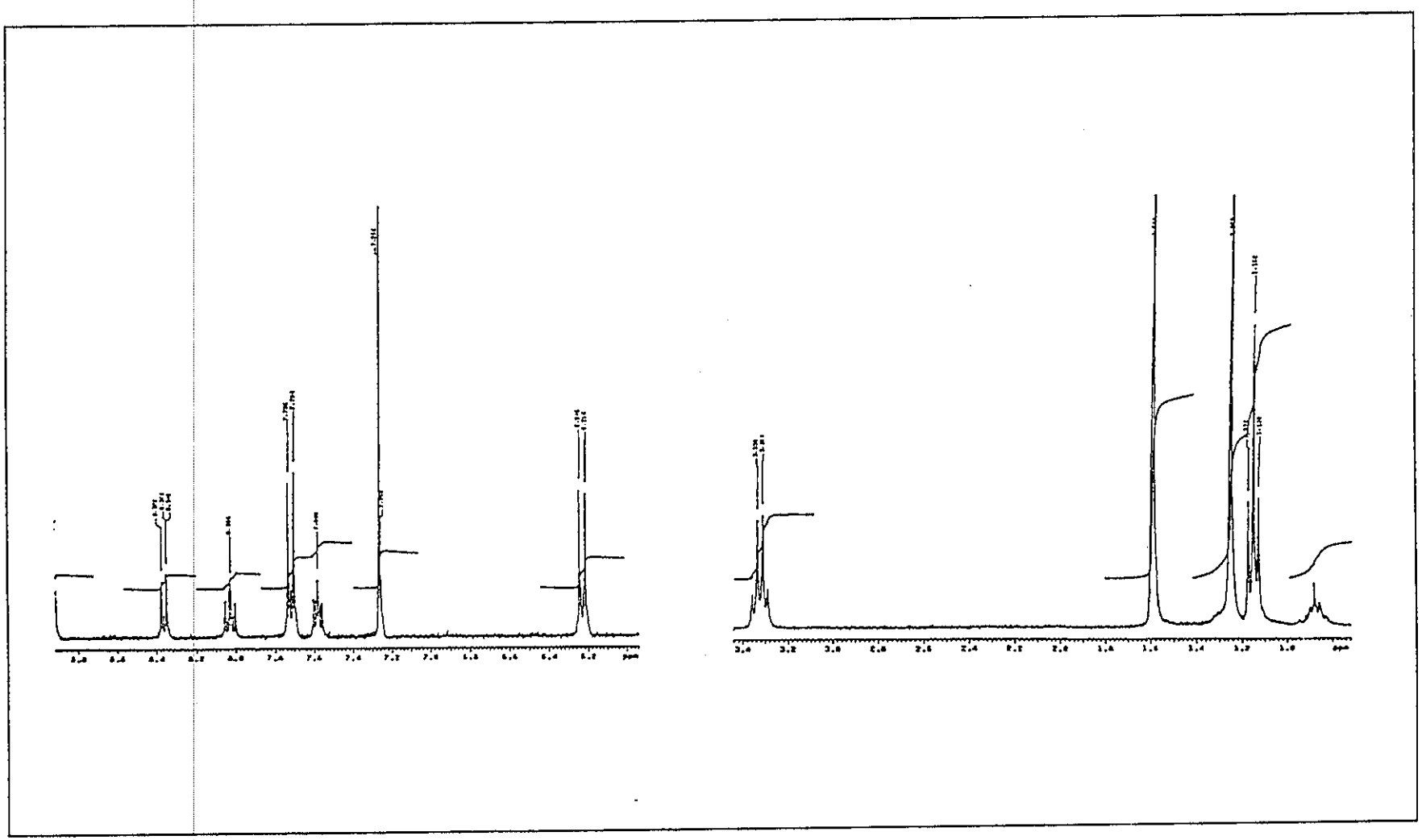

Figure 29. ^{1}H NMR spectrum of *trans*-$Ru(deazpy)_2Cl_2$

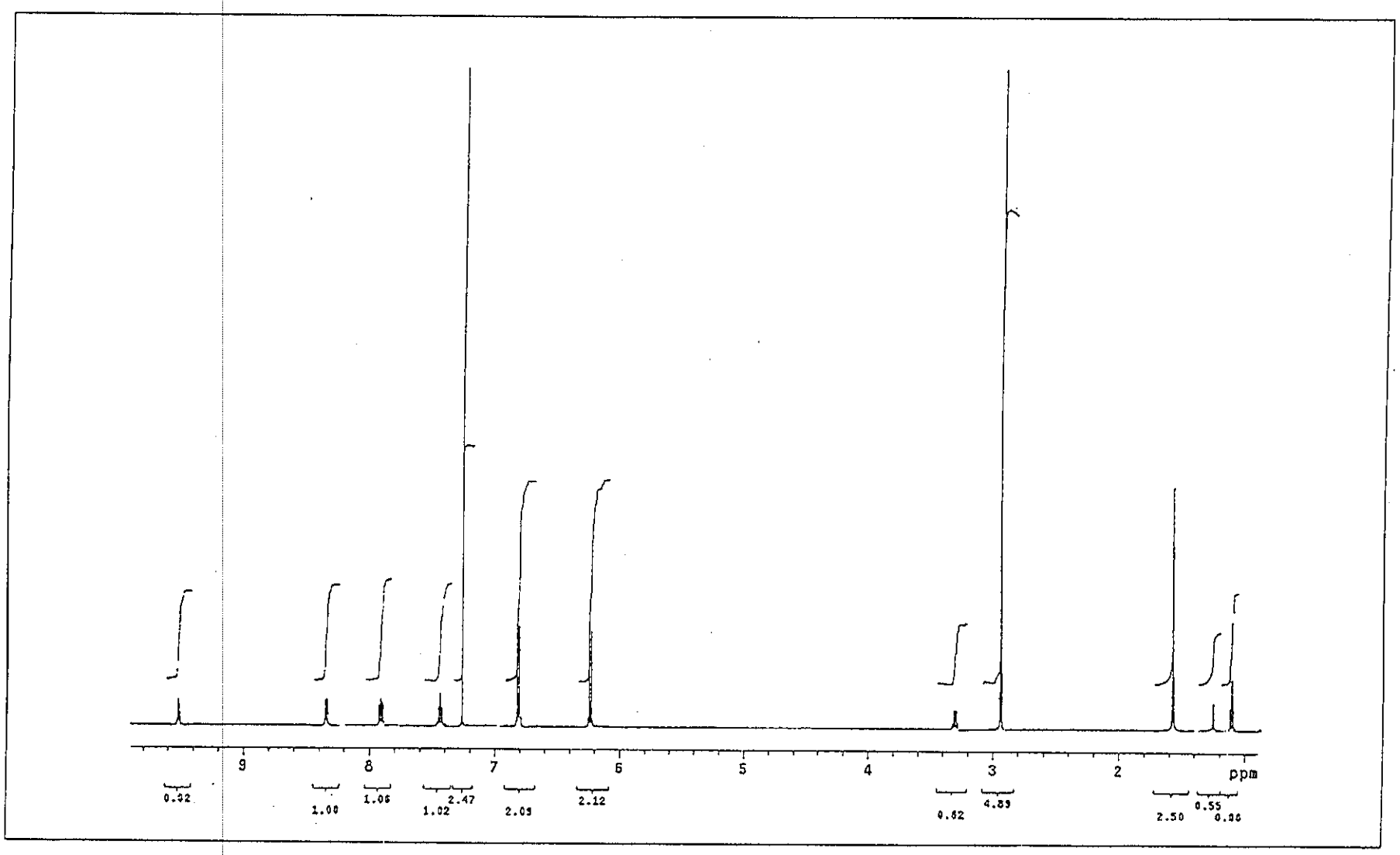

Figure 30. ^{1}H NMR spectrum of *cis*-$Ru(dmazpy)_2Cl_2$

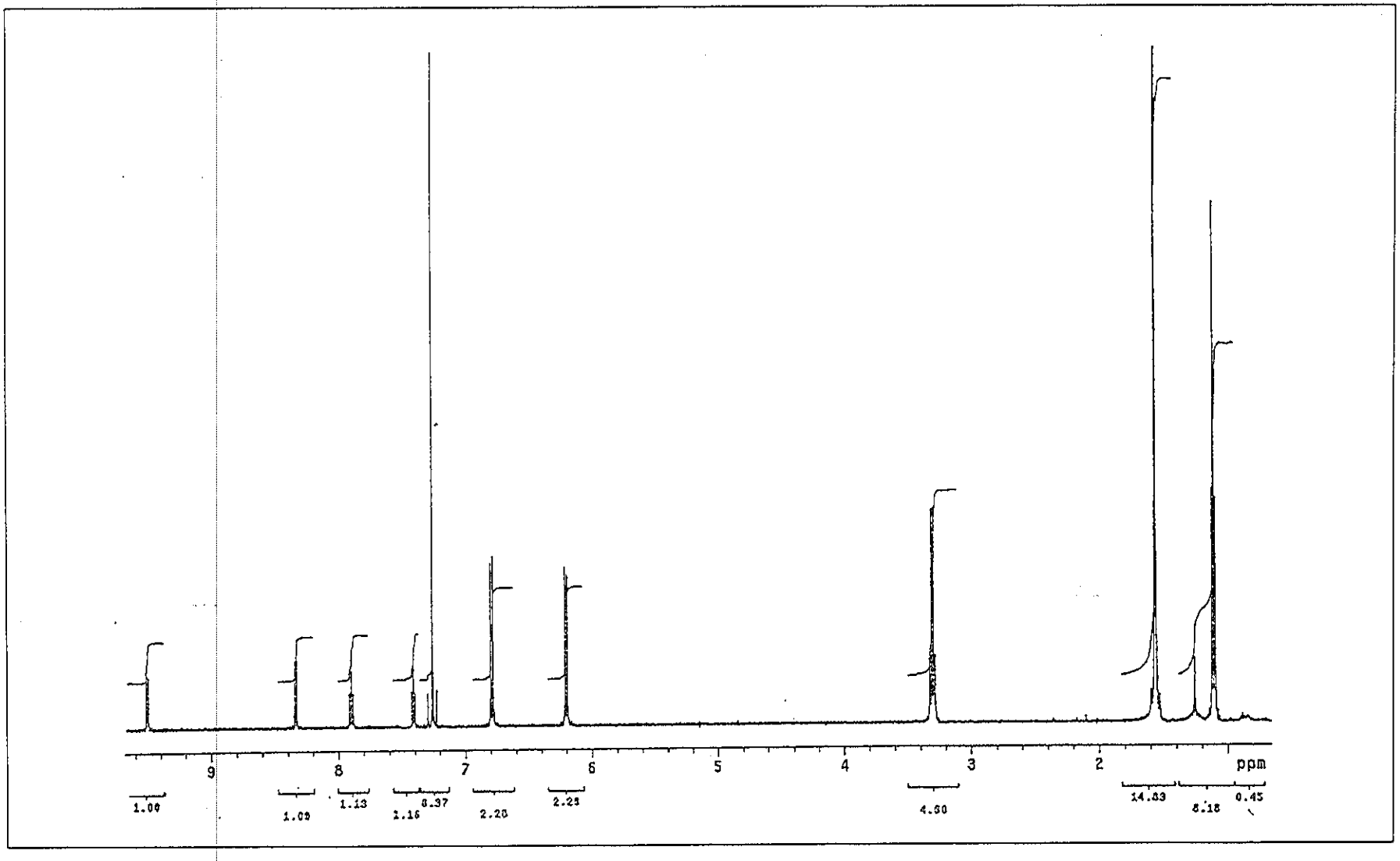

Figure 31. ^{1}H NMR spectrum of *cis*-Ru(deazpy)$_2$Cl$_2$

3.2.3.5 X-ray diffraction data

X-ray structure of *trans*-Ru(dmazpy)$_2$Cl$_2$

The single crystals of *trans*-Ru(dmazpy)$_2$Cl$_2$ complexes were grown in the mixture of CH_2Cl_2, ethanol and 0.1 M HCl (2:1:0.5 v/v). Data of the crystal and collection parameters are listed in Table 27. The structure of this complex is shown in Figure 32.

The coordinated ruthenium is distorted octahedral structure which can be seen from the angle around ruthenium ion. The average bond angles of atoms in trans position of Ru(II) center, Cl(1)-Ru-Cl(1), N(1)-Ru-N(7) and N(3)-Ru-N(5) are in the range 172-178°, sligthly deviated from the ideal octahedral (180°). Besides, the orthogonal angles around Ru(II) are in the range 86-96° to 90° in ideal octahedral. The average bond distances of Ru-Cl are 2.388(6) Å whereas, the average Ru-N(py) are 2.066(2) Å and the Ru-N(azo) bond lengths are 2.022(2) Å. The atomic arrangement in this complex involves of two *trans*-Chlorine, *cis*-N(py) and *cis*-N(azo) corresponding to *trans-cis-cis*-Ru(dmazpy)$_2$Cl$_2$ configuration, *trans*-Ru(dmazpy)$_2$Cl$_2$ (Figure 12). The planes of chelate (I) Ru(1), N(1), C(5), N(2), N(3) and chelate (II) Ru(1), N(5), C(18), N(6), N(7) are planar with dihedral angle 4.6(1)°. The pendant phenylazo rings are distorted from chelate rings with 42.3(1)° and 44.2(1)°. Selected bond distances and angles of *trans*-Ru(dmazpy)$_2$Cl$_2$ are listed in Table12. Because of the similarity of azoimine groups, we emphasize comparison of the X-ray data between the complexes of *trans*-Ru(dmazpy)$_2$Cl$_2$ and *trans*-Ru(azpy)$_2$Cl$_2$ (Velders *et al.*, 2000) in order to π-accepting properties of these ligands and effects of the -N(CH$_3$)$_2$ substituent groups. The X-ray data of *trans*-Ru(azpy)$_2$Cl$_2$ is also collected in Table 28. Furthermore, comparison of the dihedral angles in different planes of both complexes are given in Table 29.

Table 27. Crystallographic data for *trans*-$Ru(dmazpy)_2Cl_2$ and *trans*-$Ru(azpy)_2Cl_2$ complexes.

crystal parameters	*trans*-$Ru(dmazpy)_2Cl_2$	*trans*-$Ru(azpy)_2Cl_2$
empirical formula	$C_{26}H_{30}Cl_2N_8ORu$	$C_{22}H_{18}Cl_2N_6Ru$
fw	624.55	538.39
crystal system	monoclinic	hexagonal
space group	$P2_1/c$	P65
a, Å	13.3094(2)	22.2928(19)
b, Å	16.4610(2)	22.2928(19)
c, Å	12.1444(1)	8.5121(10)
α, °	90	90
β, °	91.2217(8)	90
γ, °	90	120
V, $Å^3$	2660.06(5)	3663.5(6)
Z	4	6
T,K	123(1)	150
λ, Å	0.71073	0.71073
ρ_{calcd}, g cm^{-3}	1.604	1.464
μ(Mo K_α), cm^{-1}	1.004	
abs coeff	0.827	0.881
param refined	343	281
R, %	0.0253	0.0557
R_w %	0.0308	0.1055
GOF	0.959	1.190

Table 28. Selected bond distances (Å) and angles (°) and their estimated standard deviations for *trans*-$Ru(dmazpy)_2Cl_2$ and *trans*-$Ru(azpy)_2Cl_2$

		Distances	
(i) *trans*-$Ru(dmazpy)_2Cl_2$		(ii) *trans*-$Ru(azpy)_2Cl_2$	
Ru(1)-Cl(1)	2.377(6)	Ru(1)-Cl(1)	2.377(15)
Ru(1)-Cl(2)	2.398(6)	Ru(1)-Cl(2)	2.368(16)
Ru(1)-N(1)	2.062(2)	Ru(1)-N(1)	2.116(5)
Ru(1)-N(5)	2.070(2)	Ru(1)-N(21)	2.099(5)
Ru(1)-N(3)	2.018(2)	Ru(1)-N(8)	1.986(5)
Ru(1)-N(7)	2.027(2)	Ru(1)-N(28)	1.988(5)
N(1)-C(5)	1.361(3)	N(1)-C(2)	1.356(9)
N(3)-C(6)	1.410(3)	N(8)-C(9)	1.430(9)
N(5)-C(18)	1.360(3)	N(21)-C(22)	1.347(8)
N(7)-C(19)	1.408(3)	N(28)-C(29)	1.450(9)
N(2)-N(3)	1.304(2)	N(7)-N(8)	1.302(8)
N(6)-N(7)	1.302(2)	N(27-N(28)	1.306(7)
		Angles	
Cl(2)-Ru(1)-Cl(1)	172.90(2)	Cl(2)-Ru(1)-Cl(1)	70.50(7)
N(1)-Ru(1)-N(7)	178.01(7)	N(1)-Ru(1)-N(28)	177.52(7)
N(3)-Ru(1)-N(5)	177.40(7)	N(8)-Ru(1)-N(21)	177.40(14)
Cl(1)-Ru(1)-N(1)	86.71(5)	Cl(1)-Ru(1)-N(1)	88.64(14)
Cl(2)-Ru(1)-N(1)	90.47(5)	Cl(2)-Ru(1)-N(1)	85.64(14)
Cl(1)-Ru(1)-N(5)	88.51(5)	Cl(1)-Ru(1)-N(21)	85.71(12)
Cl(2)-Ru(1)-N(5)	85.74(5)	Cl(2)-Ru(1)-N(21)	88.15(12)
Cl(1)-Ru(1)-N(7)	94.49(5)	Cl(1)-Ru(1)-N(28)	88.88(13)
Cl(2)-Ru(1)-N(7)	88.16(5)	Cl(2)-Ru(1)-N(28)	96.63(13)
Cl(1)-Ru(1)-N(3)	89.51(5)	Cl(1)-Ru(1)-N(8)	96.87(13)
Cl(2)-Ru(1)-N(3)	96.11(5)	Cl(2)-Ru(1)-N(8)	89.34(13)

N(1)-Ru(1)-N(3)	75.63(7)	N(1)-Ru(1)-N(8)	76.4(2)
N(7)-Ru(1)-N(5)	75.90(7)	N(28)-Ru(1)-N(21)	75.80(19)
N(7)-Ru(1)-N(3)	105.94(7)	N(28)-Ru(1)-N(8)	103.8(7)
N(1)-Ru(1)-N(5)	102.56(7)	N(1)-Ru(1)-N(21)	104.1(2)

Table 29. Dihedral angles of different planes.

Planes	*trans*-Ru(dmazpy)$_2$Cl$_2$	*trans*-Ru(azpy)$_2$Cl$_2$
pyridine- azo	11.1(1)	11.0(3)
	16.9(1)	11.5(4)
azo -phenyl	35.1(1)	51.72(3)
	30.5(1)	55.0(5)
pyridine - phenyl	37.1(1)	52.7(3)
	33.8(1)	54.3(3)
chelate rings	4.6(1)	3.6(3)
phenyl rings	14.2(1)	23.7(2)
Pyridine-chelate	10.9(1)	9.4(2)
	15.6(1)	10.5(2)
Phenyl - chelate	42.3(1)	58.3(2)
	44.2(1)	60.5(2)

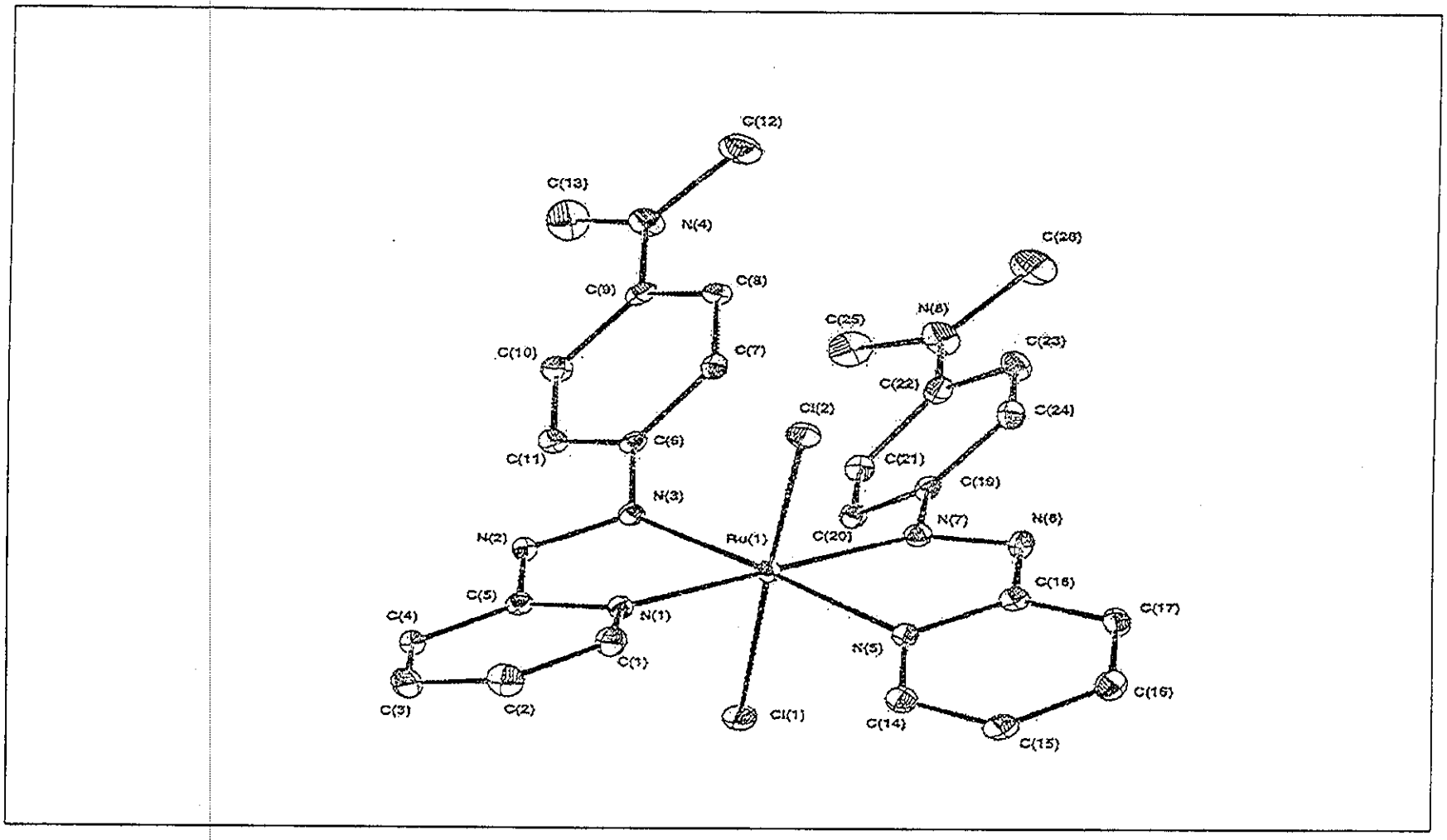

Figure 32. X-ray structure of *trans*-Ru(dmazpy)$_2$Cl$_2$

X-ray structure of *trans*-Ru(deazpy)$_2$Cl$_2$

The single crystals of *trans*-Ru(deazpy)$_2$Cl$_2$ complexes were grown in the mixture of dichloromethane, toluene and acetonitrile. The ratio by volume was 2:2:1. Crystallographic data are given in Table 30. The structure of this complex is similar to *trans*-Ru(dmazpy)$_2$Cl$_2$ which is *trans-cis-cis* configuration (Figure 33). The coordinated ruthenium is distorted octahedral structure. The average bond angles of atoms in *trans* position of Ru(II) center, Cl(1)-Ru-Cl(1), N(1)-Ru-N(7) and N(3)-Ru-N (5) are in the range 171-177° which deviated from the ideal octahedral (180°). Besides, the orthogonal angles around Ru(II) are in the range 85-96° compared to 90° in ideal octahedral. In addition, the average distances of Ru-Cl are 2.382(2) Å whereas, the average Ru-N(py) and the Ru-N(azo) bond lengths are 2.001(2) Å and 2.001 Å, respectively. The planes of two chelate rings Ru(1), N(1), C(5), N(2), N(3) and Ru(1), N(5), C(20), N(6), N(7) are planar (dihedral angle = 2.533 °). The pendant phenyl azo rings are distorted from chelate rings with angles 53.217 ° and 47.760 °. The bond distances and the dihedral angles of planes are listed in Table 31 and Table 32, respectively. The distances of Ru-Cl, Ru-N(py) and Ru-N(azo) are different from those in *trans*-Ru(dmazpy)$_2$Cl$_2$ complex. This could be due to the steric effect of substituent in deazpy ligand.

Table 30. Crystallographic data for *trans*-$Ru(deazpy)_2Cl_2$

Crystal parameters	*trans*-$Ru(deazpy)_2Cl_2$
empirical formula	$C_{30}H_{36}Cl_2N_8Ru$
fw	680.64
cryst system	monoclinic
space group	$P2_1$
a, Å	8.5023(2)
b, Å	12.4994(3)
c, Å	14.9986(4)
α, °	90
β, °	105.7788(9)
γ, deg	90
V, $Å^3$	2660.06(5)
Z	2
T, K	123(1)
λ, Å	0.71073
ρ_{calcd}, g cm^{-3}	1.474
μ(Mo Kα), cm^{-1}	7.20
R, %	0.039
R_w %	0.041
GOF	1.17

Table 31. Selected bond distances (Å) and angles (°) and their estimated standard deviations for *trans*-$Ru(deazpy)_2Cl_2$.

		Distances	
(i) *trans*-$Ru(deazpy)_2Cl_2$		(ii) *trans*-$Ru(dmazpy)_2Cl_2$	
Ru(1)-Cl(1)	2.388(2)	Ru(1)-Cl(1)	2.377(6)
Ru(1)-Cl(2)	2.377(2)	Ru(1)-Cl(2)	2.398(6)
Ru(1)-N(1)	2.088(5)	Ru(1)-N(1)	2.062(2)
Ru(1)-N(5)	2.087(5)	Ru(1)-N(5)	2.070(2)
Ru(1)-N(3)	1.990(5)	Ru(1)-N(3)	2.018(2)
Ru(1)-N(7)	2.011(5)	Ru(1)-N(7)	2.027(2)
N(1)-C(5)	1.359(7)	N(1)-C(5)	1.361(3)
N(3)-C(6)	1.433(8)	N(3)-C(6)	1.410(3)
N(5)-C(20)	1.357(7)	N(5)-C(18)	1.360(3)
N(7)-C(21)	1.421(8)	N(7)-C(19)	1.408(3)
N(2)-N(3)	1.313(6)	N(2)-N(3)	1.304(2)
N(6)-N(7)	1.299(7)	N(6)-N(7)	1.302(2)
		Angles	
Cl(2)-Ru(1)-Cl(1)	171.47(6)	Cl(2)-Ru(1)-Cl(1)	172.90(2)
N(1)-Ru(1)-N(7)	178.5(2)	N(1)-Ru(1)-N(7)	178.01(7)
N(3)-Ru(1)-N(5)	177.40(7)	N(3)-Ru(1)-N(5)	177.40(7)
Cl(1)-Ru(1)-N(1)	85.2(2)	Cl(1)-Ru(1)-N(1)	86.71(5)
Cl(2)-Ru(1)-N(1)	90.47(5)	Cl(2)-Ru(1)-N(1)	90.47(5)
Cl(1)-Ru(1)-N(5)	84.7(1)	Cl(1)-Ru(1)-N(5)	88.51(5)
Cl(2)-Ru(1)-N(5)	89.3(1)	Cl(2)-Ru(1)-N(5)	85.74(5)
Cl(1)-Ru(1)-N(7)	88.2(2)	Cl(1)-Ru(1)-N(7)	94.495)
Cl(2)-Ru(1)-N(7)	96.2(1)	Cl(2)-Ru(1)-N(7)	88.16(5)
Cl(1)-Ru(1)-N(3)	96.5(1)	Cl(1)-Ru(1)-N(3)	89.51(5)
Cl(2)-Ru(1)-N(3)	89.5(1)	Cl(2)-Ru(1)-N(3)	96.11(5)
N(1)-Ru(1)-N(3)	75.7(2)	N(1)-Ru(1)-N(3)	75.63(7)

N(7)-Ru(1)-N(5)	75.8(2)	N(7)-Ru(1)-N(5)	75.90(7)
N(7)-Ru(1)-N(3)	104.6(2)	N(7)-Ru(1)-N(3)	105.94(7)
N(1)-Ru(1)-N(5)	103.9(2)	N(1)-Ru(1)-N(5)	102.56(7

Table 32. Dihedral angles of different planes.

Planes	*trans*-Ru(deazpy)$_2$Cl$_2$	*trans*-Ru(azpy)$_2$Cl$_2$
pyridine- azo	14.2(3)	11.0(3)
	8.0(1)	11.5(4)
azo -phenyl	44.4(4)	51.72(3)
	39.5(4)	55.0(5)
pyridine - phenyl	49.0(2)	52.7(3)
	38.4(2)	54.3(3)
chelate rings	2.5(2)	3.6(3)
phenyl rings	20.7(2)	23.7(2)
pyridine-chelate	10.4(2)	9.4(2)
	11.6(2)	10.5(2)
phenyl - chelate	53.2(2)	58.3(2)
	44.8(1)	60.5(2)

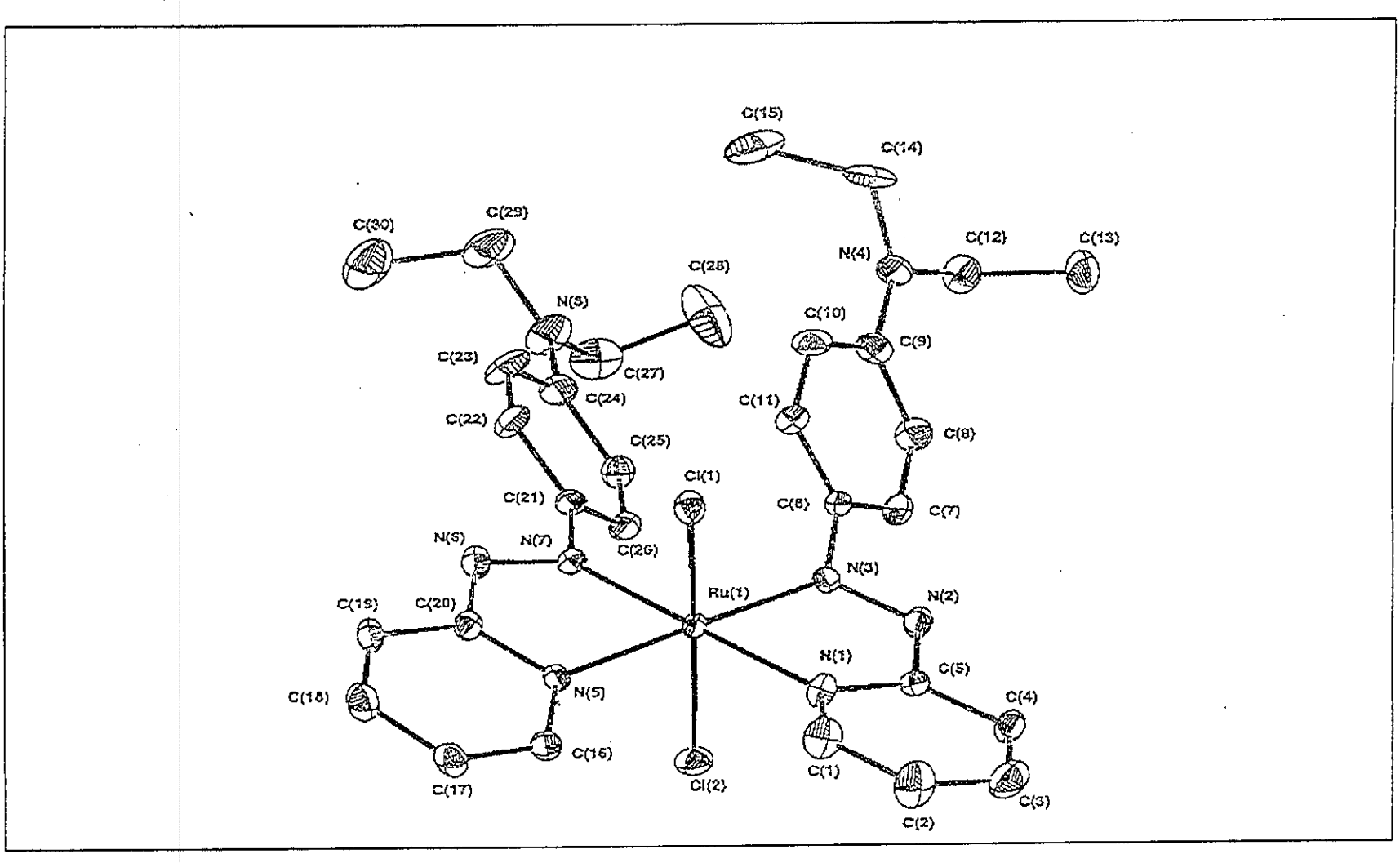

Figure 33. X-ray structure of *trans*-Ru(deazpy)$_2$Cl$_2$

X-ray structure of *cis*-Ru(dmazpy)$_2$Cl$_2$

The single crystals of *cis*-Ru(dmazpy)$_2$Cl$_2$ complex were obtained from CH_2Cl_2 : toluene : acetonitrile (2:1:1 ratio by volume). X-ray structure of this complex is shown in Figure 34. In addition, crystallographic data and collection parameters are listed in Table 33. The selected bond distances and angles are summarized in Table 34. The structure of *cis*-Ru(dmazpy)$_2$Cl$_2$ complex is distorted octahedral that one can observe from the angles of atoms which coordinated with ruthenium(II). The average bond angles of atoms in *trans* position of Ru(II) center, N(1)-Ru-N(5), Cl(1)-Ru-N(3) and Cl(2)-Ru-N(7) are in the range 170-178° which deviated from the ideal octahedral (180°). Besides, the orthogonal angles around Ru(II) are in the range 86-95° whereas, are 90° in ideal octahedral. In addition, the average distances of Ru-Cl are 2.406(8) Å whereas, the average Ru-N(py) lengths are 2.045(3) Å and the Ru-N(azo) are averaged to 2.000(3) Å. The atomic arrangement implicates Cl atoms are *cis* whereas, both N (py) atoms are *trans* geometry. The structure corresponds to *cis-trans-cis* configuration (*cis*-Ru(dmazpy)$_2$Cl$_2$) . Chelate rings Ru(1), N(5), C(18), N(6), N(7) and Ru(1), N(1), C(5), N(2), N(3) are co planar with the dihedral angle 78.839°. The dihedral angles of pyridine rings are 73.544°. Whereas, the dihedral angle of phenyl rings is 5.845°. The dihedral angles of the different planes are shown in Table 35.

Table 33. Crystallographic Data for *cis*-$Ru(dmazpy)_2Cl_2$ and *cis*-$Ru(azpy)_2Cl_2$ complexes

Crystal parameters	*cis*-$Ru(dmazpy)_2Cl_2$	*cis*-$Ru(azpy)_2Cl_2$
empirical formula	$C_{26}H_{30}Cl_2N_8Ru$	$C_{22}H_{18}Cl_2N_6Ru$
fw	624.55	538.39
cryst system	monoclinic	hexagonal
space group	$P2_1/c$	P65
a, Å	13.3094(2)	22.2928(19)
b, Å	16.4610(2)	22.2928(19)
c, Å	12.1444(1)	8.5121(10)
α,°	90	90
β,°	91.2217(8)	90
γ,°	90	120
V, $Å^3$	2660.06(5)	3663.5(6)
Z	4	6
T,K	123(1)	150
λ, Å	0.71073	0.71073
ρ_{calcd}, g cm^{-3}	1.604	1.464
μ(Mo Kα), cm^{-1}	1.004	1.004
abs coeff	0.827	0.881
param refined	343	281
R, %	0.0253	0.0557
R_w %	0.0308	0.1055
GOF	0.959	1.190

Table 34. Selected bond distances (Å) and angles (°) and their estimated standard deviations for *cis*-$Ru(dmazpy)_2Cl_2$ and *cis*-$Ru(azpy)_2Cl_2$

		Distances	
(i) *cis*-$Ru(dmazpy)_2Cl_2$		(ii) *cis*-$Ru(azpy)_2Cl_2$	
Ru(1)-Cl(1)	2.408(8)	Ru(1)-Cl(1)	2.401(1)
Ru(1)-Cl(2)	2.404(9)	Ru(1)-Cl(2)	2.397(1)
Ru(1)-N(1)	2.042(3)	Ru(1)-N(6)	2.051(4)
Ru(1)-N(5)	2.048(3)	Ru(1)-N(3)	2.045(4)
Ru(1)-N(3)	2.000(3)	Ru(1)-N(4)	1.984(4)
Ru(1)-N(7)	1.999(3)	Ru(1)-N(1)	1.977(4)
N(1)-C(5)	1.360(4)	-	-
N(3)-C(6)	1.415(4)	-	-
N(5)-C(18)	1.361(4)	-	-
N(7)-C(19)	1.415(4)	-	-
N(2)-N(3)	1.306(2)	N(4)-N(5)	1.283(6)
N(6)-N(7)	1.304(2)	N(1)-N(2)	1.279(7)
		Angles	
N(1)-Ru(1)-N(5)	177.5(1)	N(1)-Ru(1)-N(28)	177.52(7)
Cl(1)-Ru(1)-N(3)	170.06(8)	Cl(1)-Ru(1)-N(8)	96.87(13)
Cl(2)-Ru(1)-N(7)	171.16(8)	Cl(2)-Ru(1)-N(1)	89.52(16)
Cl(2)-Ru(1)-Cl(1)	92.06(3)	Cl(2)-Ru(1)-Cl(1)	89.52(6)
Cl(1)-Ru(1)-N(5)	86.28(8)	Cl(1)-Ru(1)-N(3)	95.6(1)
Cl(1)-Ru(1)-N(1)	95.22(8)	Cl(1)-Ru(1)-N(6)	89.0(1)

Cl(1)-Ru(1)-N(7)	91.81(8)	Cl(1)-Ru(1)-N(1)	-
Cl(2)-Ru(1)-N(5)	95.58(8)	Cl(2)-Ru(1)-N(3)	86.4(1)
Cl(2)-Ru(1)-N(1)	86.36(8)	Cl(2)-Ru(1)-N(6)	96.3(1)
Cl(2)-Ru(1)-N(3)	93.44(8)	Cl(2)-Ru(1)-N(4)	-
N(1)-Ru(1)-N(7)	101.2(1)	N(6)-Ru(1)-N(1)	99.2(2)
N(1)-Ru(1)-N(3)	76.9(1)	N(6)-Ru(1)-N(4)	76.6(2)
N(3)-Ru(1)-N(5)	101.4(1)	N(4)-Ru(1)-N(1)	100.5(2)
N(3)-Ru(1)-N(7)	83.9(1)	N(4)-Ru(1)-N(1)	93.5(2)
N(5)-Ru(1)-N(7)	76.7(1)	N(3)-Ru(1)-N(1)	76.1(2)

Table 35. Dihedral angles of different planes.

Planes	*cis*-Ru(dmazpy)$_2$Cl$_2$
pyridine- azo	6.4(3) 6.9(2)
azo –phenyl	39.2(3) 36.5(3)
pyridine – phenyl	42.9(1) 45.9(1)
chelate rings	78.8(1)
phenyl rings	5.8(1)
pyridine-chelate	3.8(1) 7.9(1)
phenyl – chelate	47.8(2) 44.8(1)

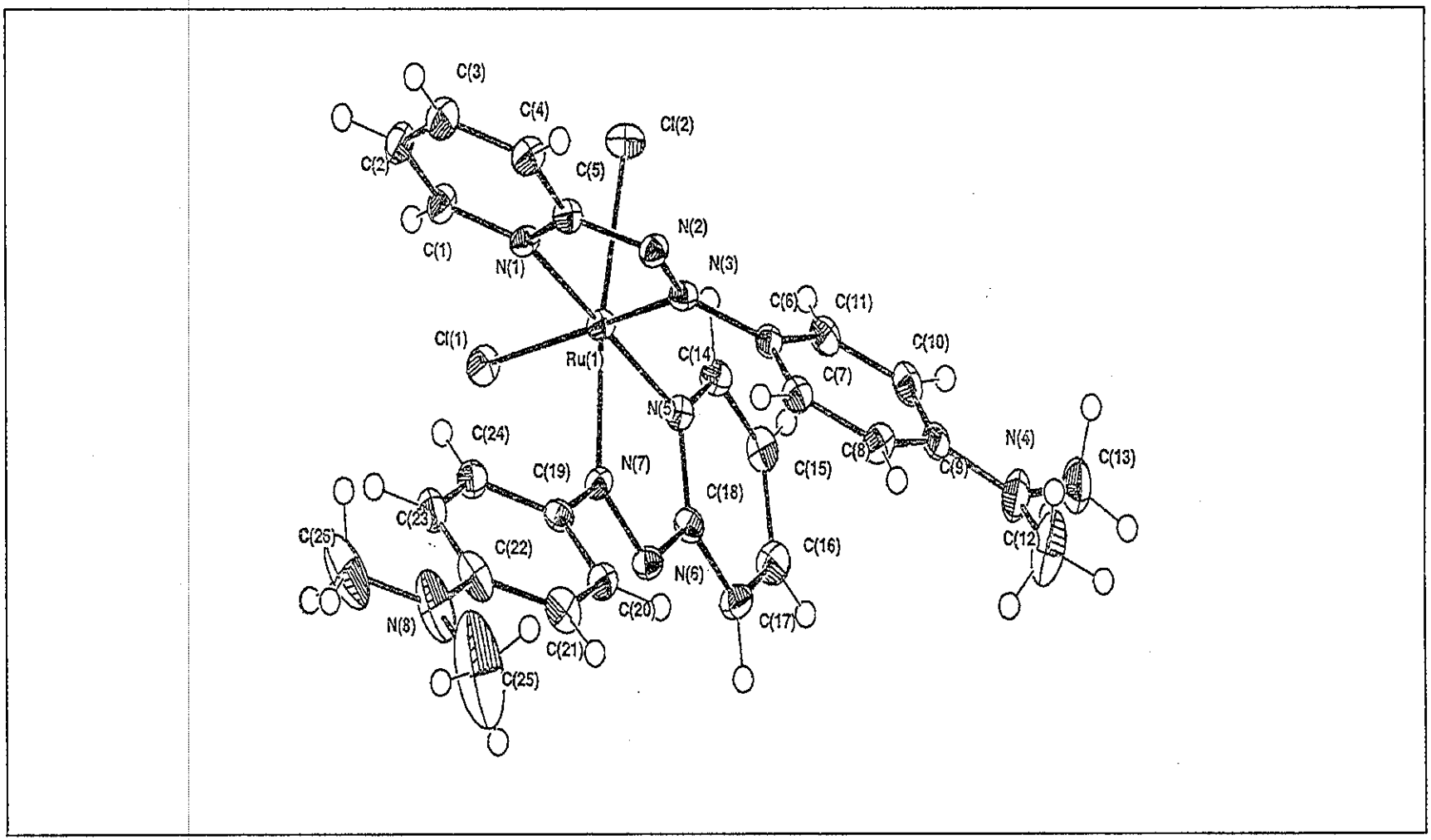

Figure 34. X-ray structure of *cis*-Ru(dmazpy)$_2$Cl$_2$

The average N=N bond distances from X-ray data of all complexes , 1.303(2) Å for *trans*-Ru(dmazpy)$_2$Cl$_2$, 1.306(6) Å for *trans*-Ru(deazpy)$_2$Cl$_2$ and 1.305(2) Å for *cis*-Ru(dmazpy)$_2$Cl$_2$, are longer than that in free ligands which were 1.270 Å for dmazpy ligand and 1.193 Å for deazpy ligand. (Hansongnern *et al.*, 2001) This was used to confirm that the π-backbonding most occurred at azo function as similar as in the case of azpy ligand.

In case of the Ru(azpy)$_2$Cl$_2$ complexes, the average N=N distances were observed at 1.281(6) Å for *cis*-Ru(azpy)$_2$Cl$_2$ complex and 1.308(8) Å for *trans*-Ru (azpy)$_2$Cl$_2$ complex whereas 1.243(2) Å was found in free azpy ligand.

The Ru-N(azo) distances were shorter than Ru-N(py). The shortening may be due to greater π-backbonding, d(Ru) $\rightarrow$ π^*(azo). Furthermore, Ru-N(azo) distances of azpy complexes were shorter than that in dmazpy and deazpy complexes whereas, the Ru-N(py) distances of dmazpy and deazpy complexes were shorter. This result will be considered further in discussion part.

3.3 Electrochemistry of Complexes.

3.3.1 Electrochemistry of dmazpy and deazpy ligands.

Electrochemical behaviors of those complexes were investigated by cyclic voltammetric methods. The cyclic voltammograms of their ligands should be considered first. Because of the similarity structures between dmazpy, deazpy and azpy ligands, it is important to compare their cyclic voltammograms. The cyclic voltammograms of azpy, dmazpy and deazpy ligands in acetonitrile solution are shown in Figure 35. The cyclic voltammograms of dmazpy and deazpy ligands are very similar. The four peaks are observed, two of those are in reduction potential range (negative potential) and the other two are in oxidation potential range (positive potential). Whereas, azpy ligand has no peaks in positive potential. All potentials are collected in Table 36. The potentials are compared with the unique potential of ferrocene couple ($E_{1/2}$ 0.090 V, ΔEp = 56 mV).

In this work, the different scan rates were applied to the electrochemical cell for inducing to redox reaction and for prove that the oxidized or reduced species in order to study if the reduced or oxidized species could be reversed back to show the redox reaction. If the redox reaction occurred, the cyclic voltammogram was shown as a couple. The couple which gave anodic currents equal to cathodic currents were referred to reversible couple. In contrast, the unequal currents were referred to the transfer of the electron in reduction and oxidation was not equal. This could lead to irreversible reaction.

Table 36. Cyclic voltammetric data of dmazpy, deazpy and azpy ligands in 0.1 M TBAH acetonitrile at scan rate 50 mV/s. (ferrocene couples occurred at 0.090 V., ΔEp = 56 mV)

compounds	$E_{1/2}$, V (ΔEp,mV)	
	Oxidation	reduction
dmazpy	+0.634 (84) +0.832 (84)	-1.671[a]
deazpy	+0.688 (96) +0.897 (84)	-1.619[a]
azpy	-	-1.487(171)

a = irreversible cathodic peak

Reduction range

The cathodic peaks at Ep_c = -1.671 V (for dmazpy) and -1.619 V (for deazpy) in reduction potential are irreversible peaks eventhough high scan rates(500, 1000, 2000 mV/s) were applied. In both dmazpy and deazpy the anodic peaks appeared at -1.172 V. However, these anodic peak could not occur spontaneously. Comparison with azpy ligand, the reduction potential displays a reversible couple at $E_{1/2}$ = -1.487 V (ΔE_p 171) which was two electron transfer process related to the ΔE_p of ferrocene.

Oxidation range

The cyclic voltammogram of azpy showed two quasi-reversible couples at $E_{1/2}$ 0.634 V (72 mV) and 0.832 V (82 mV) respectively. The deazpy ligand gave similar results and the two quasi-reversible couples appeared at $E_{1/2}$ 0.688 V (96 mV) and 0.897

V (84 mV). These two quasi-reversible couples of both ligands displayed the same characters as described below.

The group I was studied in the range 400-700 mV. The voltammograms showed the irreversible peaks at low scan rate (50 and 100 mV/s). However, this group became clearly quasi-reversible peaks at higher scan rates (1000-4000 mV/s). In addition, the peak separation (ΔE_p) and the peak currents of this couple gave a detail that this couple occurred from one electron transfer compared with ferrocene couples. This couple occurs spontaneously (Figure 39 Appendix B).

The group II actually differed from the couple I because this couple could not individually arise eventhough higher scan rates were applied. It must be produced from the couple I species (scan in the range 750-1150 mV) (Figure 40 Appendix B).

Whereas, in azpy ligand there was no peaks in oxidation potential and only responses in reduction potential were observed. Thus the interpretation of Ru(II/III) couples of complexes of $Ru(azpy)_2Cl_2$ were easily assigned. The difference should be due to substituent effects in dmazpy and deazpy molecules. The cyclic voltammograms of the starting materials of both ligands, *N,N*-dimethyl-1,4-nitrosoaniline and *N,N*-diethyl-1,4-nitrosoaniline were also studied to confirm this information. In the oxidation ranges of both substances. There were quasi-reversible couples (as shown in Figure 41 Appendix B) at the adjacent potentials to couple I of both ligands. Therefore, it can confirm that oxidative couples are from the substituents groups.

3.3.2 $Ru(L)_2Cl_2$ (L = dmazpy and deazpy)

Cyclic voltammograms of *cis* and *trans* isomers of $Ru(L)_2Cl_2$ (L = dmazpy and deazpy) gave the similar patterns but the peak potentials were shifted. The cyclic voltammograms of the *trans* complexes were shown in Figure 36 and the *cis* form were displayed in Figure 37. There were three couples in positive potential. The two

couples were ligand characters and one couple for the redox of Ru(II/III). Whereas, the two cathodic peaks occurred in reduction range (Table 37).

Table 37. Cyclic voltammetric data of *trans*-$Ru(L)_2Cl_2$ and *cis*-$Ru(L)_2Cl_2$ (L= dmazpy and deazpy) in 0.1 M TBAH acetonitrile at scan rate 50 mV/s compared with *trans*- and *cis*-$Ru(azpy)_2Cl_2$. (ferrocene couples occurred at 0.090 V., $\Delta Ep = 56$ mV)

Compounds	$E_{1/2}$, V (ΔEp,mV)	
	oxidation	reduction
trans-$Ru(dmazpy)_2Cl_2$	I → +0.389 (52) **Ru(II/III)→ +0.891 (80)** II → +1.174 (44)	-1.088
trans-$Ru(deazpy)_2Cl_2$	I → +0.340 (60) **Ru(II/III)→ +0.895 (50)** II → +1.100 (40)	-1.087
trans-$Ru(azpy)_2Cl_2$	**Ru(II/III)→ +0.643 (60)**	-0.937(50) -1.541
cis-$Ru(dmazpy)_2Cl_2$	I → +0.509 (50) **Ru(II/III)→ +0.906 (50)** II → +1.139 (58)	-1.066
cis-$Ru(deazpy)_2Cl_2$	I → +0.500 (60) **Ru(II/III)→ +0.890 (80)** II → +1.090 (100)	-1.095
cis-$Ru(azpy)_2Cl_2$	**Ru(II/III)→ +0.820 (63)**	-0.853 (64) -1.676

Oxidation potential

The group I belong to the ligand character which occurred spontaneously when scaned in 300-600 mV (Figure 42 Appendix B). This couple was quasi-reversible couple. The current increased when higher scan rates were applied. In addition, it was one electron transfer process compared with ferrocene couple.

The Ru(II/III) couple was quasi-reversible in the potential range of 600 – 1000 mV (Figure 38). It can individually occur and transfer of one electron.

The group II was quasi-reversible of ligand because it showed the character similar to those of ligand couple II. It can not spontaneously occur in the range 1000 to 1400 mV. This couple was detected as shoulder at high scan rates (1000-4000 mV/s) as shown in Figure 43 Appendix B.

Reduction potential

Two cathodic peaks appeared in the range 0 to –1800 mV at scan rate 50 mV/s at 1.10 and 1.28 V. The peak at 1.10 V was quasi-reversible couple when higher scan rates were applied. Whereas, the peak at 1.28 V dissapeared and became anodic peaks only at around 1.02 V (Figure 44 Appendix B).

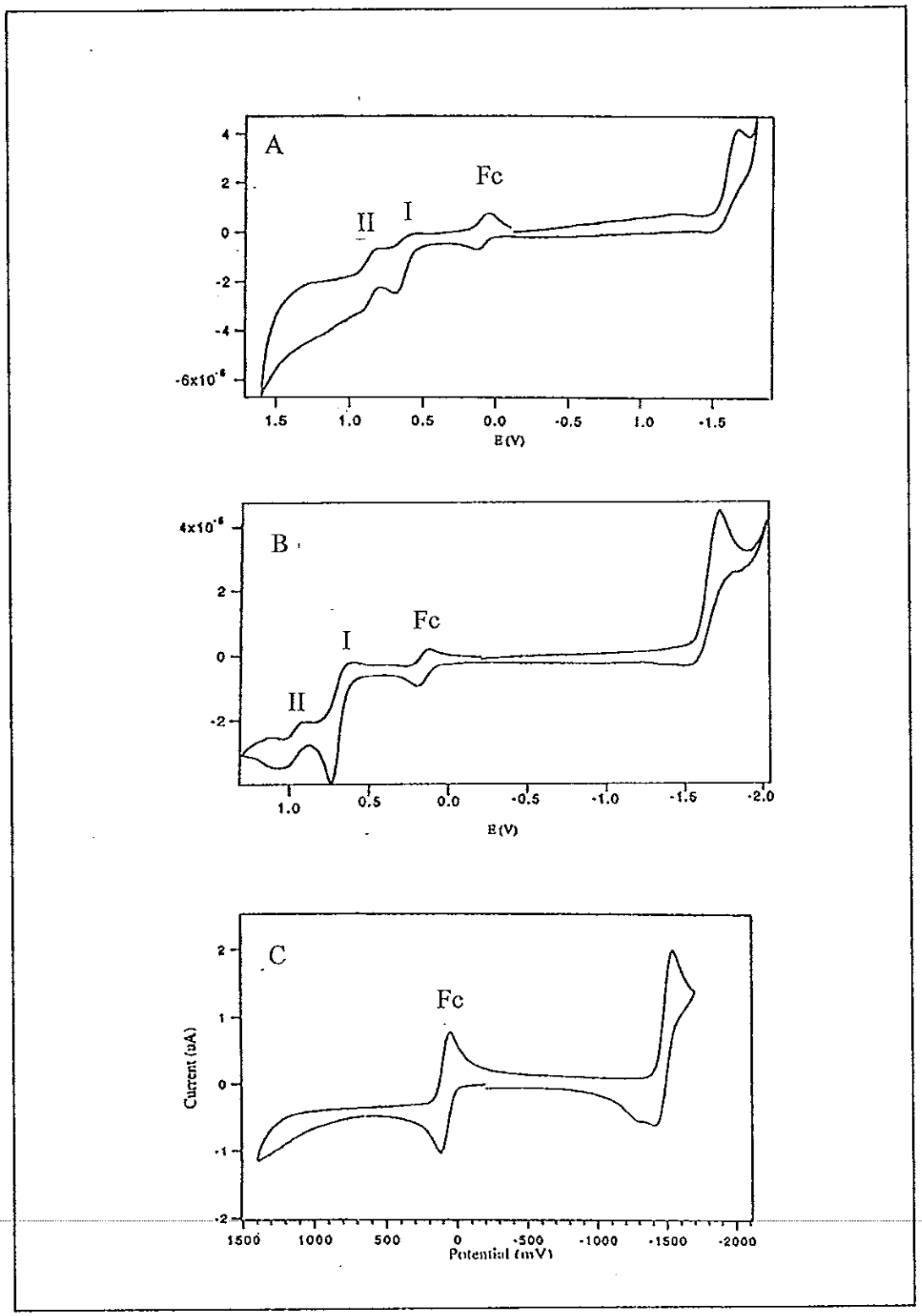

Figure 35. Cyclic voltammograms of (A) dmazpy, (B) deazpy and (C) azpy in 0.1 M TBAH CH_3CN at scan rate 50 mV/s

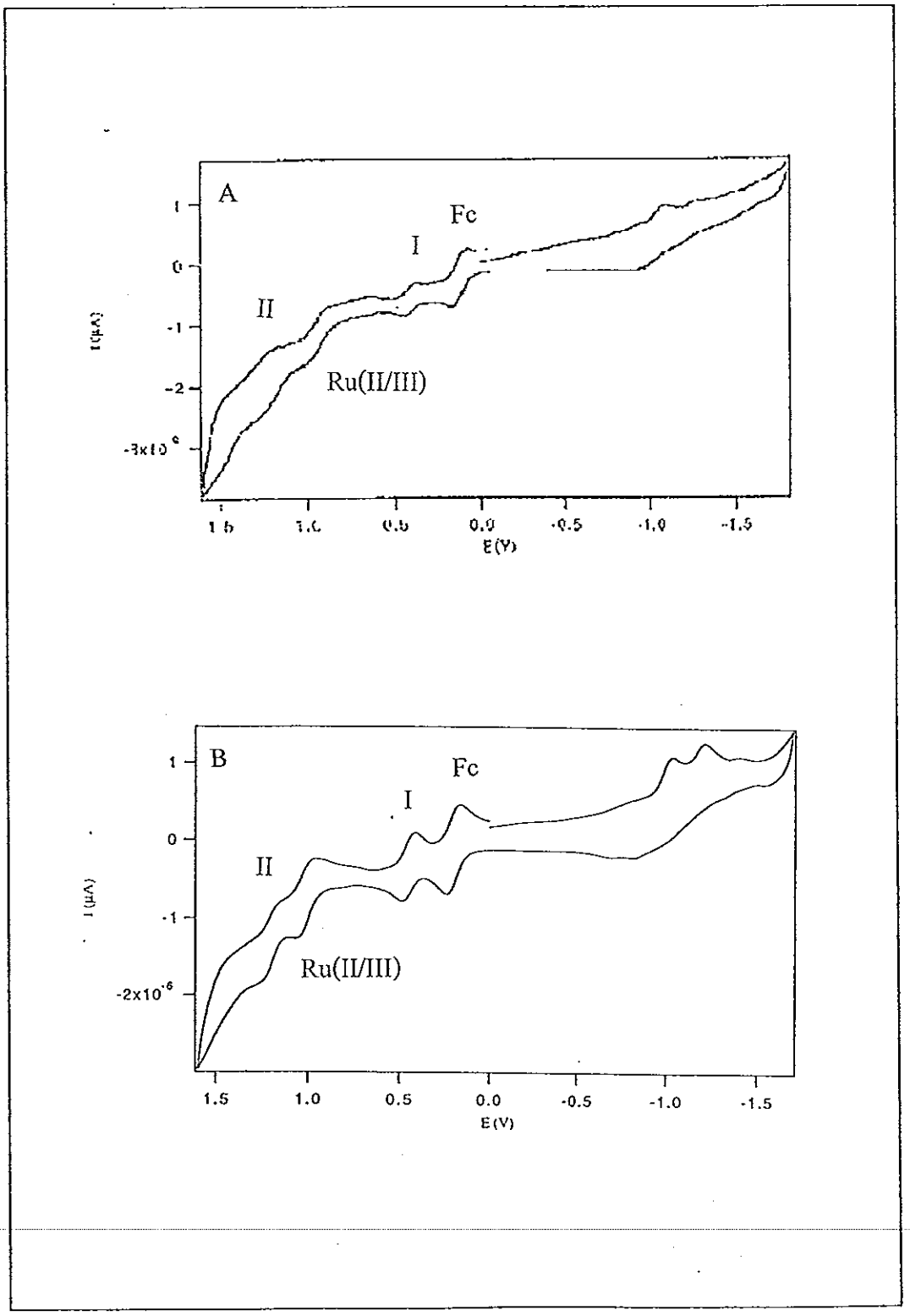

Figure 36. Cyclic voltammograms of (A) *trans*-$Ru(dmazpy)_2Cl_2$,

(B) *trans*-$Ru(deazpy)_2Cl_2$ in 0.1 M TBAH CH_3CN at scan rate 50 mV/s

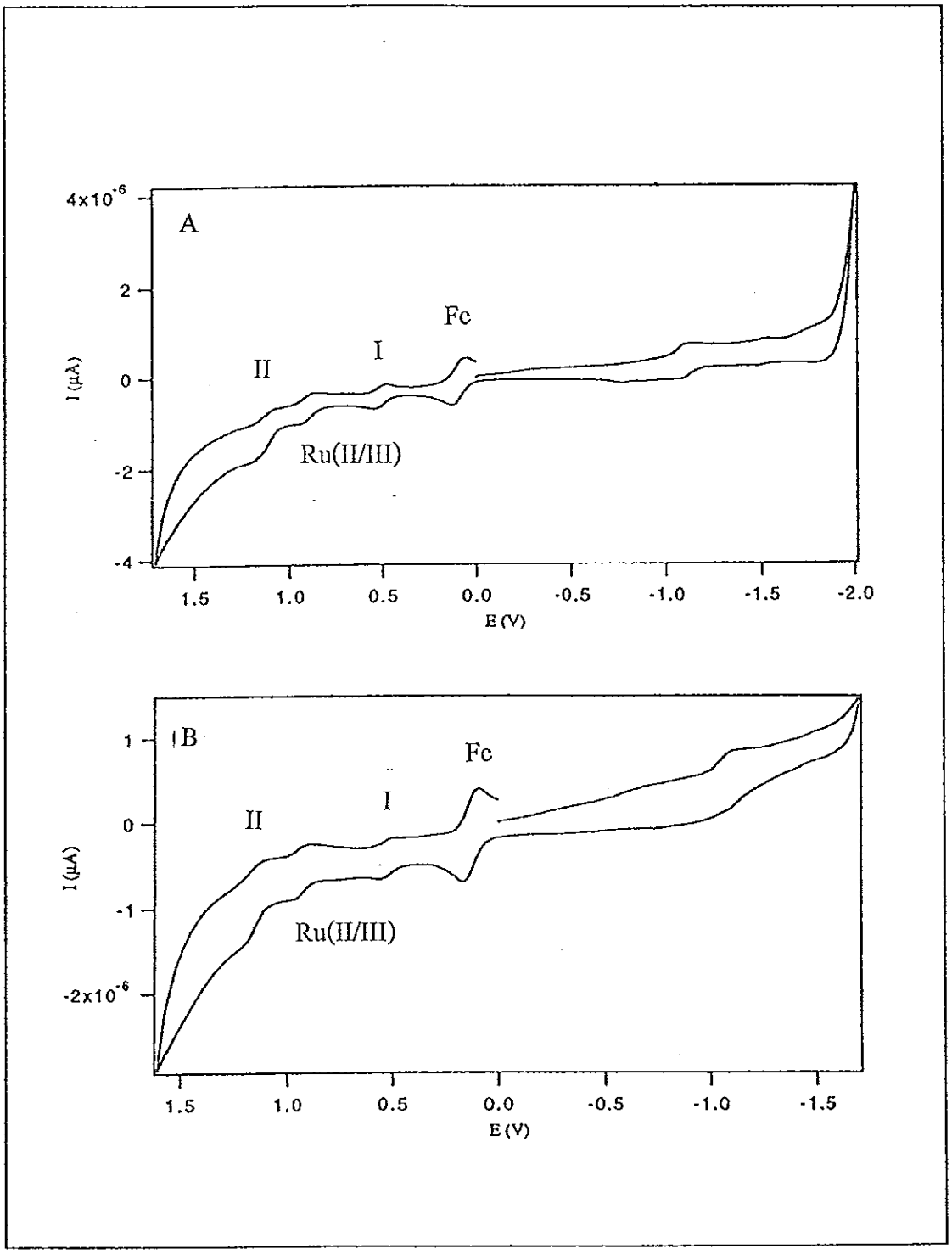

Figure 37. Cyclic voltammograms of (A) *cis*-$Ru(dmazpy)_2Cl_2$, (B) *cis*-$Ru(deazpy)_2Cl_2$ in 0.1 M TBAH CH_3CN at scan rate 50 mV/s

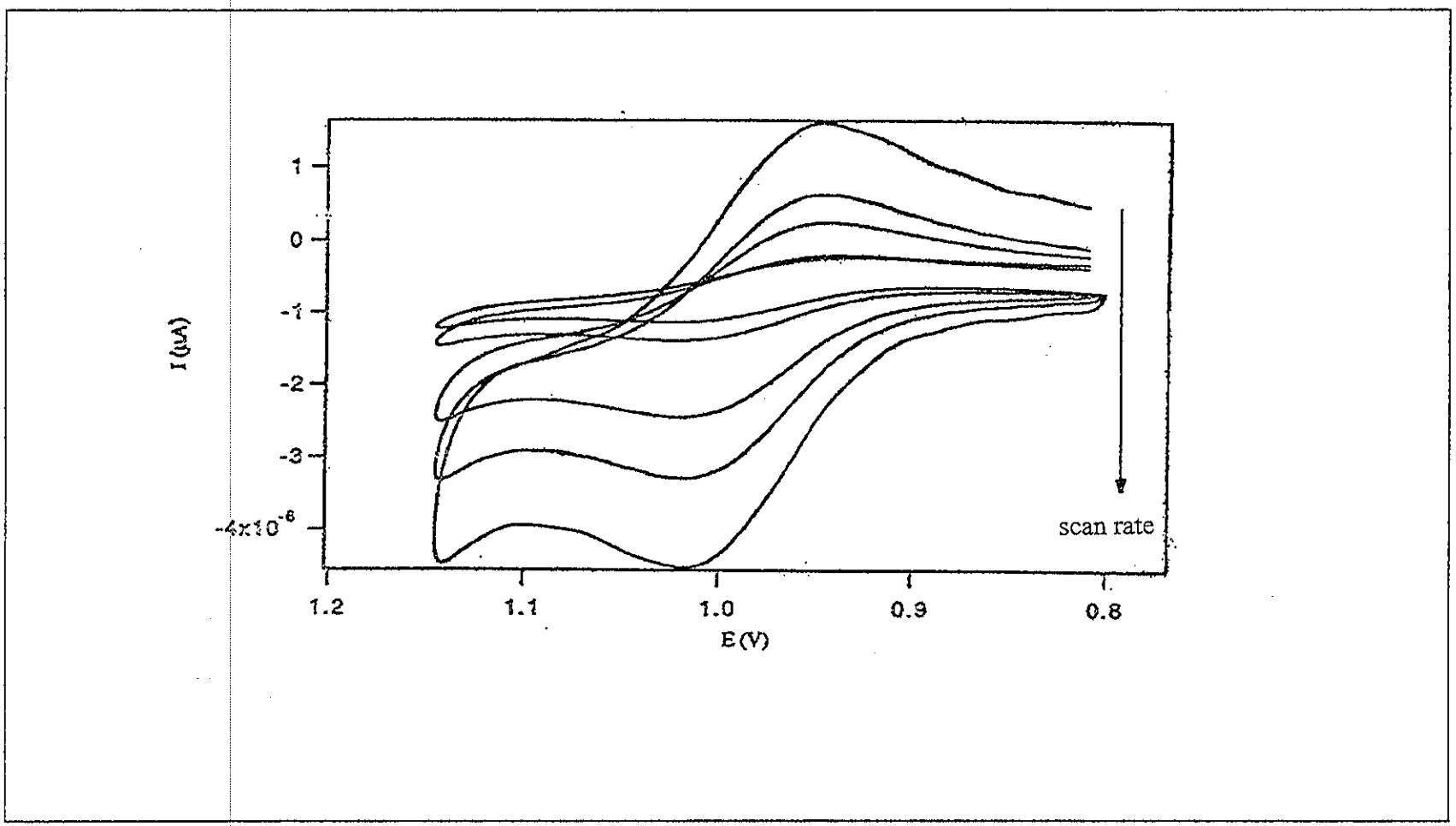

Figure 38. Cyclic voltammograms of quasi-reversible couples of Ru(II/III) scanned with various scan rates (50, 100, 200, 500, 1000 mV/s)

Chapter4

DISCUSSION

It is well documented that the 2-(phenylazo)pyridine (azpy) is a good π−acid ligand with azoimine function. It is known as the great stabilizer of ruthenium(II) by coordination to be the complexes such as in $Ru(azpy)_2Cl_2$ and $Ru(azpy)_2(NO_3)_2$ complexes. These complexes have been studied for their chemistry and their applications. The isomeric of *cis*-$Ru(azpy)_2Cl_2$ shows the high in Vitro toxicity against tumor cell lines (Velder *et al.*,2000). In addition, these complexes are catalyts in the epoxidation reaction (Barf and Sheldon, 1995). Besides, the complex of α–Ru-$(azpy)_2$ $(NO_3)_2$ showed strong binding to DNA-model bases. (Holtze *et al.*,2000). From these variety applications, the chemistry of the azoimine groups is in progress for finding the other new π−acid ligands which has azoimine function.

In this present work, the chemistry of ruthenium(II) complexes with new azoimine ligands are studied. These ligands are dmazpy and deazpy. Both ligands are the derivatives of azpy which have the substituents as electron-donating groups (-NR_2 ; R = CH_3 , C_2H_5). The objectives of this work are to study the chemical effects of electron donating groups on the azpy structure and to find the σ−donor and π−acceptor on the basis of X-ray structure, electrospray mass spectrometry, proton nuclear magnetic resonance, infrared spectroscopy, UV-Vis absorption spectroscopic data and redox properties.

4.1 Electrospray mass spectroscopic technique

The electrospray mass spectroscopy is a basis technique to determination of the molecular weight of molecules. In principal, it cannot give us the arrangement of atoms in the molecule directly. However in this work, one can divide the fragmentation patterns of all complexe into 2 groups. The further characterizations based on X-ray and ^{1}H NMR methods reveal that 2 different groups are *trans*- and *cis*- isomers.

Fragmentation characters of *trans*- isomers showed that Cl atoms still remained in their structures. In contrast to the *trans*-isomers the *cis*-forms usually lose the Cl atom. Both *trans* complexes also give the intense peak of protonated $[Ru(L)_2xHCl_2]^+$ (L = dmazpy and deazpy, x = the number of protons) species. In addition, the *trans*-Ru $(dmazpy)_2 Cl_2$ gives $[RuCl_2]^+$ at m/z 171.0 but *trans*-$Ru(deazpy)_2Cl_2$ does not give that fragment directly. The peak at m/z 288.3 corresponds to $[Ru(NC_5H_4N{=}NC_6H_5)4H]^+$ ion which loses two chlorine atoms, one ligand and the substituent $-NR_2$ (R = CH_3 or C_2H_5) of the other ligand. However, this peak appeared less intense than others.

The *cis*-$Ru(dmazpy)_2Cl_2$ complexes show the most intense peaks at m/z 589, which is assigned to $[Ru(dmazpy)_2Cl]^+$ (100 %). One chlorine atom is lost from the complex. The two Cl in cis structure are orthogonal (92.06(3)°, 3.464(2) Å. There is electron repulsion between two Cl atoms. It leads to longer Ru-Cl bond distances than trans isomer. Therefore, the Cl atom in *cis* isomer is usually lost first.

The purple deazpy complex which has not identified from X-ray structure show the fragmentation pattern similar to the *cis* form of dmazpy complex. Besides, the abundant m/z values are agree well with the *cis*-$Ru(deazpy)_2Cl_2$. There is a notable fragmentation mechanism of some peaks in *cis*-$Ru(deazpy)_2Cl_2$ complex. The electerospray mass spectrum of this complex was repeated the peaks at m/z 413.2 and 391.2 .

are still observed. The mechanisms of both peaks can be proposed in the Scheme I and II.

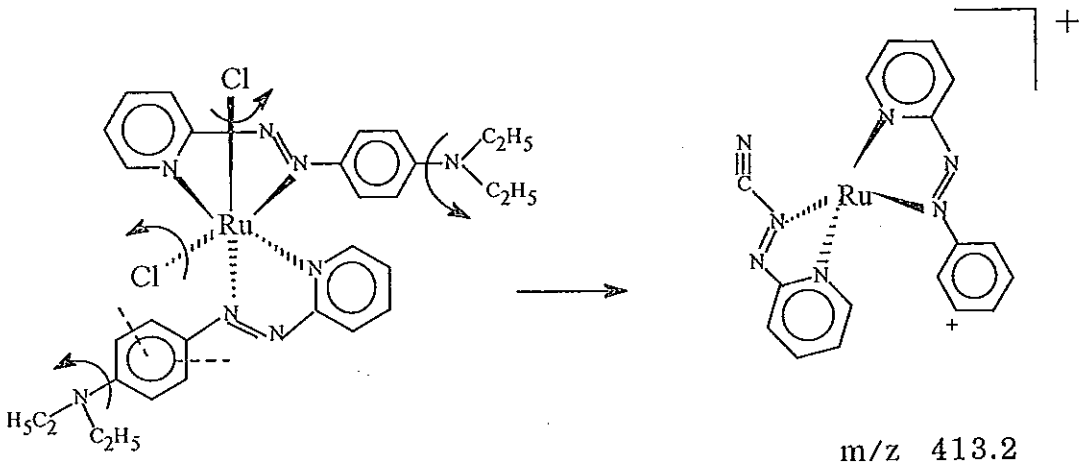

Scheme I

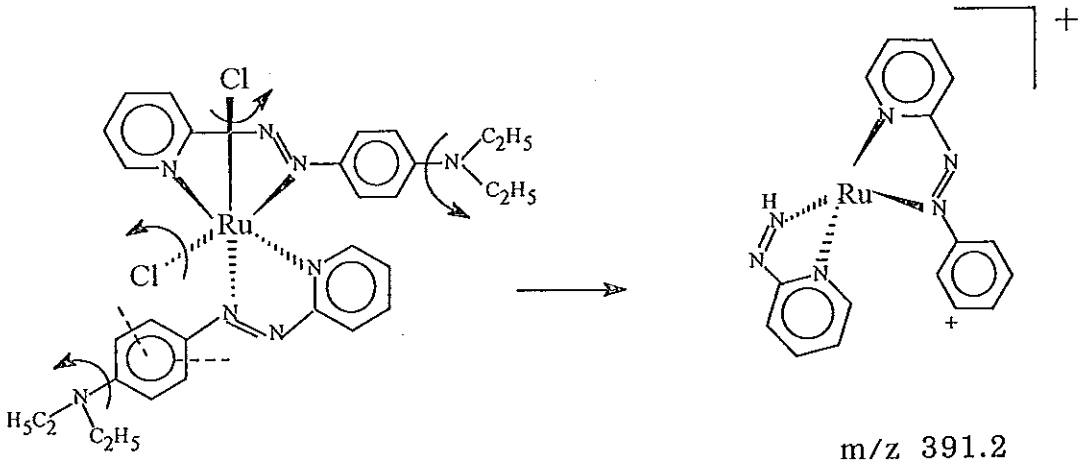

Scheme II.

After the Cl atoms and $-NR_2$ (R = CH_3 and C_2H_5) lost, the cationic benzene were not stable and it became fragmentation to be the other species at m/z 413.2 and 391.2 (as shown in Scheme I and II).

4.2 Infrared spectroscopic technique

IR spectra of dmazpy an deazpy ligands show the important peaks in the range 1600-400 cm^{-1} and the IR spectra of complexes are recorded from 1600-200 cm^{-1}. The objects in studying the IR spectra were to locate the important functional groups such as C=N stretching, N=N stretching, Ru-Cl stretching, Ru-N(py) stretching and Ru-N(azo) stretching modes. Besides, the IR results can be used to determine the π-acceptor properties of ligands.

The N=N stretching vibrations of free dmazpy and deazpy have been observed at 1399 and 1396 cm^{-1}, respectively. Whereas, N=N stretching frequency of azpy ligand appears at 1420 cm^{-1}, higher energy than those found in dmazpy and deazpy. This can be explained that the substituents, $-NR_2$ (R = CH_3 and C_2H_5) of dmazpy and deazpy donate electrons to phenyl ring. The delocalized electrons are filled into the π-π^* orbital of azo function. This leads to decrease the N=N bond order. The N=N bond is weaker than that of free azpy. Since the azo modes in dmazpy and deazpy appear at closed frequencies. It means that the electron donating abilities of methyl and ethyl groups are comparable.

The N=N stretching modes in complexes were shifted to lower frequencies than that in free ligands approximately to 150 cm^{-1}. This is the case of azpy complex similar to azpy complex. This is the strong evidence for the most π-backbonding bonding from ruthenium to azo, $t_{2g} \rightarrow \pi^*$ (azo). The $Ru(azpy)_2Cl_2$ displayed the N=N stretching mode at the higher energy than that in dmazpy and deazpy complexes because dmazpy and deazpy accept electrons both from Ru(II) and substituent groups. The bond order was decreased. From these results, it can be suggested that the apzy is a stronger π-acid than dmazpy and deazpy ligand.

The spectra of metal-ligand stretching modes appear in the range 400-200 cm^{-1}. The characteristic peaks are Ru-Cl, Ru-N(py) and Ru-N(azo) stretching modes. The *cis*-

and *trans*-$Ru(azpy)_2Cl_2$ complexes is respectively C_2 and C_{2v} symmetries (Krause and Krause, 1980). There symmetries are also applied to the corresponding dmazpy and deazpy complexes. Therefore, it should show IR active for two bands of each modes but the Ru-N modes appear as weak signal. Thus, it is hard to assign those peaks. However, the Ru-Cl stretching mode is a sharp single band, different from the Ru-N modes.

4.3 UV-Visible absorption spectrometry

The absorption spectra of *cis*- and *trans*-$Ru(L)_2Cl_2$ (L = dmazpy and deazpy) in various solvents were carried out in 200-820 nm. The absorption bands in UV region (200-400 nm) have characters of intraligand transitions similar to that in free ligands. Both of dmazpy and deazpy ligands exhibit two intense bands which are assigned as $n \rightarrow \pi^*$ at 274 nm ($\varepsilon\sim$ 1,000 $M^{-1}cm^{-1}$) and $\pi \rightarrow \pi^*$ transitions ($\varepsilon\sim$ 30,000 $M^{-1}cm^{-1}$) in the range 430-440 nm. The $\pi \rightarrow \pi^*$ absorption bands are the lowest energies. In contrast with azpy ligand, the $n \rightarrow \pi^*$ transition at 450 nm ($\varepsilon\sim$ 950 $M^{-1}cm^{-1}$) is the lowest energy. The different behavior is due to the substituent effect. The substituents ($-NR_2$, R = CH_3 and C_2H_5) are high polarity auxochrome which have strong effect to the absorption of bonded chromophores. The most effective chromophore should be phenyl part which leads to moderate intense color of dmazpy and deazpy ligands. (Shriver *et al.*., 1994) Besides, the substituents are the electron donating groups which can donate electrons to $\pi*$ orbitals of phenyl ring. From these results, it leads to stabilize the π^* orbital in the more polar solvents. Therefore, the $\pi \rightarrow \pi^*$ transition are shifted to lower energy and give more intense band than azpy ligand. Besides, the higher polarity of solvents give rise to the bathochromic shift of $\pi \rightarrow \pi^*$ transitions. In case of dmazpy and deazpy, the excited state (π^*) is stabilized while the ground state of azpy (n) is stabilized when the polarity of solvents increased. The absorption data of complexes

are specified to metal-to-ligand charge transfer, MLCT ($t_{2g} \rightarrow \pi^*$) bands in visible region (400-820 nm) which is the important character of these complexes. The absorption spectra of *trans*-isomers differ from *cis*-isomer. The spectrum consists of two MLCT intense bands with different molar extinction coefficients. The maximum wavelength which is the most intense band of *trans* forms occur in the range 630-652 nm ($\varepsilon\sim$ 23,000 M^{-1} cm^{-1}). Whereas, the cis isomers occur in the range 500-510 nm ($\varepsilon\sim$ 24,000 M^{-1} cm^{-1}). The colors of *trans* and *cis* isomers are green and purple, respectively. The wavelength of 500-560 nm is the absorption of the green wave and the desorption is purple wave. Thus, the *cis*-isomers are purple. For the *trans*- isomers, they absorb the orange color (592-650) and desorb the green-blue therefore, the *trans*- are green. The other weaker bands of *cis*- form appear in the range 628-654 nm which in the same range of the maxima intense bands of *trans* form absorbed. Whereas, the weaker intense bands of the *trans* forms absorb in the range (482-494 nm). The same situation occurs with the *cis*-,*trans*-$Ru(azpy)_2Cl_2$ complexes. The lowest absorption wavelengths of the isomeric of dmazpy and deazpy complexes are a few bathochromic shift of those in the azpy complexes. It indicates equally stabilization of the t_{2g} ruthenium orbitals in the dmazpy and deazpy complexes. Furthermore, the dmazpy and deazpy complexes show the solvent effect in various solvents when the polarity of solvents increased, the bathochromic shift was observed.

4.4 Proton Nuclear Magnetic resonance spectrometry

The ^{1}H-NMR data of *trans*-$Ru(L)_2Cl_2$ (L = dmazpy and deazpy) have similar assignments to their ligands. Whereas, ^{1}H-NMR data of the *cis*-$Ru(L)_2Cl_2$ display different patterns from both of ligands and *trans*-$Ru(L)_2Cl_2$. The different is particularly useful in determination of isomer configuration. However, the spectra of both ligands and all complexes are divided into three parts. The signal downfield are

owing to protons on pyridine ring, the upfield signals refer to phenyl protons and the alkyl groups on substituents which appear at the high field side.

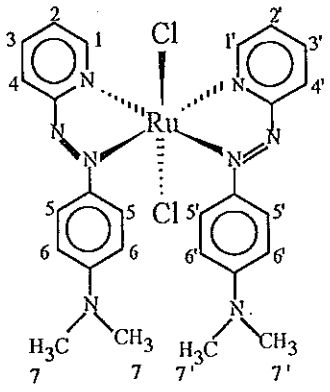

trans-Ru(dmazpy)$_2$Cl$_2$

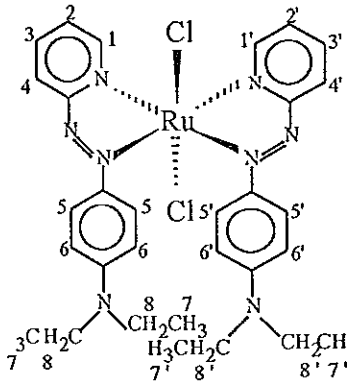

trans-Ru(deazpy)$_2$Cl$_2$

Table 38. ^{1}H NMR data for dmazpy, deazpy and *cis*- and *trans*-Ru(L)$_2$Cl$_2$ (L = dmazpy, deazpy) complexes.

H-position	δ (ppm)					
	dmazpy	deazpy	*trans*-Ru(dmazpy)$_2$Cl$_2$	*trans*-Ru(deazpy)$_2$Cl$_2$	*cis*-Ru(dmazpy)$_2$Cl$_2$	*cis*-Ru(deazpy)$_2$Cl$_2$
1,1'	8.678	8.668	8.925	8.923	9.517	9.506
4,4'	8.012	7.987	8.423	8.441	8.342	8.348
2,2'	7.828	7.818	8.050	8.028	7.529	7.900
5,5'	7.762	7.751	7.594	7.720	6.524	6.790
3,3'	7.286	7.271	7.612	7.582	7.434	7.413
6,6'	6.754	6.724	6.195	6.230	6.234	6.240
7,7'	3.100	3.464	2.989	3.314	2.989	3.305
8,8'	-	1.239	-	1.152	-	1.660

d = doublet dt = doublet of triplet t = triplet q = quatet

In the *trans*-Ru(dmazpy)$_2$Cl$_2$ complex the protons at the 1,1', 4,4', 2,2' and 5,5' position are shift downfield whereas 6,6' and 7,7' appear in the upfield region compare to the signal of free dmazpy. The shifted of proton is influenced by the electron density surround it. These results are similar to the *trans*-Ru(deazpy)$_2$Cl$_2$ complex. The protons at the 1,1' and the 4,4' position appear at lower downfield while protons at 5,5'-8,8' positions are shifted upfield. In these complexes the ligands coordinated with ruthenium ion and the Cl atoms are in trans position. Even the Cl atoms located with different planes from chelate rings but the distances between chlorine atoms (Cl1) and pyridine protons are 5.058 Å. Thus protons of pyridine rings (1,1' to 3,3' and 5,5') are effected by the electronegative Cl atoms and the signals accordingly move to downfield. Furthermore, protons at 4,4' are phenyl protons which nearly located to Cl (2) therefore they have been consequently effected from chlorine atom. The results contrast with 6,6 to 7,7' or 6,6' to 8,8' positions. It can be explained that these protons are far from chlorine atoms hence they have not got any interaction from chlorine atoms (average 6.309 Å for 6,6'-H, 8.269 Å for 7,7'-H and 9.142 Å for 8,8'-H).

The signals of 4,4' and 5,5'-H positions in cis-Ru(dmazpy)$_2$Cl$_2$ differ from free ligands and trans-Ru(L)$_2$Cl$_2$ complexes.

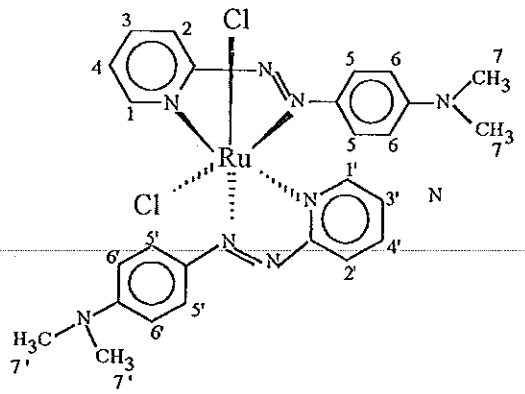

cis-Ru(dmazpy)$_2$Cl$_2$

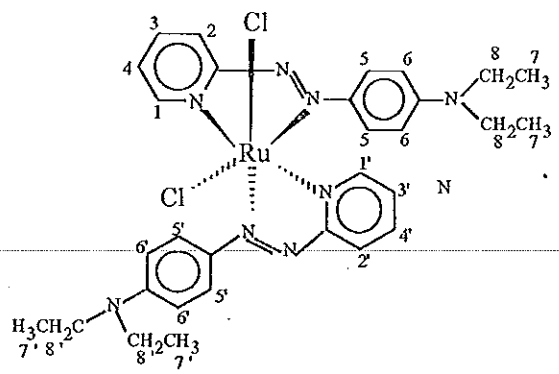

cis-Ru(deazpy)$_2$Cl$_2$

The 3,3'-H are protons on pyridine rings and the 5,5'-H are protons on phenyl rings. Therefore, the observed signals are different, the 3,3'-H is observed to be doublet of triplet peaks and occur at the downfield range with greater chemical shift than 5,5'-H. It is due to the inductive Cl atom. The average distances between 3,3'-H to Cl(1) is 5.115 Å and they are approximately in the same plane (dihedral angle 9.624° data from single crystal of *cis*-$Ru(dmazpy)_2Cl_2$. Thus, the electrons around the 3,3'-H are induced by chlorine atom. The signals accordingly occur at downfield. Whereas, 5,5'-H have got less effect than 3,3'-H. The distances of chlorine atom and 5,5'-H are 6.629 Å. It is worthy noted that all protons at 1,1' and 4,4' are shifted to downfield. The doublet signal of 1,1'-H appear at the lowest chemical shifts relative to free dmazpy and *trans*-$Ru(L)_2Cl_2$. It may be due to chlorine and N(py) which are in the same plane and adjacent locating. On the other hand, the signals of other positions move to lower frequencies.

Since the single crystal of *cis*-$Ru(deazpy)_2Cl_2$ was not obtainable, then result from other techniques can be used to characterize the structure. The ^{1}H-NMR spectra of *cis*-$Ru(deazpy)_2Cl_2$ can be used to confirm that the isolated purple complex is *cis-trans-cis* configuration according to similar the ^{1}H-NMR pattern of *cis*-$Ru(dmazpy)_2Cl_2$. In addition, the chemical shifts which are observed appear nearly to values in *cis*-Ru $(dmazpy)_2Cl_2$.

4.5 X-ray structure

There are four complexes , *trans*-$Ru(dmazpy)_2Cl_2$, *trans*-$Ru(deazpy)_2Cl_2$, *cis*-$Ru(dmazpy)_2Cl_2$ and *cis*-$Ru(deazpy)_2Cl_2$ complexes, which obtained from the reactions but only three of them were supported by single crystal X-ray technique. Although the *cis*-$Ru(deazpy)_2Cl_2$ could not crystallize to give single crystal. It was characterized from spectroscopic techniques ^{1}H-NMR spectra and electrospray mass spectrum.

The configurations of Ru(II) complexes are normally six coordination. The structures of all complexes are distorted octahedral. The *trans*-form has C_{2v} symmetry. The structure of *trans*-isomer is symmetric owing to C_2 axis with two vertical planes. The atom configuration is *trans-cis-cis* which referred to Cl atom, N(py) and N(azo), respectively. Whereas, the *cis* isomer has configuration as *cis-trans- cis*. The structures are approached to C_2 symmetry which has no vertical planes.

On the other hand, the two chelated planes of *cis*-Ru(dmazpy)$_2$Cl$_2$ are orthogonal (dihedral angle 78.8(1)°). The bond distances and the dihedral angles of phenyl planes with the other planes are different results. It should be effected from their geometrical structure and the substituent on phenyl rings.

The substituent groups of –NR$_2$ (R = CH$_3$,C$_2$H$_5$) showed the extensive effects to bond distances of Ru-N(azo), N=N and Ru-N(py) in *trans*-complexes

The planarity between substituent planes and phenyl plane is observed with dihedral angle less than 10 ° (average dihedral angle 3.318(4) ° for *cis*-Ru(dmazpy)$_2$Cl$_2$ and 4.516(2) ° for *trans*-Ru(dmazpy)$_2$Cl$_2$). The lone pair electrons at N-atom can delocalize into the phenyl ring. The conjugated structure is suggested in scheme III. The –N$^+$(CH$_3$)$_2$ was stabilized by electrons from the methyl groups.

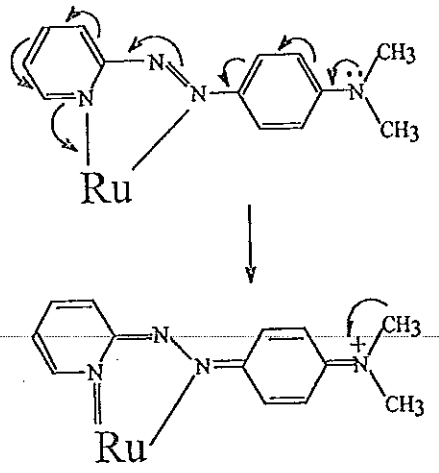

Scheme III

From the conjugated structure, the Ru-N(azo) distances should be longer. Whereas, the Ru-N(py) bonds should be shorter related to the azpy complex. The donated electrons are delocalized in the ligand structure which extends conjugated system than that of azpy complexes. These results are shown in Table 38.

Table 39. Bond distances of all complexes (Å).

Bonds	*trans* $Ru(dmazpy)_2Cl_2$	*trans* $Ru(deazpy)_2Cl_2$	*trans* $Ru(azpy)_2Cl_2$	*cis* $Ru(dmazpy)_2Cl_2$	*cis* $Ru(azpy)_2Cl_2$
Ru-Cl	2.398 (6)	2.388 (2)	2.368 (16)	2.408 (8)	2.401 (1)
	2.378 (6)	2.377 (2)	2.378 (15)	2.404 (9)	2.397 (1)
Ru-N(py)	2.062 (2)	2.088 (5)	2.115 (5)	2.042 (3)	2.051 (4)
	2.071 (2)	2.011 (5)	2.099 (5)	2.048 (3)	2.045 (4)
Ru-N(azo)	2.018 (2)	1.990 (5)	1.986 (5)	2.000 (3)	1.984 (4)
	2.027 (2)	2.011 (5)	1.988 (5)	1.999 (3)	1.977 (4)
N=N	1.304 (2)	1.313 (6)	1.302 (8)	1.306 (2)	1.283 (6)
	1.302 (2)	1.299 (7)	1.306 (7)	1.304 (2)	1.279 (7)

4.5.1 X-ray data of Ru-N(azo) bond

The Ru-N(azo) bond distances of all complexes are shorter than the Ru-N(py) bonds due to the most π–backbonding from Ru(II) to azo function. Amoung the in *trans*-isomers, the average Ru-N(azo) distances are arranged in order of $Ru(azpy)_2Cl_2$ (1.987 Å) (Velder *et al.*, 2000) < $Ru(deazpy)_2Cl_2$ (2.001 Å) < $Ru\text{-}(dmazpy)_2Cl_2$ (2.022 Å). However, the bond strength of Ru-N(azo) are conversely order. The Ru-N(azo) bond of $Ru\text{-}(azpy)_2Cl_2$ is stronger than that in RuL_2Cl_2 (L= dmazpy, deazpy) because the substituent in the donate electrons into the π^* orbital of azo character. The π–backbonding from Ru(II) is decreased. Thus, the Ru-N(azo) of dmazpy and deazpy

complexes weaker than that in azpy complex. From these data, the π-acceptor order are azpy > deazpy > dmazpy.

The Ru-N(azo) distance of deazpy complex is shorter than that in dmazpy complex because of the different electron donating groups. The ethyl group of substituent was bent from the plane of phenyl with average dihedral angle 57.8(4)°, then less electrons delocalized into donate electron to phenyl plane.

4.5.2 X-ray data of N=N bond

The azo function, -N=N-, is known as the accepting function of the π electrons from Ru(II). The N=N bond distances are decreased in complexes from the π-backbonding of $t_{2g} \rightarrow \pi^*$ orbital. The N=N distances in coordinated dmazpy ligands are longer (1.303 Å) than that in uncoordinated ligand (1.270 Å, Hansongnern *et al.*, 2001).

In *trans*-complexes, the N=N bond distances showed almost the same values, 1.304 Å for $Ru(azpy)_2Cl_2$ (Velder *et al.*, 1.306 Å for $Ru(deazpy)_2Cl_2$ and 1.303 Å for $Ru(dmazpy)_2Cl_2$. In contrast with the IR data, the N=N stretching modes of dmazpy and deazpy complexes appeared at the lower frequencies than azpy which indicated that the N=N bond of azpy is stronger than dmazpy and deazpy. The reason is due to more conjugated structure of dmazpy and deazpy which allowed electrons continually delocalize in azo π^* orbital. Therefore, the amount of electrons in π^* orbital are closely to azpy. The N=N distances are very similar in *trans*-complexes. Thus, it is not easy to arrange the π--acid properties of the ligands based on the azo distance.

In case of the *cis*-isomers, the *cis*-$Ru(dmazpy)_2Cl_2$ showed the N=N distances similar to that of *trans*-isomer (1.305(2) Å). Whereas, the *cis*-$Ru(azpy)_2Cl_2$ give shorter N=N distances (1.281(6) Å). It may be due to that the *cis*- configuration has (C_2 symmetry) less strain than *trans*- isomer.

4.5.3 X-ray data of Ru-N(py) bond

The electron donating substituents, $-NR_2$ (R = CH_3 and C_2H_5), show the dramatically effect to the Ru-N(py) bond distances in the *trans*- forms of dmazpy and deazpy complexes. The Ru-N(py) distances are shorter than that in *trans*-$Ru(azpy)_2Cl_2$ complex (2.066 Å for *trans*-$Ru(dmazpy)_2Cl_2$, 2.088 Å for *trans*-$Ru(deazpy)_2Cl_2$. Whereas, the Ru-N(py) distances in $Ru(azpy)_2Cl_2$ are 2.116 A. This results are due to the delocalization of electrons followed by scheme III. The pyridine rings donate more σ-electrons to ruthenium(II) center. Therefore, the Ru-N(py) bonds are strong. Ruthenium(II) are rich of electrons then, it give electron back (π-backbonding) to the π* orbital of azo character. It is suggested that there are some of π-backbonding to pyridine as well. Therefore, the bond distance of Ru-N(py) bonds are decreased. The Ru-N(py) lengths became shorter which similar to Ru-N(py) distances in *trans*-$[Ru(phen)_2(py)_2]PF_6$ complex, 2.096(5) – 2.100(5) Å and 2.013(2) – 2.054(2) Å for *cis*-$Ru(bpy)_2Cl_2$ complex (Ye *et al.*, 1994).

According to the Ru-N(py) distances, it can be arranged in order: *trans*-$Ru(dmazpy)_2Cl_2$ < *trans*-$Ru(deazpy)_2Cl_2$ < *trans*-$Ru(azpy)_2Cl_2$. Thus, the σ donation ability of pyridine in ligands are arranged into the order azpy < deazpy < dmazpy. The $-N(CH_3)_2$ is located in the same plane of phenyl whereas, the $-N(C_2H_5)_2$ is distortion from phenyl plane for average 57.3 °. Therefore, the $-N(CH_3)_2$ group shows the σ donation ability greater than the $-N(C_2H_5)_2$ group. On the other hand, the azpy ligand has no electron donating group in the structure.

In case of *cis*-isomers, the Ru-N(py) distances do not show the different character between *cis*-$Ru(dmazpy)_2Cl_2$ and *cis*-$Ru(azpy)_2Cl_2$. The complexes of *cis*-$Ru(dmazpy)_2Cl_2$ shows the average Ru-N(py) distances of 2.045 Å similar to the cis-$Ru(azpy)_2Cl_2$ (2.048 Å) and those *trans*-isomers.

4.5.4 X ray data of Ru-Cl bond

All *trans*- and *cis*-isomers show the average of Ru-Cl distances in the order of $Ru(dmazpy)_2Cl_2$ (2.388 Å) > $Ru(deazpy)_2Cl_2$ (2.382 Å) > *trans*-$Ru(azpy)_2Cl_2$ (2.373 Å). The Ru-Cl distances of dmazpy and deazpy complexes in the pyridine plane are observed to longer than the one in phenyl plane. It should be due to decreasing the strain of structures by lenghtening the Ru-Cl bond.

4.6 Cyclic Voltammetry technique

4.6.1 Reduction range (negative potential)

The potential 0.3 to –1.8 V was scanned and referred to the reduction range. The reduction peaks of ligand, dmazpy and deazpy are less stable. At the low scan rate (50 mV/s), the forward scanned showed one cathodic peak at –1.671 V for dmazpy and –1.619 V for deazpy. It did not show any reversed anodic peak in this range. The reduced species at Ep_c –1.671 V could not occur reversible oxidation. Higher scan rates (100 to 2000 mV/s) were applied to stimulate the oxidation. However, the oxidation were not found. The species at Ep_c –1.671 V were irreversible peak in the cyclic voltammogram which were defined to the dmazpy, deazpy species. The azo, -N=N-, was the accepting function as shown in equation (3)

$$\text{dmazpy} + e^- \longrightarrow \text{dmazpy}^- \qquad (3)$$
$$\text{deazpy} + e^- \longrightarrow \text{deazpy}^-$$

It was different characters from free azpy ligand. The azpy showed the reversible couple of two electron transfer in one process at $E_{1/2}$ = -1.487 V
(ΔEp 171 mV) which suggested the following mechanism of the azpy reduction in equation (4) (Shelder and Barf, 1968).

$$\text{azpy} + 2e^- \rightleftharpoons \text{azpy}^{2-} \qquad (4)$$

$$\text{-C-N=N-C-} + 2e^- \rightleftharpoons \text{-C-N=N-C}^{2-}$$

The reduction potential species of azpy, dmazpy and deazpy are compared and showed that the azpy can accept the electron better than deazpy and dmazpy, respectively. This corresponds to X-ray data and IR data. The reduction potential represents the electron accepting ability of the ligand. The more positive potential are greater electron accepting ability.

The reduction range of *trans*-$Ru(L)_2Cl_2$ (L = dmazpy and deazpy) give the quasi-reversible couple at $E_{1/2}$ –1.088 V(ΔEp 55 mV) for dmazpy complex and –1.087 V (ΔEp 53 mV) for deazpy complex. The electron transfer process is one electron and they also show an irreversible cathodic potential at –1.275 V and 1.250 V, respectively. Besides, comparison with *trans*-$Ru(azpy)_2Cl_2$, it showed two reversible reduction couple at $E_{1/2}$ –0.937 V(ΔEp 50 mV) and $E_{1/2}$ –1.541 V(ΔEp 80 mV). From these reduction potential, it can be arranged the π–accepting ability as order, azpy > dmazpy~deazpy. Because the reduction potentials of dmazpy and deazpy complexes are very close to each other, the one cannot exactly determine π–accepting ability from this technique. However, these results from the X-ray data and IR data supported that the azpy has the greatest π–accepting ability.

In case of *cis*-$Ru(L)_2Cl_2$ (L = dmazpy and deazpy), the quasi-reversible couple occur at $E_{1/2}$ –1.066 V(ΔEp 84 mV) for dmazpy complex and –1.095 V (ΔEp 50 mV) for deazpy complex. Whereas, the *cis*-$Ru(azpy)_2Cl_2$ shows two quasi-reversible couple at $E_{1/2}$ –0.853 V(ΔEp 64 mV) and $E_{1/2}$ –1.676 V(ΔEp 86 mV). All of *cis*- isomers give more positive reduction potential than that in *trans*-isomers because the structure of *cis*-isomer is less symmetric than *trans*-form. Therefore, *cis*- isomers is less rigidity and more stable than *trans*-isomer.

Oxidation range (positive potential)

The free ligands of dmazpy and deazpy show the two quasi-reversible couples in oxidative cyclic voltammograms (group I and group II). Whereas, this phenomena is not available for azpy ligand. From ligand structures, the hypothesis is the different from the substituent groups. To prove out the reason, the starting materials of *N,N*-dimethyl-1,4-nitrosoaniline and *N,N*-diethyl-1,4-nitrosoaniline were carried out by cyclic voltammetric method. The cyclic voltammograms of both compounds (Figure 45 Appendix B) obtain one quasi-reversible couple in oxidation range which leads to be the group I in dmazpy and deazpy voltammograms.

The character of the group I of dmazpy and deazpy was studied in the 0.3-0.7 V. At the low scan rate (50 mV/s), the scanned forward showed one anodic peak at +0.624 V for dmazpy and + 0.659 V for deazpy. It showed the quasi-reversible cathodic peak in this range at high scan rates (200-2000 mV/s). The $E_{1/2}$ potential is +0.634 V (ΔEp 81 mV) for dmazpy and +0.688 V (ΔEp 96 mV). Besides, the currents of anodic peak are higher than that of cathodic peak but currents of cathodic peak will increase when high potentials are supplied. The electron transfer process is followed by equation (5) which the redox reaction occurred at phenyl ring. In general, the redox of azobenzene was found at high potential (more than +2.000 V). The available of electron donating groups, R referred to $-N(CH_3)_2$ and $-N(C_2H_5)_2$ provides the ease of redox reaction on phenyl (benzene) ring.

$$NC_5H_4N{=}NC_6H_5{-}N(R)_2 \rightleftharpoons NC_5H_4N{=}NC_6^{+}H_5{-}N(R)_2 + e^{-} \qquad (5)$$

The cyclic voltammograms of this couple of both ligands are shown in Figure 46, Appendix B.

The ligand group II are studied in the potential range 0.3-1.4 V. The group II has a specific character that it must be produced from (Figure 47, Appendix B) the anodic species, $NC_5H_4N=NC_6^+H_5\text{-}N(R)_2$, of the couple I at higher potential +0.832 V (ΔEp 84 mV) for dmazpy and +0.897 V (ΔEp 84 mV) for dmazpy followed the equation (6).

$$NC_5H_4N=NC_6^+H_5\text{-}N(R)_2 \rightleftharpoons NC_5H_4N=NC_6^{2+}H_5\text{-}N(R)_2 + e^- \qquad (6)$$

The character of this couple is useful for indicating Ru(II/III) couple in complexes.

All complexes show the redox of the three groups in oxidation range, the first group is the redox of ligand group I, the second group is the redox of Ru(II/III) and the final group is the redox of ligand group II.

The ligand couple I is shifted to more positive potential at +0.389 V (52 mV) for *trans*-$Ru(dmazpy)_2Cl_2$, +0.340 V (60 mV) for *trans*-$Ru(deazpy)_2Cl_2$, +0.509 (50 mV) for *cis*-$Ru(dmazpy)_2Cl_2$ and +0.500 V for *cis*-$Ru(deazpy)_2Cl_2$. The shifts of the ligand couple I to less positive potential in complexes, are due to greater conjugation in ligands. This leads to lower the π^* energy level. Therefore, the redox potential of phenyl ring occurs at lower potential than that in free ligand. Besides from the X-ray results, the substituent $-N(C_2H_5)_2$ can donate electron less than $-N(CH_3)_2$. Therefore, the *cis*- and *trans*-$Ru(dmazpy)_2Cl_2$ are more stable with higher positive potentials than *cis*- and *trans*-$Ru(deazpy)_2Cl_2$.

The redox of Ru(II/III) in all complexes are found to be quasi-reversible couples when scanned in the range +700-+1000 mV (as shown in Figure 48 , Appendix B). The $E_{1/2}$ potentials of *trans*-isomer are +0.891 V (80 mV) for *trans*-$Ru(dmazpy)_2Cl_2$ and +0.895 V (50 mV). Whereas, the *trans*-$Ru(azpy)_2Cl_2$ gives the potential at +0.643 V(60 mV). One can assign the stability of Ru(II) in order of *trans*-$Ru(dmazpy)_2Cl_2$ ~ *trans*-

$Ru(deazpy)_2Cl_2$ > *trans*-$Ru(azpy)_2Cl_2$. The dmazpy and deazpy ligand can stabilize the Ru(II) in the complexes more than azpy due to the pyridine σ donating ability and the more conjugation. This result is similar to case of *cis*-isomers, the *cis*-$Ru(dmazpy)_2Cl_2$ give the highest positive potentials than *cis*-$Ru(deazpy)_2Cl_2$ and *cis*-$Ru(azpy)_2Cl_2$, at +0.906 V (50 mV) and +0.890 V (80 mV) and +0.820 (63), respectively. It can be noted that the dmazpy is greatly stabilize Ru(II). The results agree well with the X-ray data and IR results. It is noted the substituent, $-N(C_2H_5)_2$, can donate electrons to the parent molecule and increase that the strength of σ bonding at pyridine toward Ru(II). The deazpy also has this character but it can provide electrons less than the dmazpy. Therefore, the σ bonding ability is summarized in order dmazpy > deazpy > azpy supported the X-ray data. The happened redox is given in equation (7).

$$Ru^{III}(L)_2Cl_2^{+} \rightleftharpoons Ru^{II}(L)_2Cl_2 \text{ (L = dmazpy and deazpy)} \qquad (7)$$

In addition, the Ru(II) *cis*-isomers are stabilized more than *trans*- isomers due to the less symmetry in *cis*- form.

The final group is the ligand couple II in all complexes occur at higher potential than those in free ligands, +1.174 V (44 mV) for *trans*-$Ru(dmazpy)_2Cl_2$, +1.100 V (40 mV) for *trans*-$Ru(deazpy)_2Cl_2$, +1.139 V (58 mV) for *cis*-$Ru(dmazpy)_2Cl_2$ and + 1.090 V for *cis*-$Ru(deazpy)_2Cl_2$. The shifting to higher potentials than that in free ligands causes by the complex is oxidized with two electrons before reaching to the potential of this species in forward scan oxidation side. Those oxidized electrons are from the ligand group I and the other one from Ru center. Thus, the losing an other one electron is difficult. The supplied potentials are higher than that of free ligands.

Chapter 5

SUMMARY

The isomeric complexes of $Ru(L)_2Cl_2$ (L = dmazpy and deazpy) were synthesized. The structures of isolated complexes were identified as *trans*- and *cis*- configurations referred to Cl atoms. The isomers of *trans*-$Ru(L)_2Cl_2$ and *cis*-$Ru(dmazpy)_2Cl_2$ were determined by the single crystal X-ray diffraction method and other spectroscopic techniques which correspond to the proposed structures. Although, the *cis*-$Ru(deazpy)_2Cl_2$ has not been determined from single crystal X-ray diffraction but the ^1H NMR and electrospray mass spectroscopic data can determine to be the *cis*- configuration as similar as the *cis*-$Ru(dmazpy)_2Cl_2$.

The different isomers show the specific characters in electrospray mass spectra and ^1H-NMR results. From the electrospray mass spectra, the *cis*- forms are preferable to lose a chlorine atom whereas, the Ru-Cl bond strength is greater in the *trans*-complex. In addition, the ^1H-NMR assignment gives the data that the proton on pyridine rings of *cis*- isomers are shifted to downfield than that of *trans*- isomers caused by the effective from electronegative chlorine atoms. The *cis* isomers exhibit a MLCT transition at higher energy than the *trans*- complexes with a strong molar absorptivity due to less symmetry of *cis*- forms.

The effects of the substituents are studied from X-ray structure, infrared spectroscopic data and cyclic voltammetric technique. The substituents, $-N(CH_3)_2$ and $-N(C_2H_3)_2$ on the para position make the different chemical properties from azpy. These substituents are electron donating groups and are planar to the phenyl plane. Therefore, the electrons from the substituents can be donated to the phenyl ring. The $-N(C_2H_3)_2$ give less donated electrons to phenyl ring than the $-N(CH_3)_2$. The electrons delocalized in the conjugated system. The pyridine shows the strong donation to Ru(II) and then leads to decreasing of Ru-N(py) distances related to the results from azpy complexes. It can be

in the conjugated system. The pyridine shows the strong donation to Ru(II) and then leads to decreasing of Ru-N(py) distances related to the results from azpy complexes. It can be suggested that dmazpy and deazpy are the stronger σ donor than azpy ligand. Besides, the increase of conjugated system in dmazpy and deazpy complexes make the Ru(II) stabilized. Thus, the electrochemistry of Ru(II/III) occur at more positive potential than that of azpy complexes.

However, the azpy is still the strong π acceptor. The substituents, $-N(CH_3)_2$ and $-N(C_2H_3)_2$ of dmazpy and deazpy are possible to donate electrons to the π* orbital of the azo function thus the bond order of azo,–N=N-, is decreased. The N=N stretching mode in IR spectra are observed at lower energy than azpy complexes. Furthermore, the distances of Ru-N(azo) of azpy give the shorter than dmazpy and deazpy complexes.

From these results, the π acceptor properties of those ligands are provided in the order azpy > deazpy > dmazpy. Whereas, the σ donation ability of pyridine are assigned in the reverse order of dmazpy > deazpy > azpy.

BIBLIOGRAPHY

Bag N., Pramanik A., Lahiri G. K. and Chakravorty A. 1992. "Chemistry of the [Ru(RQ $(tap)_2)]^z$ Family : Authentic Catecholates, Reduction Potentials, and Spectra (RQ = Quinone/Semiquinone/Catecholate; tap = 2-(m-Tolylazo)pyridine; z = 0, ±, ±2", Inorg. Chem. 31(1992), 40-45.

Bao T., Krause K. and Krause R. A. 1988. "Hydroxide-Assisted Stereospecific Isomerization of a *trans*-Dichloro Bis Chelate of Ruthenium(II)", Inorg. Chem. 27(1988), 759-761.

Barf G. A. and Sheldon R. A. 1995. "Ruthenium(II) 2-(phenylazo)pyridine Complexes as Epoxidation Catalyst", J. Mol. Catal., 98 (1995), 143-147.

Carol C. 1993. "Encyclopedia of Chemistry". 2d ed. McGraw-Hill Inc. United State, 972-975.

Colton R., Harrison K. L., Mah Y. A. and Traeger J. C. 1995. "Cationic Phosohine Complexes of Gold(I): an Electrospray Mass Spectrometric Study", Inorg. Chim. Acta. 231(1995), 65-71.

Crutchley R. J. and Lever A. B. P. 1982. "Comparative Chemistry of Bipyridyl Metal Complexes: Spectroscopy, Electrochemistry and Photoanation", Inorg. Chem. 21(1982), 2276-2282.

Eklund J. C. and Bond A. M. 1998. "Perspectives in Modern Voltammetry: Basic Concepts and Mechanistic Analysis", Department of Chemistry, Monash University, Clayton, Australia and Physical and Chemistry Laboratory, Oxford University, Oxford, UK., 4-12.

Evans I. P., Spencer A. and Wilkinson G. 1973. "Dichlorotetrakis(dimethyl sulphoxide) ruthenium(II) Complexes", J. Chem. Soc., (1973), 204-209.

Goswami S., Chakravarty A. R., Chakravorty A. 1981. " Chemistry of Ruthenium. 2.[1] Synthesis, Structure and Redox Properties of 2-(Arylazo)pyridine Complexes", Inorg. Chem. 20(1981), 2246-2250.

Hansongnern K., Onganusorn S., Pakawatchai C. and White A. 2001. " The molecular structure of 2-(4'-*N,N*-dimethylaminophenylazo) pyridine", submitted for publication.

Hansongnern K., Onganusorn S., Kawaminami M. 2001. " The molecular structure of 2-(4'-*N,N*-diethylaminophenylazo) pyridine", paper submitted for publication.

Hotze A. C. H., Velders A. H., Ugozzoli F., Cinji M. B., Anna M. M. L., Haasnoot J. G. and Reedijk J. 2000. "Synthesis, Characterization, and Crystal Structure of α-$[Ru(azpy)_2(NO_3)_2]$ (azpy = 2-(phenylazo)pyridine) and the Products of Its Reactions with Guanine Derivatives" Inorg. Chem. 39 (2000), 3838-3844.

Irving M., Klotz M. and Ming W. C. L. 1953. "Stability Constants for Some Metal Chelates of Pyridine-2-azo-*p*-dimethylaniline", J. Am. Chem. Soc. 75(1953), 4159-4162.

Jeffrey J., Gray, H. B. 1999. "Spectroscopy and Electrochemistry of mer-[$RuCl_3$(dmso)(tmen)]. Dimethylsulfoxide Is Sulfur-Bonded to Ru(II), Ru(III) and Ru(IV)", Inorg. Chem. 38(1999), 2-3.

Krause R. A. and Krause, K. 1980. "Chemistry of Bipyridyl-like Ligands. Isomeric Complexes of Ruthenium(II) with 2-(phenylazo)pyridine[1]", Inorg. Chem. 19 (1980), 2600-2603.

Krause R. A. and Krause, K. 1984. "Chemistry of Bipyridyl-like Ligands. 3. Complexes of Ruthenium(II) with 2-((4-Nitrophenyl)azo)pyridine[1]", Inorg. Chem. 23 (1984), 2195-2198.

Misra T. K., Das D., Sinha, C., Ghosh, P. and Pal C. K. 1998. "Chemistry of Azoimidazoles: Synthesis, Spectral Characterization, Electrochemical Studies and X-Ray Crystal Structures of Isomeric Dichloro Bis[1-alkyl-2-arylazo)imidazole] Complexes of Ruthenium(II)" Inorg. Chem. 37(1998), 1672-1678.

Meyer G. J. 1997. "Effeciect Light-to-Electrical Energy Conversion : Nanocrystalline TiO_2 Films Modified with Inorganic Sensitizers" J. Chem. Ed. 74(1997), 652-656.

Norman R. O. C. 1978. "Principles of Organic Synthesis" 2d ed. Chapman and Hall, London, New York.

Penneerselvam K., Hansongnern K., Rattanawit N., Liao F. L. and Lu T. H. 2000. "Crystal Structure of the [Protonated 2-(phenylazo)pyridine and Protonated 2-(4-hydroxyphenylazo)pyridine (3:1)]tetrafluoroborate", Anal. Sci . 16 (2000),1107-1108.

Sadler J. L. and Bard A. J. 1968. "The Electrochemical Reduction of Aromatic Azo Compounds", J. Am. Chem. Soc. 90(1968), 1979-1989.

Santra P. K., Misra T. K., Das D., Sinha C., Slawin A. M. Z. and Wollins J. D. 1999. "Chemistry of azopyrimidines. Part II. Synthesis, Spectra, Electrochemistry and X-ray Crystal Structures of Isomeric Dichloro bis[2-(arylazo)pyrimidine] Complexes of Ruthenium(II)", Polyhedron. 18(1999), 2869-2878.

Seal A. and Ray S. 1984. "Structures of Two Isomers of Dichlorobis(2-phenylazopyridine)ruthenium(II) $[RuCl_2(C_{11}H_9N_3)_2]$", Acta Cryst. 40, (1984), 929-932.

Shriver, D. F., Atkins, P. W. and Langford, C. H. 1994. Inorganic Chemistry. 2nd ed., Oxford : Oxford University Press , UK., 595-600.

Sullivan P. Salmon D. J., Meyer T. J. and Peedin J. 1979. " Monomeric and Dimeric Pyrazole and Pyrazolyl Complexes of Ruthenium", Inorg. Chem. 18(1979), 3369-3374.

Velder A. H., Kooijman H., Spek A. L., Haasnoot D. V. and Reedijk J. 2000. "Strong Differences in the in Vitro Cytotoxicity of Three Isomeric Dichlorobis(2-phenylazopyridine)ruthenium(II) Complexes", Inorg. Chem. 39 (2000), 2966-2967.

Wolfgang S., Strekas T. C. Gafney H. Krause R. and Krause K. 1984. "Spectral and Photophysical Properties of Ruthenium(II) 2-(phenylazo)pyridine Complexes", Inorg. Chem. 23(1984), 2650-2655.

Ye B-H., Chen X-M., Zeng T. Z., Ji L-N. 1995. "Syntheses, spectra and crystal structures of ruthenium(II) complexes with polypyridyl: $[Ru(bipy)_2(phen)](ClO_4)_2.H_2O$and $[Ru(bipy)_2(Me\text{-}phen)\ )](ClO_4)_2$", Inorg. Chim. Acta. 240 (1995), 5-11.

Appendix A.

Table 40. The bond distances (Å) and bond angles (°) of *trans*-Ru(dmazpy)$_2$Cl$_2$ complex.

Bond distances

Atoms	Distance (Å)
Ru(1)-Cl(1)	2.3767(5)
Ru(1)-Cl(2)	2.3978(5)
Ru(1)-N(1)	2.062(1)
Ru(1)-N(3)	2.018(2)
Ru(1)-N(5)	2.070(2)
Ru(1)-N(7)	2.027(1)
N(1)-C(1)	1.344(3)
N(1)-C(5)	1.361(3)
N(2)-N(3)	1.305(2)
N(2)-C(5)	1.390(3)
N(3)-C(6)	1.410(3)
N(4)-C(9)	1.364(3)
N(4)-C(12)	1.453(3)
N(4)-C(13)	1.449(3)
N(5)-C(14)	1.345(3)
N(5)-C(18)	1.360(3)
N(6)-N(7)	1.302(2)
N(6)-C(18)	1.387(3)
N(7)-C(19)	1.409(3)
N(8)-C(22)	1.367(3)

Table 40.(continued)

Atoms	Distance (Å)
N(8)-C(25)	1.449(3)
N(8)-C(26)	1.452(3)
C(1)-C(2)	1.380(3)
C(2)-C(3)	1.389(4)
C(3)-C(4)	1.382(3)
C(4)-C(5)	1.387(3)
C(6)-C(7)	1.399(3)
C(6)-C(11)	1.403(4)
C(7)-C(8)	1.377(3)
C(8)-C(9)	1.412(4)
C(9)-C(10)	1.416(3)
C(10)-C(11)	1.378(3)
C(14)-C(15)	1.372(3)
C(15)-C(16)	1.398(3)
C(16)-C(17)	1.379(3)
C(17)-C(18)	1.380(3)
C(19)-C(20)	1.398(4)
C(19)-C(24)	1.398(3)
C(20)-C(21)	1.380(3)
C(21)-C(22)	1.413(3)
C(22)-C(23)	1.421(4)
C(23)-C(24)	1.370(3)

Table 40. (continued)

Bond angle (°)

Atoms	Angles (°)
Cl(1)-Ru(1)-Cl(2)	172.90(2)
Cl(1)-Ru(1)-N(1)	86.71(4)
Cl(1)-Ru(1)-N(3)	89.54(4)
Cl(1)-Ru(1)-N(5)	88.52(4)
Cl(1)-Ru(1)-N(7)	94.48(4)
Cl(2)-Ru(1)-N(1)	90.47(4)
Cl(2)-Ru(1)-N(3)	96.08(4)
Cl(2)-Ru(1)-N(5)	85.74(4)
Cl(2)-Ru(1)-N(7)	88.17(4)
N(1)-Ru(1)-N(3)	75.65(6)
N(1)-Ru(1)-N(5)	102.55(6)
N(1)-Ru(1)-N(7)	178.01(6)
N(3)-Ru(1)-N(5)	177.43(5)
N(3)-Ru(1)-N(7)	105.93(6)
N(5)-Ru(1)-N(7)	75.91(6)
Ru(1)-N(1)-C(1)	130.4(1)
Ru(1)-N(1)-C(5)	110.8(1)
C(1)-N(1)-C(5)	118.3(2)
N(3)-N(2)-C(5)	111.9(2)
Ru(1)-N(3)-N(2)	118.0(1)
Ru(1)-N(3)-C(6)	129.1(1)
N(2)-N(3)-C(6)	112.8(2)
C(9)-N(4)-C(12)	120.2(2)

Table 40. (continued)

Atoms	Angles (°)
C(9)-N(4)-C(13)	121.9(2)
C(12)-N(4)-C(13)	117.6(2)
Ru(1)-N(5)-C(14)	130.4(1)
Ru(1)-N(5)-C(18)	111.7(1)
C(14)-N(5)-C(18)	117.7(2)
N(7)-N(6)-C(18)	112.5(1)
Ru(1)-N(7)-N(6)	118.5(1)
Ru(1)-N(7)-C(19)	128.6(1)
N(6)-N(7)-C(19)	112.4(1)
C(22)-N(8)-C(25)	122.3(2)
C(22)-N(8)-C(26)	120.6(2)
C(25)-N(8)-C(26)	117.0(2)
N(1)-C(1)-C(2)	122.2(2)
C(1)-C(2)-C(3)	119.0(2)
C(2)-C(3)-C(4)	119.4(2)
C(3)-C(4)-C(5)	118.6(2)
N(1)-C(5)-N(2)	117.3(2)
N(1)-C(5)-C(4)	122.0(2)
N(2)-C(5)-C(4)	120.3(2)
N(3)-C(6)-C(7)	118.7(2)
N(3)-C(6)-C(11)	122.7(2)
C(7)-C(6)-C(11)	118.6(2)
C(6)-C(7)-C(8)	120.8(2)
C(7)-C(8)-C(9)	121.3(2)

Table 40. (continued)

Atoms	Angles (°)
N(4)-C(9)-C(8)	121.1(2)
N(4)-C(9)-C(10)	121.4(2)
C(8)-C(9)-C(10)	117.5(2)
C(9)-C(10)-C(11)	120.7(2)
C(6)-C(11)-C(10)	121.1(2)
N(5)-C(14)-C(15)	122.9(2)
C(14)-C(15)-C(16)	118.9(2)
C(15)-C(16)-C(17)	118.9(2)
C(16)-C(17)-C(18)	119.0(2)
N(5)-C(18)-N(6)	117.8(2)
N(5)-C(18)-C(17)	122.4(2)
N(6)-C(18)-C(17)	119.5(2)
N(7)-C(19)-C(20)	119.8(2)
N(7)-C(19)-C(24)	120.8(2)
C(20)-C(19)-C(24)	119.3(2)
C(19)-C(20)-C(21)	120.2(2)
C(20)-C(21)-C(22)	121.0(2)
N(8)-C(22)-C(21)	122.0(2)
N(8)-C(22)-C(23)	120.2(2)
C(21)-C(22)-C(23)	117.8(2)
C(22)-C(23)-C(24)	120.6(2)
C(19)-C(24)-C(23)	120.9(2)

Appendix A.

Table 41. The bond distances (Å) and bond angles (°) of *trans*-Ru(deazpy)$_2$Cl$_2$ complex.

Bond distances

Atoms	Distance (Å)
Ru(1)-Cl(1)	2.389(2)
Ru(1)-Cl(2)	2.376(2)
Ru(1)-N(1)	2.088(4)
Ru(1)-N(3)	1.990(5)
Ru(1)-N(5)	2.087(5)
Ru(1)-N(7)	2.011(4)
N(1)-C(1)	1.342(8)
N(1)-C(5)	1.359(7)
N(2)-N(3)	1.313(6)
N(2)-C(5)	1.371(7)
N(3)-C(6)	1.433(7)
N(4)-C(9)	1.380(8)
N(4)-C(12)	1.45(1)
N(4)-C(14)	1.47(1)
N(5)-C(16)	1.342(8)
N(5)-C(20)	1.357(6)
N(6)-N(7)	1.299(7)
N(6)-C(20)	1.390(8)
N(7)-C(21)	1.421(7)
N(8)-C(24)	1.383(8)

Table 41. (continued)

Atoms	Distance (Å)
N(8)-C(27)	1.45(1)
N(8)-C(29)	1.454(9)
C(1)-C(2)	1.391(8)
C(2)-C(3)	1.39(1)
C(3)-C(4)	1.39(1)
C(4)-C(5)	1.388(7)
C(6)-C(7)	1.386(9)
C(6)-C(11)	1.391(9)
C(7)-C(8)	1.378(9)
C(8)-C(9)	1.403(9)
C(9)-C(10)	1.421(9)
C(10)-C(11)	1.380(9)
C(12)-C(13)	1.527(9)
C(14)-C(15)	1.52(1)
C(16)-C(17)	1.382(9)
C(17)-C(18)	1.398(8)
C(18)-C(19)	1.379(9)
C(19)-C(20)	1.395(8)
C(21)-C(22)	1.392(8)
C(21)-C(26)	1.398(9)
C(22)-C(23)	1.377(9)
C(23)-C(24)	1.39(1)
C(24)-C(25)	1.412(9)
C(25)-C(26)	1.387(8)

Table 41. (continued)

Bond angles (°)

Atoms	Angle (°)
C(27)-C(28)	1.51(1)
C(29)-C(30)	1.516(9)
Cl(1)-Ru(1)-Cl(2)	171.48(5)
Cl(1)-Ru(1)-N(1)	90.4(1)
Cl(1)-Ru(1)-N(3)	96.5(1)
Cl(1)-Ru(1)-N(5)	84.7(1)
Cl(1)-Ru(1)-N(7)	88.1(1)
Cl(2)-Ru(1)-N(1)	85.2(1)
Cl(2)-Ru(1)-N(3)	89.5(1)
Cl(2)-Ru(1)-N(5)	89.3(1)
Cl(2)-Ru(1)-N(7)	96.2(1)
N(1)-Ru(1)-N(3)	75.7(2)
N(1)-Ru(1)-N(5)	103.9(2)
N(1)-Ru(1)-N(7)	178.5(2)
N(3)-Ru(1)-N(5)	178.8(2)
N(3)-Ru(1)-N(7)	104.6(2)
N(5)-Ru(1)-N(7)	75.8(2)
Ru(1)-N(1)-C(1)	130.2(4)
Ru(1)-N(1)-C(5)	111.2(3)
C(1)-N(1)-C(5)	118.5(4)
N(3)-N(2)-C(5)	112.0(5)
Ru(1)-N(3)-N(2)	119.8(4)

Table 41. (continued)

Atoms	Angle (°)
Ru(1)-N(5)-C(16)	130.3(3)
Ru(1)-N(5)-C(20)	111.8(4)
C(16)-N(5)-C(20)	117.5(5)
N(7)-N(6)-C(20)	112.9(4)
Ru(1)-N(7)-N(6)	119.2(3)
Ru(1)-N(7)-C(21)	130.8(3)
N(6)-N(7)-C(21)	109.5(4)
C(24)-N(8)-C(27)	122.2(5)
C(24)-N(8)-C(29)	122.0(6)
C(27)-N(8)-C(29)	115.8(5)
N(1)-C(1)-C(2)	121.5(6)
C(1)-C(2)-C(3)	120.1(7)
C(2)-C(3)-C(4)	118.5(5)
C(3)-C(4)-C(5)	118.7(6)
N(1)-C(5)-N(2)	118.1(4)
N(1)-C(5)-C(4)	122.6(5)
N(2)-C(5)-C(4)	118.8(5)
N(3)-C(6)-C(7)	122.0(5)
N(3)-C(6)-C(11)	118.8(6)
C(7)-C(6)-C(11)	119.1(5)
C(6)-C(7)-C(8)	120.8(6)
C(7)-C(8)-C(9)	121.2(6)
N(4)-C(9)-C(8)	121.8(6)
N(4)-C(9)-C(10)	120.6(6)

Table 41. (continued)

Bond Angles	Angle (°)
C(8)-C(9)-C(10)	117.6(6)
C(9)-C(10)-C(11)	120.3(6)
C(6)-C(11)-C(10)	120.9(6)
N(4)-C(12)-C(13)	113.2(6)
N(4)-C(14)-C(15)	112.8(6)
N(5)-C(16)-C(17)	122.4(5)
C(16)-C(17)-C(18)	119.7(6)
C(17)-C(18)-C(19)	118.7(6)
C(18)-C(19)-C(20)	118.3(5)
N(5)-C(20)-N(6)	117.3(5)
N(5)-C(20)-C(19)	123.3(5)
N(6)-C(20)-C(19)	119.4(4)
N(7)-C(21)-C(22)	120.2(6)
N(7)-C(21)-C(26)	121.1(5)
C(22)-C(21)-C(26)	118.7(5)
C(21)-C(22)-C(23)	120.4(6)
C(22)-C(23)-C(24)	122.1(6)
N(8)-C(24)-C(23)	120.4(6)
N(8)-C(24)-C(25)	122.0(6)
C(23)-C(24)-C(25)	117.5(5)
C(24)-C(25)-C(26)	120.5(6)
C(21)-C(26)-C(25)	120.8(5)
N(8)-C(27)-C(28)	113.1(6)
N(8)-C(29)-C(30)	112.4(6)

Appendix A.

Table 42. The bond distances (Å) and bond angles (°) of *cis*-Ru(dmazpy)$_2$Cl$_2$ complex.

Bond distances

Atom	Distance (Å)
Ru(1)-Cl(1)	2.4083(7)
Ru(1)-Cl(2)	2.404(1)
Ru(1)-N(1)	2.042(3)
Ru(1)-N(3)	2.000(2)
Ru(1)-N(5)	2.048(3)
Ru(1)-N(7)	1.999(3)
N(1)-C(1)	1.340(4)
N(1)-C(5)	1.361(4)
N(2)-N(3)	1.306(4)
N(2)-C(5)	1.385(4)
N(3)-C(6)	1.415(4)
N(4)-C(9)	1.362(4)
N(4)-C(12)	1.420(5)
N(4)-C(13)	1.461(6)
N(5)-C(14)	1.348(5)
N(5)-C(18)	1.361(5)
N(6)-N(7)	1.304(4)
N(6)-C(18)	1.389(5)
N(7)-C(19)	1.415(5)
N(8)-C(22)	1.356(6)

Table 42. (continued)

Atom	Distance (Å)
N(8)-C(25)	1.413(7)
N(8)-C(26)	1.443(6)
C(1)-C(2)	1.380(4)
C(2)-C(3)	1.388(4)
C(3)-C(4)	1.380(5)
C(4)-C(5)	1.392(4)
C(6)-C(7)	1.404(5)
C(6)-C(11)	1.392(5)
C(7)-C(8)	1.369(4)
C(8)-C(9)	1.411(5)
C(9)-C(10)	1.416(5)
C(10)-C(11)	1.378(4)
C(14)-C(15)	1.378(5)
C(15)-C(16)	1.386(6)
C(16)-C(17)	1.388(5)
C(17)-C(18)	1.383(5)
C(19)-C(20)	1.395(5)
C(19)-C(24)	1.404(5)
C(20)-C(21)	1.374(6)
C(21)-C(22)	1.414(6)
C(22)-C(23)	1.410(6)
C(23)-C(24)	1.376(6)
Cl(3)-C(27)	1.745(4)
Cl(4)-C(27)	1.764(5)

Table 42. (continued)

Atom	Distance (Å)
C(28)-C(29)	1.24(1)
C(28)-C(31)	1.59(2)
C(28)-C(32)	1.65(1)
C(29)-C(30)	1.568(9)
C(29)-C(31)	1.19(1)
C(29)-C(32)	1.32(1)
C(29)-C(30)	1.52(1)
C(30)-C(32)	1.16(1)
C(30)-C(31)	1.15(1)

Bond angles (°)

Atom	Angle (°)
Cl(1)-Ru(1)-Cl(2)	92.06(3)
Cl(1)-Ru(1)-N(1)	95.22(7)
Cl(1)-Ru(1)-N(3)	170.1(1)
Cl(1)-Ru(1)-N(5)	86.28(7)
Cl(1)-Ru(1)-N(7)	91.80(7)
Cl(2)-Ru(1)-N(1)	93.41(9)
Cl(2)-Ru(1)-N(5)	95.58(9)

Table. 42 (continued)

Atom	Angle (°)
Cl(2)-Ru(1)-N(7)	171.2(1)
N(1)-Ru(1)-N(3)	76.9(1)
N(1)-Ru(1)-N(5)	177.50(9)
N(1)-Ru(1)-N(7)	101.2(1)
N(3)-Ru(1)-N(5)	101.4(1)
N(3)-Ru(1)-N(7)	84.0(1)
N(5)-Ru(1)-N(7)	76.8(1)
Ru(1)-N(1)-C(1)	128.7(2)
Ru(1)-N(1)-C(5)	113.0(2)
C(1)-N(1)-C(5)	118.2(3)
N(3)-N(2)-C(5)	112.0(2)
Ru(1)-N(3)-N(2)	119.8(2)
Ru(1)-N(3)-C(6)	124.8(2)
N(2)-N(3)-C(6)	114.1(2)
C(9)-N(4)-C(12)	121.8(4)
C(9)-N(4)-C(13)	120.8(3)
C(12)-N(4)-C(13)	116.6(4)
Ru(1)-N(5)-C(14)	128.6(2)
Ru(1)-N(5)-C(18)	112.9(2)
C(14)-N(5)-C(18)	118.3(3)
N(7)-N(6)-C(18)	111.7(3)
Ru(1)-N(7)-N(6)	120.3(3)
Ru(1)-N(7)-C(19)	124.8(2)

Table 42. (continued)

Atom	Angle (°)
N(6)-N(7)-C(19)	114.0(3)
C(22)-N(8)-C(25)	122.0(4)
C(22)-N(8)-C(26)	121.1(4)
C(25)-N(8)-C(26)	116.9(4)
N(1)-C(1)-C(2)	122.2(3)
C(1)-C(2)-C(3)	119.7(3)
C(2)-C(3)-C(4)	118.9(3)
C(3)-C(4)-C(5)	118.7(3)
N(1)-C(5)-N(2)	117.9(3)
N(1)-C(5)-C(4)	122.3(3)
N(2)-C(5)-C(4)	119.7(3)
N(3)-C(6)-C(7)	121.2(3)
N(3)-C(6)-C(11)	120.0(3)
C(7)-C(6)-C(11)	118.8(3)
C(6)-C(7)-C(8)	120.6(3)
C(7)-C(8)-C(9)	121.5(3)
N(4)-C(9)-C(8)	121.9(3)
N(4)-C(9)-C(10)	120.8(3)
C(8)-C(9)-C(10)	117.2(3)
C(9)-C(10)-C(11)	121.0(3)
C(6)-C(11)-C(10)	120.8(3)
N(5)-C(14)-C(15)	122.1(4)

Table 42. (continued)

Atom	Angle (°)
C(14)-C(15)-C(16)	119.5(3)
C(15)-C(16)-C(17)	119.1(3)
C(16)-C(17)-C(18)	118.7(4)
N(5)-C(18)-N(6)	118.0(3)
N(5)-C(18)-C(17)	122.2(4)
N(6)-C(18)-C(17)	119.7(4)
N(7)-C(19)-C(20)	121.5(3)
N(7)-C(19)-C(24)	119.3(3)
C(20)-C(19)-C(24)	119.2(3)
C(19)-C(20)-C(21)	120.5(3)
C(20)-C(21)-C(22)	121.4(3)
N(8)-C(22)-C(21)	121.6(4)
N(8)-C(22)-C(23)	121.2(4)
C(21)-C(22)-C(23)	117.2(4)
C(22)-C(23)-C(24)	121.6(3)
C(19)-C(24)-C(23)	120.1(3)
Cl(3)-C(27)-Cl(4)	110.3(3)
C(29)-C(28)-C(31)	47.8(6)
C(29)-C(28)-C(32)	52.0(6)
C(31)-C(28)-C(32)	99.4(7)
C(28)-C(29)-C(30)	126.6(8)
C(28)-C(29)-C(31)	80.1(8)
C(28)-C(29)-C(30)	129.7(7)

Table 42. (continued)

Atom	Angle (°)
C(30)-C(29)-C(31)	151(1)
C(30)-C(29)-C(32)	46.6(6)
C(30)-C(29)-C(30)	103.2(6)
C(31)-C(29)-C(32)	160(1)
C(31)-C(29)-C(30)	48.3(8)
C(32)-C(29)-C(30)	149.2(8)
C(29)-C(30)-C(32)	55.4(6)
C(29)-C(30)-C(29)	76.8(5)
C(29)-C(30)-C(31)	127.1(9)
C(32)-C(30)-C(29)	131.7(7)
C(32)-C(30)-C(31)	177.2(9)
C(29)-C(30)-C(31)	50.7(7)
C(28)-C(31)-C(29)	50.8(7)
C(28)-C(31)-C(30)	131.8(9)
C(29)-C(31)-C(30)	81.0(8)
C(28)-C(32)-C(29)	48.0(6)
C(28)-C(32)-C(30)	126.0(9)
C(29)-C(32)-C(30)	78.0(8)

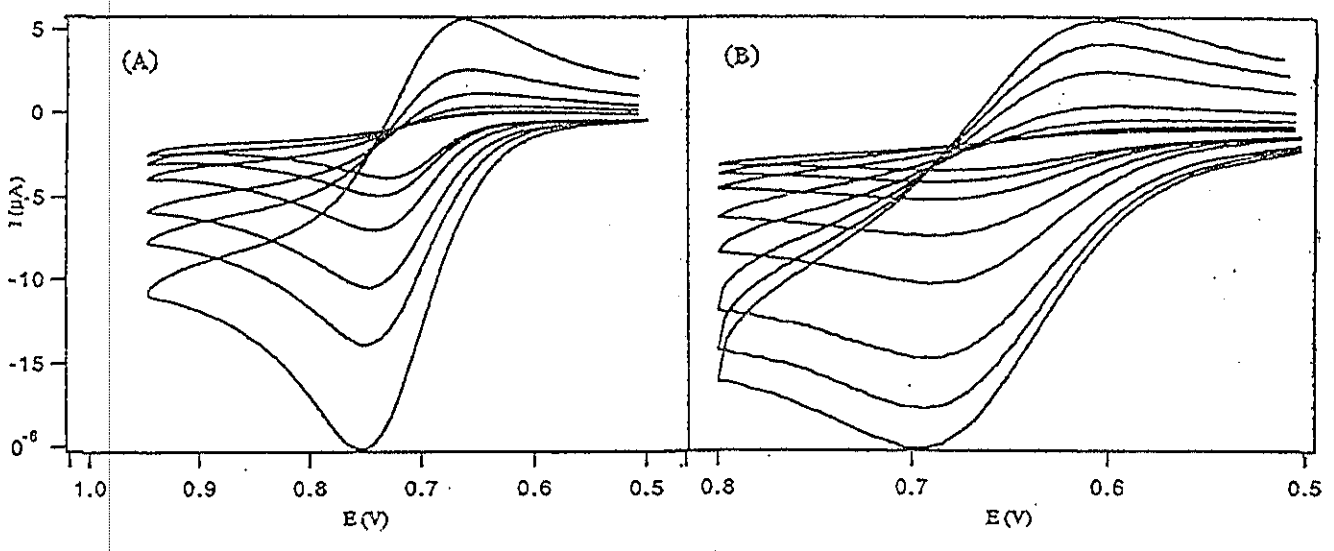

Figure 39. Cyclic voltammograms of ligand group I (A) dmazpy, (B) deazpy scanned with various scan rates (50-2000 mV/s)

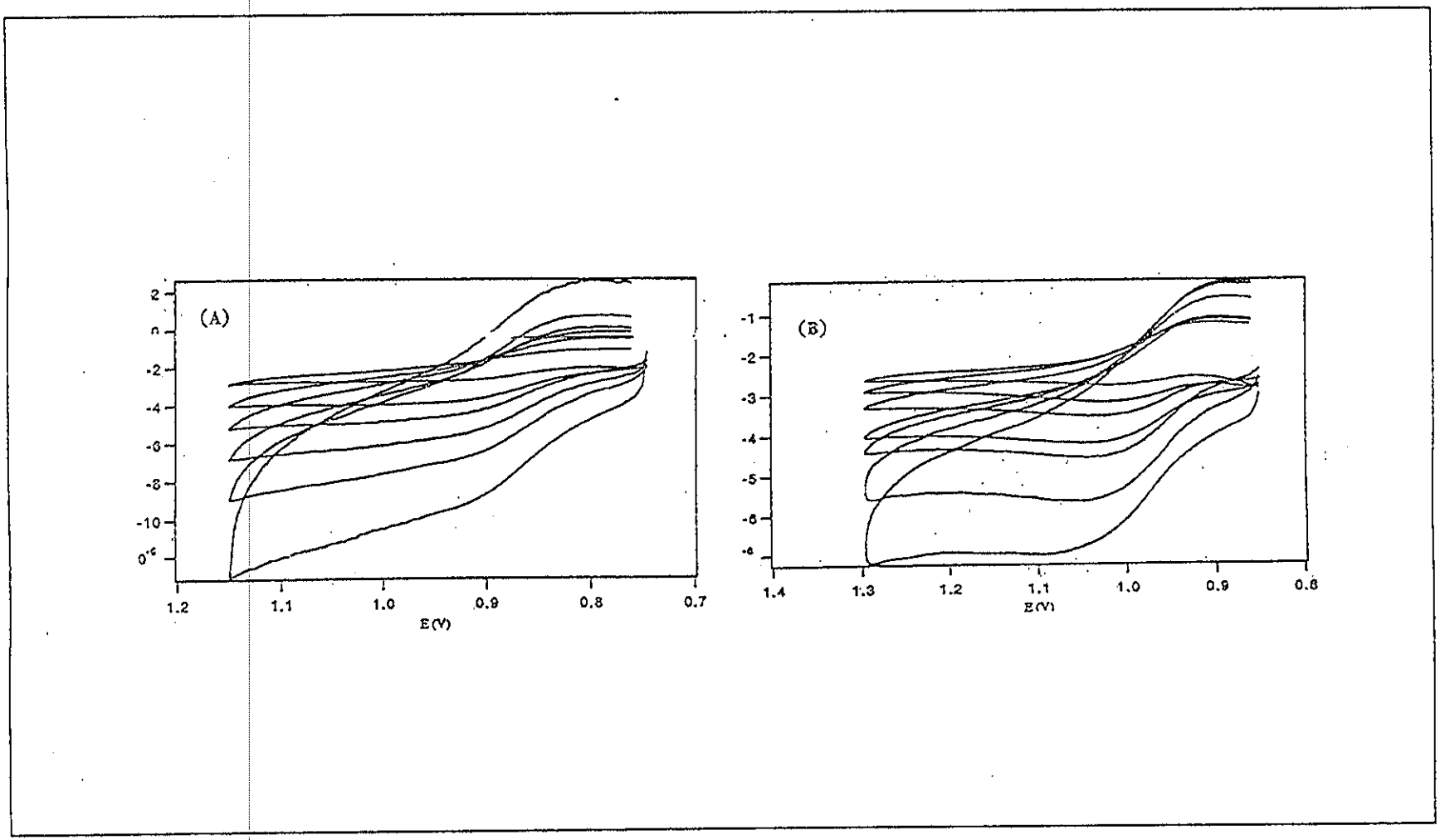

Figure 40. Cyclic voltammograms of ligand group II (A) dmazpy, (B) deazpy scanned with various scan rates (50-2000 mV/s)

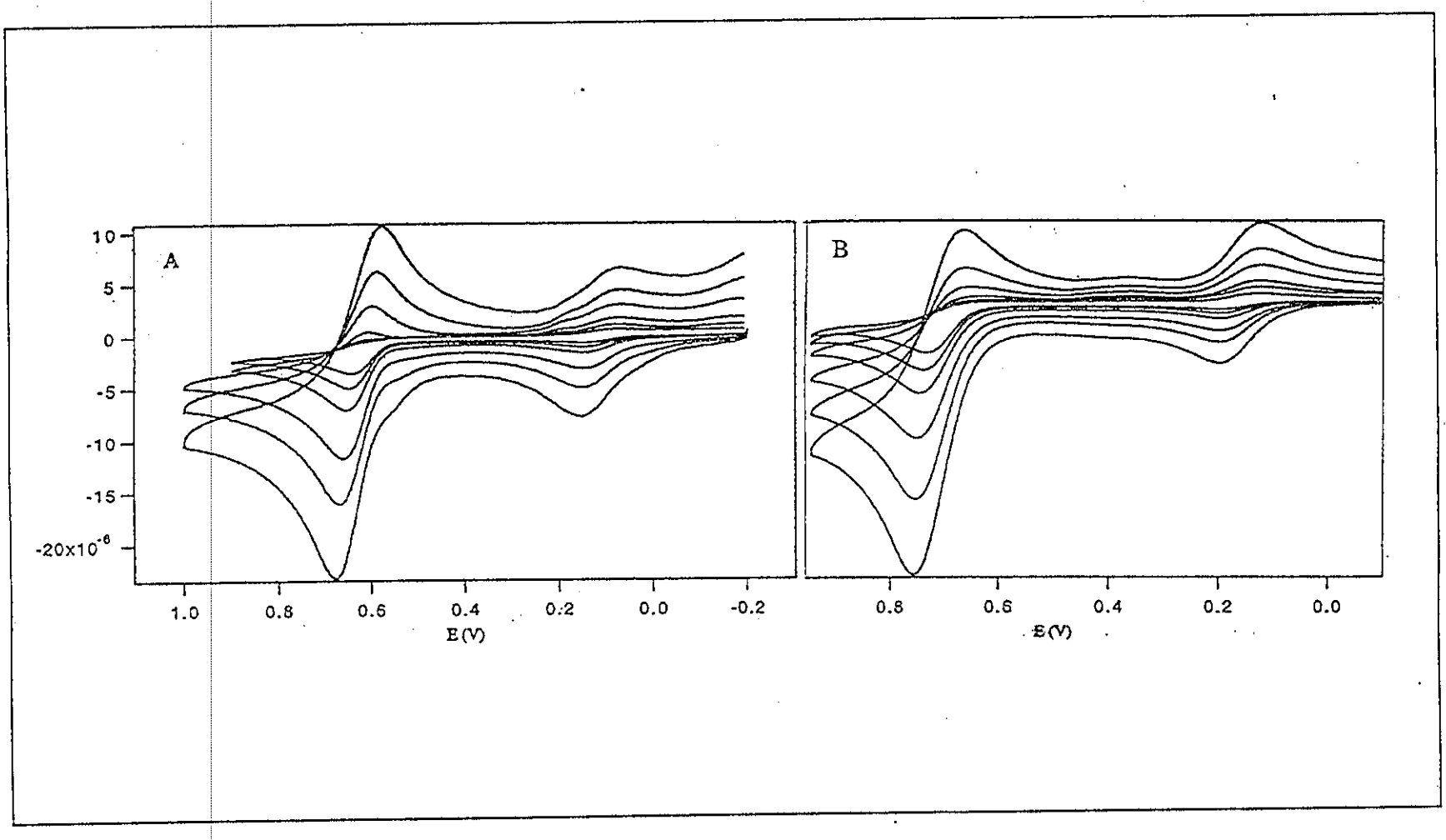

Figure 41. Cyclic voltammograms of (A) *N,N*-dimethyl-1,4-nitrosoaniline and (B) *N,N*-diethyl-1,4-nitrosoaniline scanned with various scan rates (50-2000 mV/s)

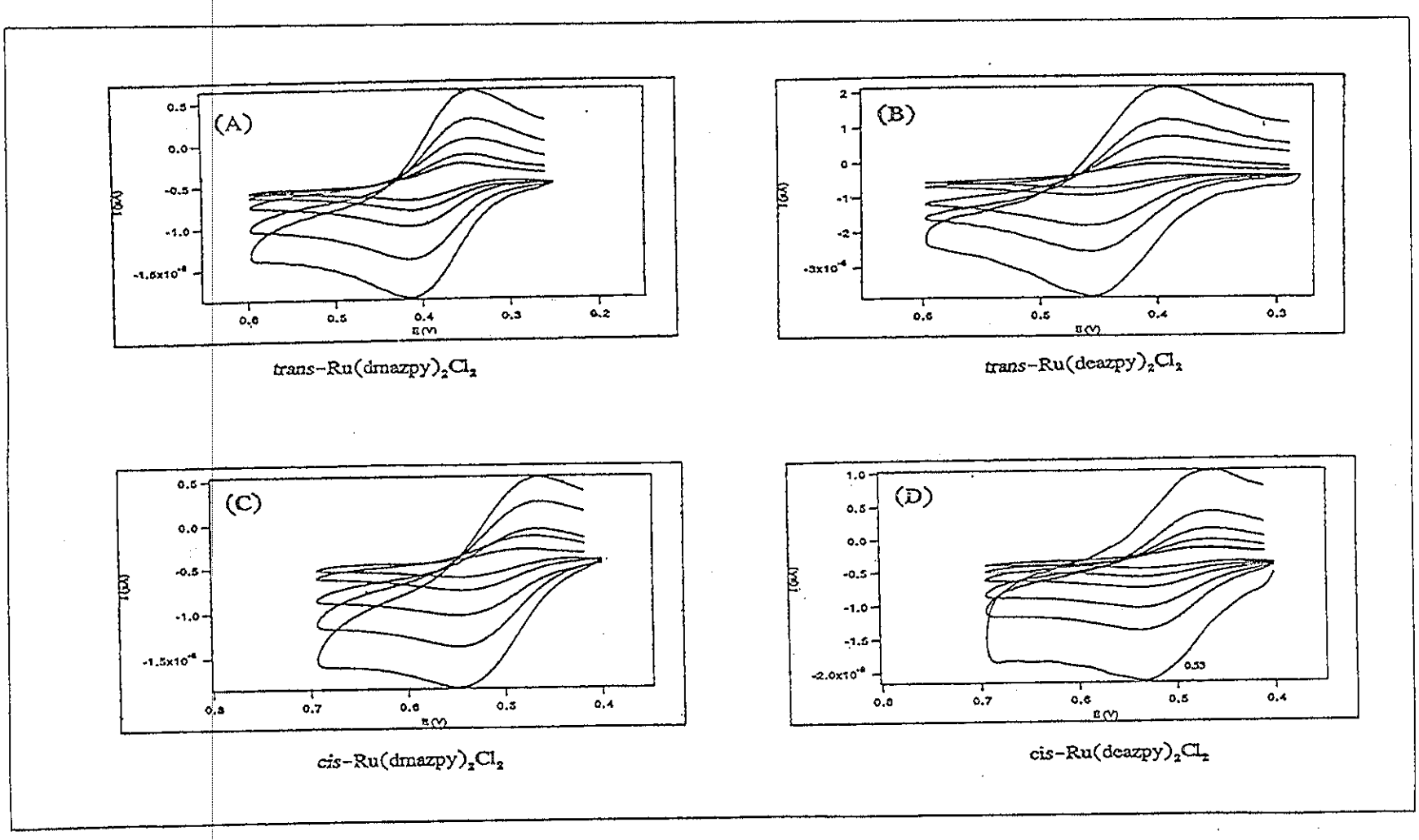

Figure 42. Cyclic voltammograms of couple I in oxidation range of A-D *trans*- and *cis*- $Ru(L)_2Cl_2$ (L = dmazpy and deazpy) by varying scan rates (50-2000 mV/s)

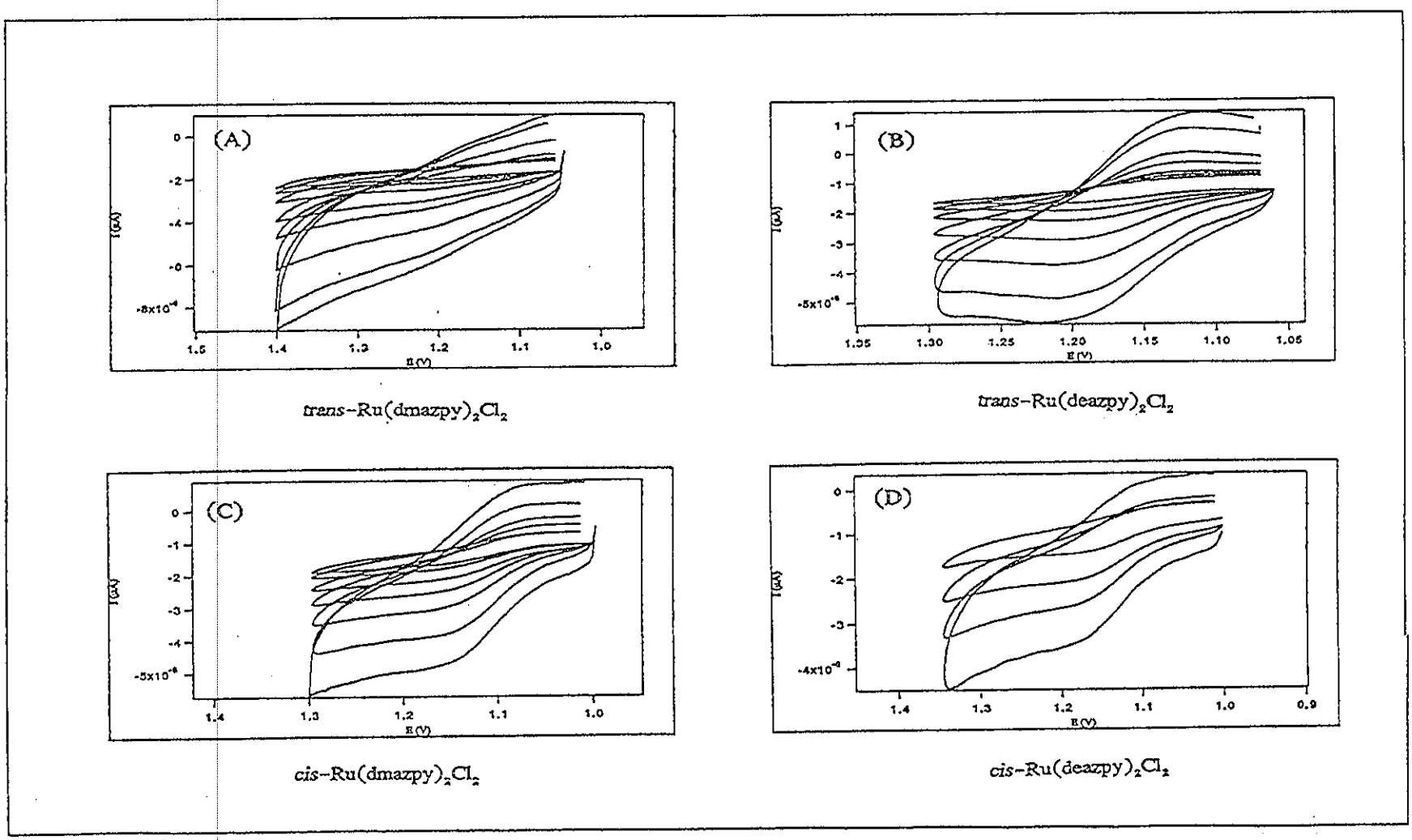

Figure 43. Cyclic voltammograms of couple II in oxidation range of A-D *trans*- and *cis*- $Ru(L)_2Cl_2$ (L = dmazpy and deazpy) by varying scan rates (50-2000 mV/s)

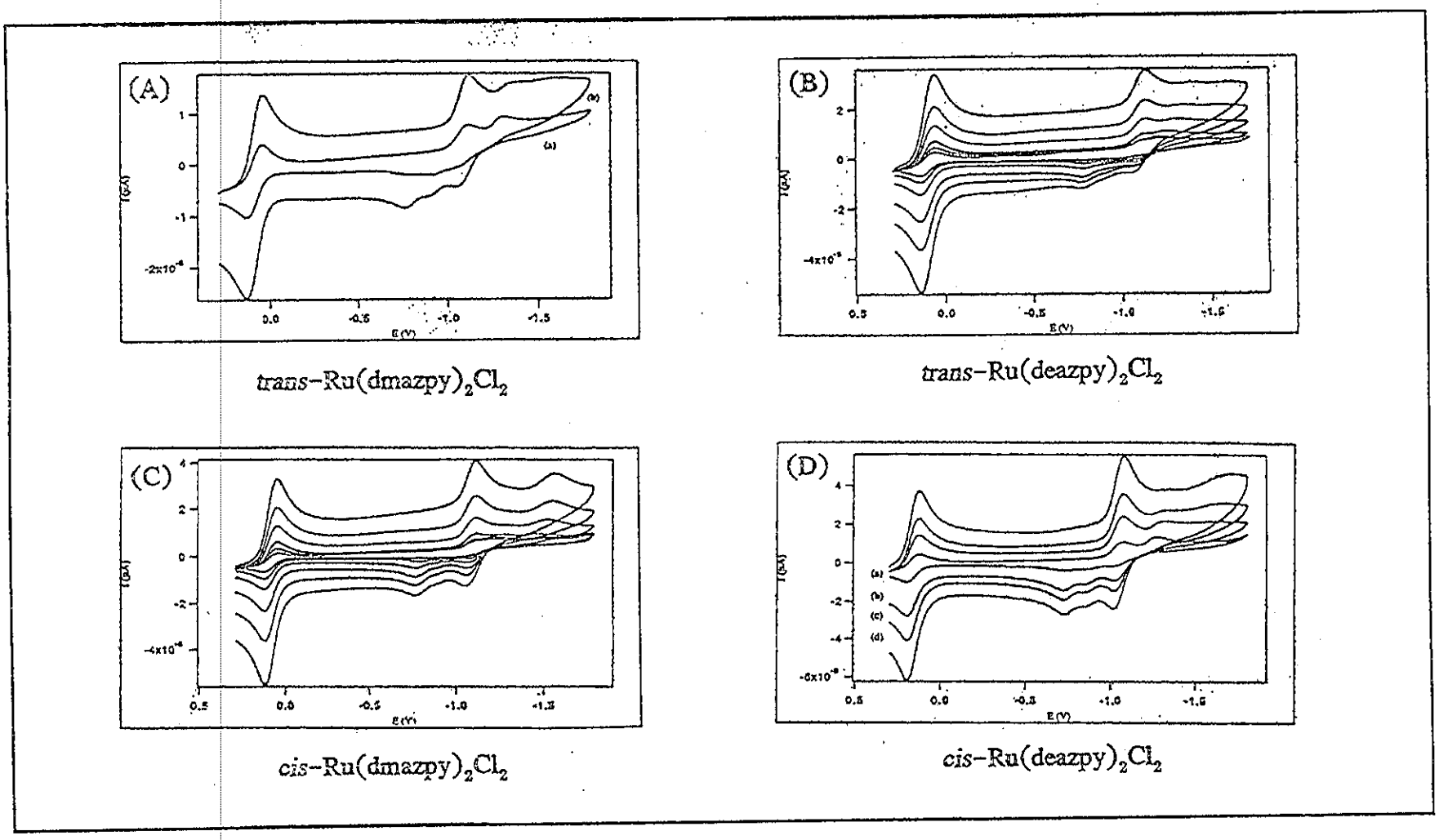

Figure 44. Cyclic voltammograms of reduction range of A-D *trans*- and *cis*- $Ru(L)_2Cl_2$ (L = dmazpy and deazpy) by varying scan rates (50-2000 mV/s)

VITAE

Name Miss Nararak Leesakul

Birth Date 23 January 1977

Educational Attainment

Degree	Name of Institution	Year of Graduate
Bachelor of Science (Chemistry)	Prince of Songkla University	1998

Scholarship Awards during Enrolment

Postgraduate Education and Research Program in Chemistry (2000-2001).